Electronic Supplementary Material (ESI) for Organic & Biomolecular Chemistry.


*Supporting Information for*

# Optimization of a Synthetic Receptor for Dimethyllysine using a Biphenyl-2,6-Dicarboxylic Acid Scaffold: Insights into Selective Recognition of Hydrophilic Guests in Water

*Isaiah N. Gober and Marcey L. Waters**

Department of Chemistry, CB 3290, UNC Chapel Hill, Chapel Hill, NC 27599

mlwaters@email.unc.edu

**Scheme S1**. Synthesis of Monomer **I**

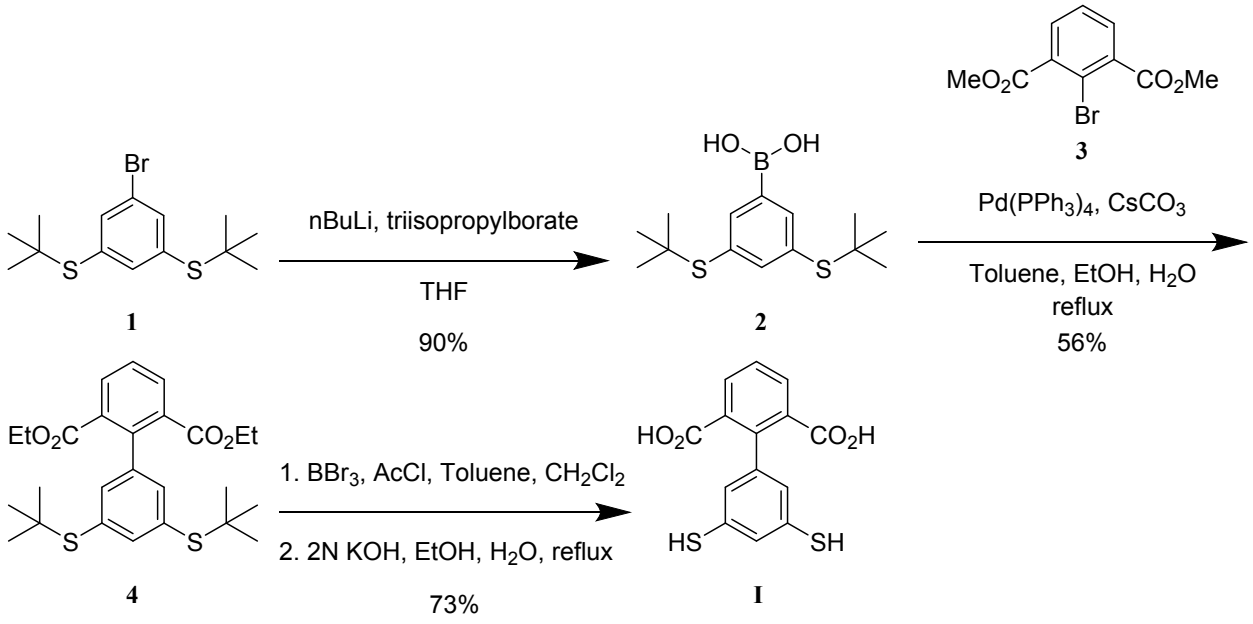


**Synthesis of 1**. Compound **1** was synthesized according to published procedure.[1]

**Synthesis of 2**. Compound **1** (0.50 g, 1.51 mmol) was dissolved in anhydrous THF (6 mL) at -78 $^{o}$C, and n-butyl lithium (2.5 M in hexanes, 0.75 mL, 1.9 mmol) was added dropwise. The solution was stirred at -78 $^{o}$C for 1 h, and then triisopropyl borate (1.2 mL, 6.4 mmol) was added dropwise. The reaction was stirred at -78 $^{o}$C for 3 h and then allowed to warm to room temperature overnight. Water (1 mL) was added to the reaction, and the solvent was removed under reduced pressure. The crude product was dissolved in dichloromethane, and 1N HCl (3 mL) was added. After stirring for 1 h, the organic fraction was separated, and the product was purified by column chromatography (ethyl acetate/hexanes gradient from 10% to 35%) to give a white solid (0.404 g, 90% yield). $^{1}$H NMR ($CDCl_3$, 600 MHz): 7.857,7.854 (d, 1H, CH), 7.752-7.857 (m, 2H, CH), 1.275 (s, 18H, $CH_3$). $^{13}$C NMR ($CDCl_3$, 600 MHz): 148.130, 147.303, 142.906, 142.777, 132.515, 46.284, 31.088. MS (calculated): 577.23 [cyclic boronic ester dimer + OH], 875.35 [open boronic ester trimer + OH], 1137.45 [cyclic boronic ester + OH], 1417.57 [cyclic boronic ester pentamer + OH]. HRMS (observed, ESI-): 577.23339 [cyclic boronic ester dimer + OH], 875.35906 [open boronic ester trimer + OH], 1137.46613 [cyclic boronic ester + OH], 1417.58859 [cyclic boronic ester pentamer + OH].

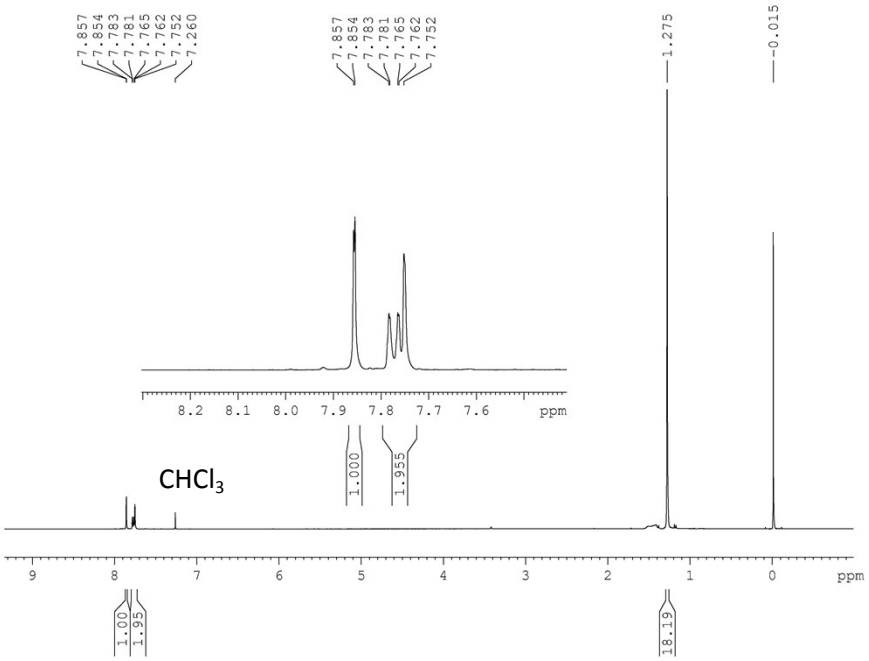


**Figure S1**. 1D $^{1}$H-NMR (600 MHz) of Compound **2** in $CDCl_3$.

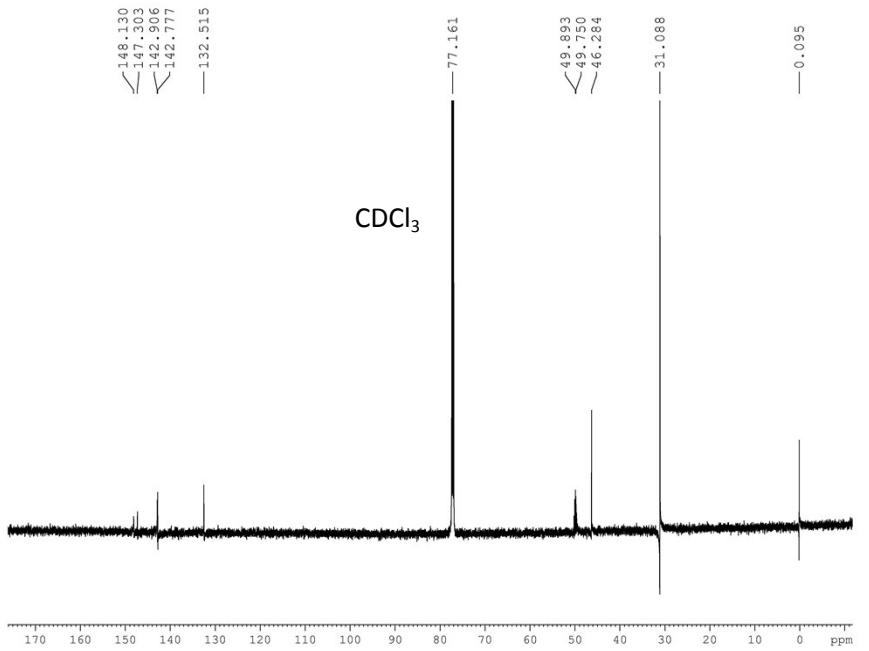


**Figure S2**. 1D $^{13}$C-NMR (600 MHz) of Compound **2** in $CDCl_3$.

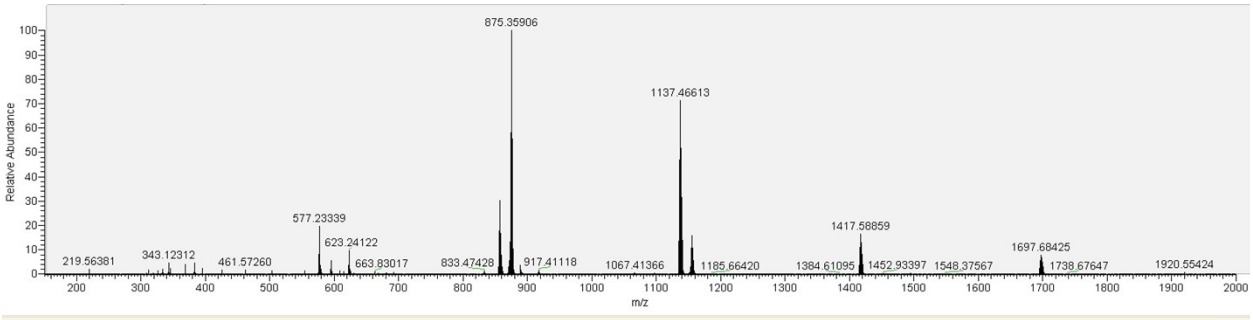


**Figure S3**. High resolution mass spectrum of Compound **2**.

**Synthesis of 3**. Compound **3** was synthesized according to published procedure.[2]

**Synthesis of 4**. A solution of $CsCO_3$ (3.60 g, 11 mmol) in $H_2O$ (4.8 mL), toluene (21 mL), and EtOH (21 mL) was degassed by bubbling with argon for 2 h. To this flask under an atmosphere of argon were added **3** (0.69 g, 2.5 mmol), **2** (0.78 g, 2.6 mmol), and $Pd(PPh_3)_4$ (0.30 g, mmol). The solution was heated to reflux and vigorously stirred overnight. After cooling to room temperature, the solvent was removed under reduced pressure. The resulting crude solid was purified by column chromatography (ethyl acetate/hexanes gradient from 15% to 35%) to give a white solid (0.59 g, 56% yield). $^1$H NMR ($CDCl_3$, 600 MHz): 7.935, 7.922 (d, 2H, CH), 7.722 (s, 1H, CH), 7.506 (t, 1H, CH), 7.400, 7.398 (d, 2H), 4.024, 4.012 (q, 4H, $CH_2$), 1.303 (s, 18H, $CH_3$), 1.010 (t, 6H, $CH_3$). $^{13}$C NMR ($CDCl_3$, 600 MHz): 167.580, 144.815, 139.949, 137.854, 133.349, 132.343, 127.801, 61.324, 46.339 31.069, 14.004. MS (calculated): 475.20 [M+H], 949.39 [2M+H], 971.37 [2M+$Na^+$]. HRMS (observed, ESI+): 475.19894 [M+H], 949.39195 [2M+H], 971.37069 [2M+$Na^+$].

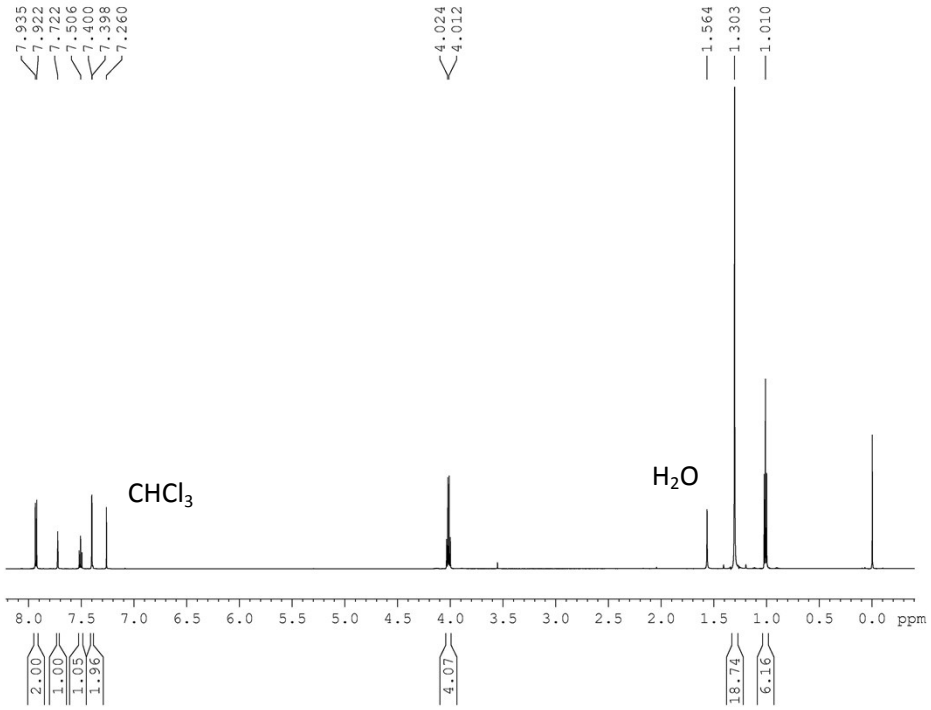


**Figure S4**. 1D $^{1}$H-NMR (600 MHz) of Compound **4** in $CDCl_3$.

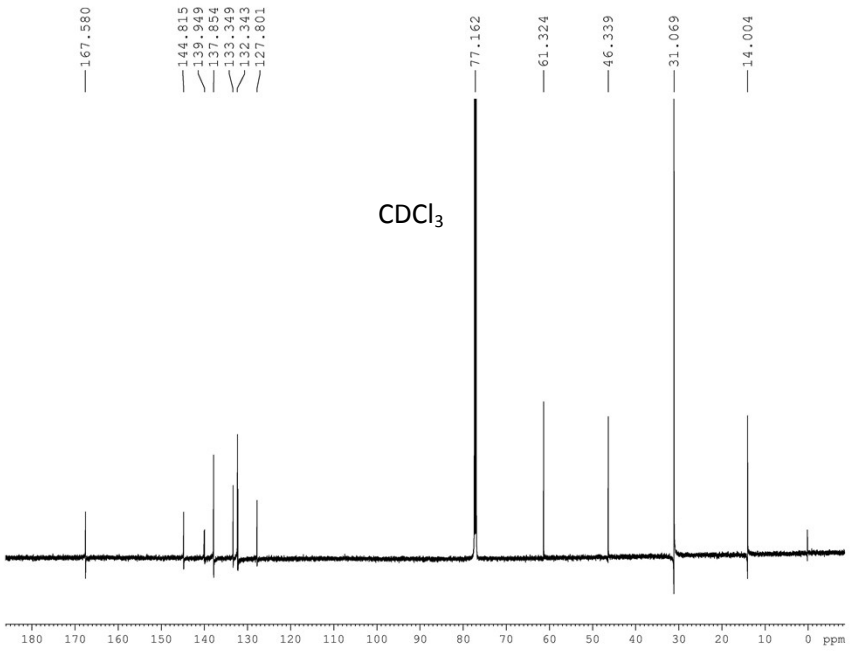


**Figure S5**. 1D $^{13}$C-NMR (600 MHz) of Compound **4** in $CDCl_3$.

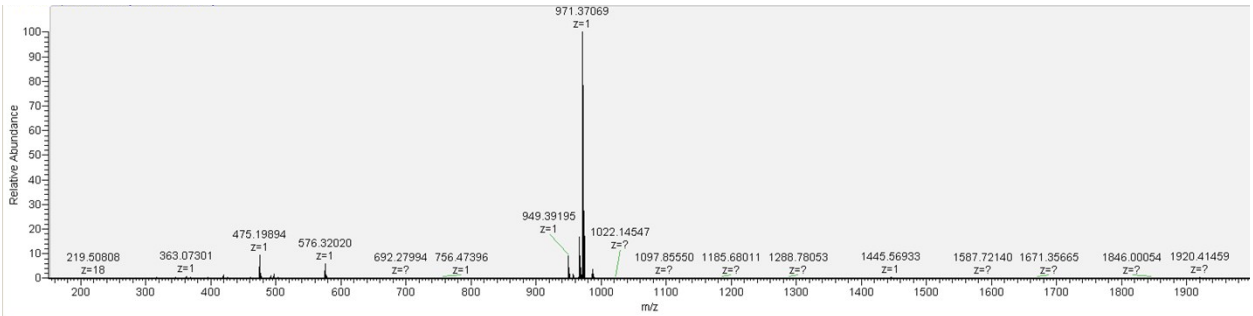


**Figure S6**. High resolution mass spectrum of Compound **4**.

**Synthesis of I**. Compound **4** (0.50 g, 1.1 mmol) was dissolved in a solution of toluene (2.2 mL) and acetyl chloride (1.12 mL, 15.7 mmol) under an atmosphere of nitrogen. The solution was cooled on an ice bath, and a 1.0 M solution of $BBr_3$ in dichloromethane (2.47 mL, 2.5 mmol) was added dropwise. Afterward, the ice bath was removed and the reaction was allowed to warm to room temperature. After 2h, the reaction was quenched by slow, dropwise addition of water (10 mL). The organic phase was separated, washed with water (3 x 10 mL), and dried over magnesium sulfate. The solvent was removed under reduce pressure to provide a crude thioacetate intermediate. A solution of potassium hydroxide (0.80 g, 14.3 mmol) in water (4.5 mL) and ethanol (2 mL) was degassed by bubbling with nitrogen for 2 h. To this solution was the thioacetate intermediate (0.38 g, 0.91 mmol) under an atmosphere of nitrogen. The reaction was heated at reflux for 3 h. After cooling to room temperature, the solution was concentrated under reduced pressure. The product was precipitated out by addition of 3N HCl. The precipitate was collected by vacuum filtration and dried under vacuum overnight to give a white solid (0.24 g, 73% yield over 2 steps). $^1$H NMR ($CD_3OD$ 600 MHz): 7.892, 7.879 (d, 2H, CH), 7.537 (t, 1H, CH), 7.170 (s, 1H, CH), 6.905, 6.902 (s, 2H, CH). $^{13}$C NMR ($CDCl_3$, 600 MHz): 171.071, 142.068, 140.533, 135.252, 133.333, 132.375, 128.777, 128.331, 127.169. MS (calculated): 304.99 [M-H], 610.99 [2M-H]. HRMS (observed, ESI+): 304.99499 [M-H], 610.99692 [2M-H].

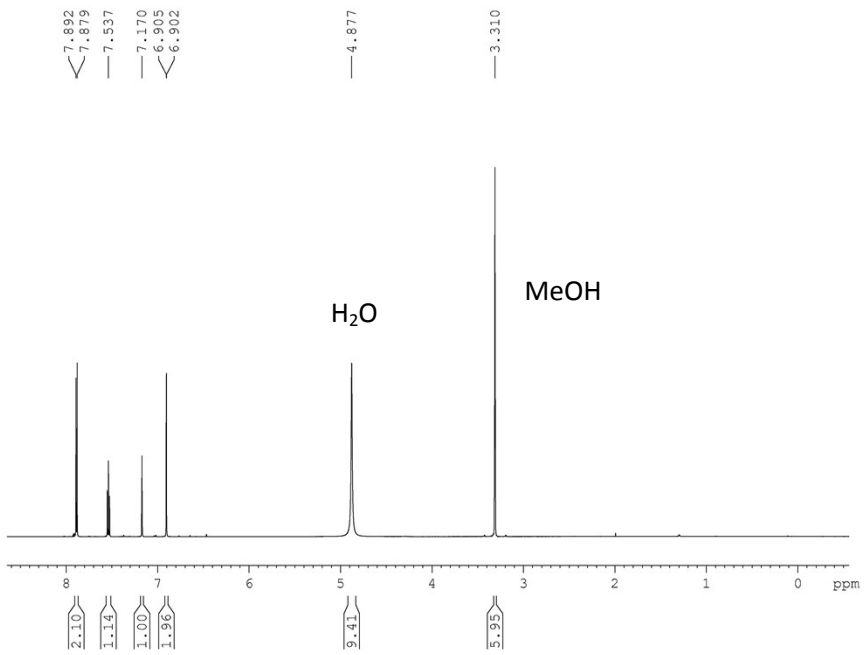


**Figure S7**. 1D $^{1}$H-NMR (600 MHz) of Monomer **I** in $CD_3OD$.

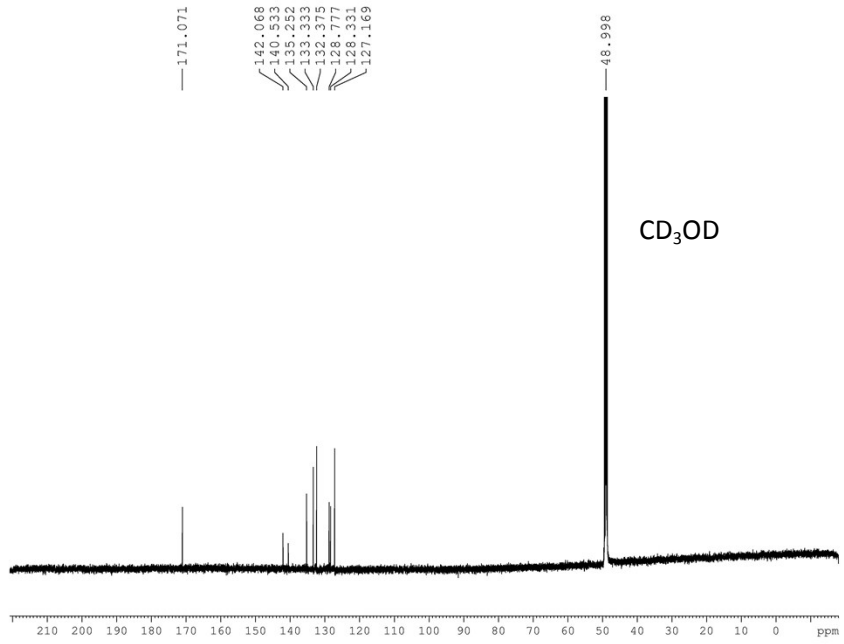


**Figure S8**. 1D $^{13}$C-NMR (600 MHz) of Monomer **I** in $CD_3OD$.

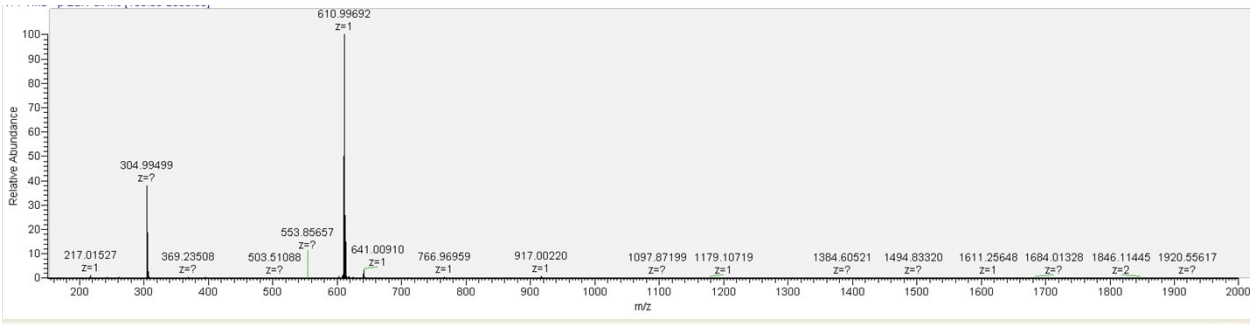


**Figure S9**. High resolution mass spectrum of Monomer **I**.

**Scheme S2**. Synthesis of Monomer J

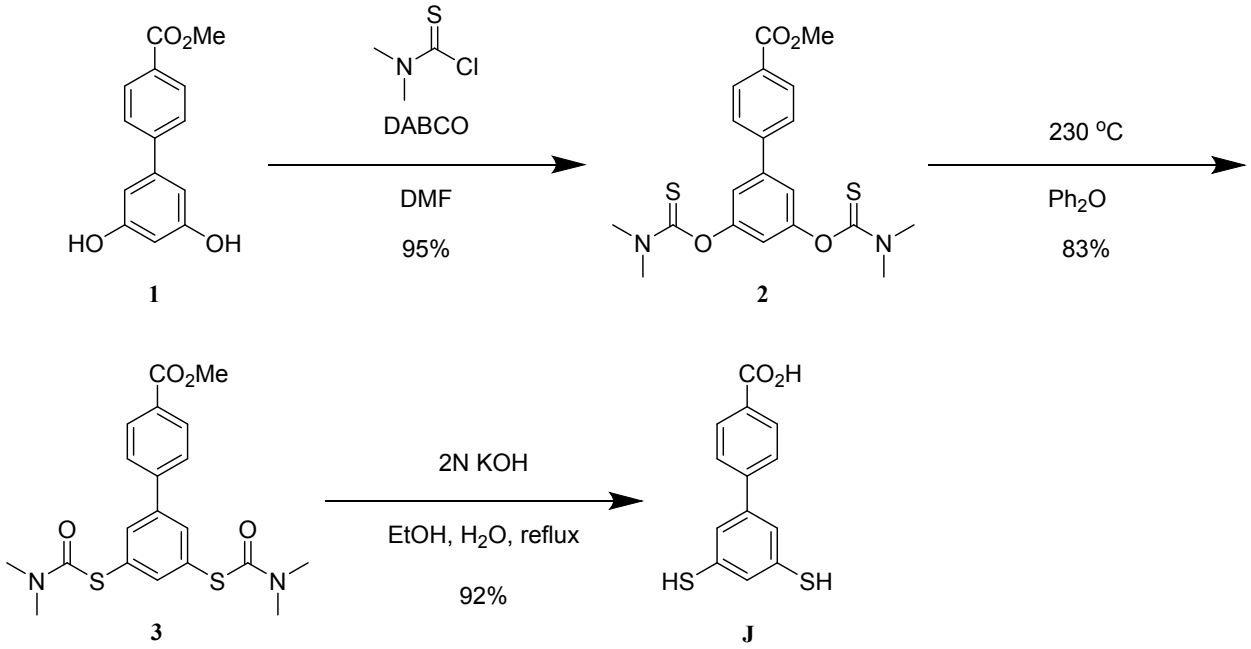


**Synthesis of 5**. Compound **5** was prepared according to published procedure.[3]

**Synthesis of 6**. Compound **5** (0.23 g, 0.94 mmol, 1 equiv.) was dissolved in 2 mL of anhydrous DMF under a nitrogen atmosphere, and the solution was cooled to 0°C. To this solution was added 1,4-diazabicyclo[2.2.2]octane (0.42 g, 3.7 mmol, 4 equiv.) in small portions. A solution of dimethylthiocarbamoyl chloride (0.47 g, 3.7 mmol, 4 equiv.) in 2 mL anhydrous DMF was added dropwise to the resulting suspension. The reaction mixture was allowed to warm to room temperature and stirred for 24 hours. Afterward, 40 mL of water was added to the reaction mixture to precipitate out the crude solid, which was collected by filtration to yield a white solid (0.37 g, 95%). $^{1}$H NMR ($CDCl_3$, 600 MHz): 8.087,8.073 (d, 2H, CH), 7.664,7.650 (d, 2H, CH), 7.249,7.245 (d, 2H, CH), 6.893 (t, 1H, CH), 3.935 (s, 3H, $CH_3$), 3.466 (s, 6H, N-$CH_3$), 3.361 (s, 6H, N-$CH_3$). $^{13}$C NMR ($CDCl_3$, 600 MHz): 187.336, 167.000, 154.586, 143.833, 141.448, 130.241, 127.288, 119.516, 117.731, 52.324, 43.498, 39.025. MS (calculated): 419.11 [M+H], 441.09 [M+$Na^+$], 837.23 [2M+H], 859.21 [2M+$Na^+$]. HRMS (observed, ESI+): 419.10986 [M+H], 441.09189 [M+$Na^+$], 837.21382 [2M+H], 859.19383 [2M+$Na^+$].

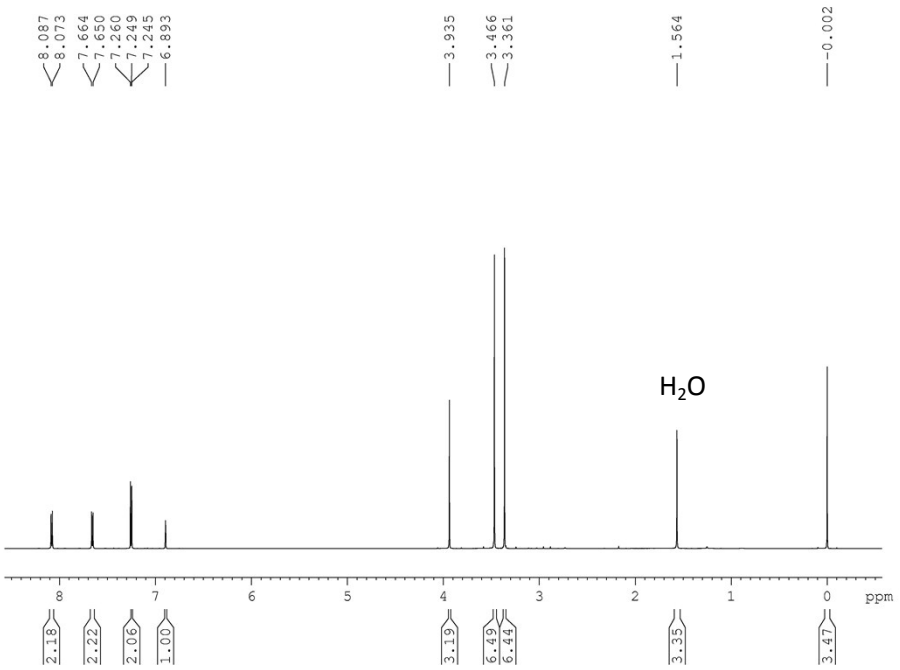


**Figure S10**. 1D $^{1}$H-NMR (600 MHz) of Compound **6** in $CDCl_3$.

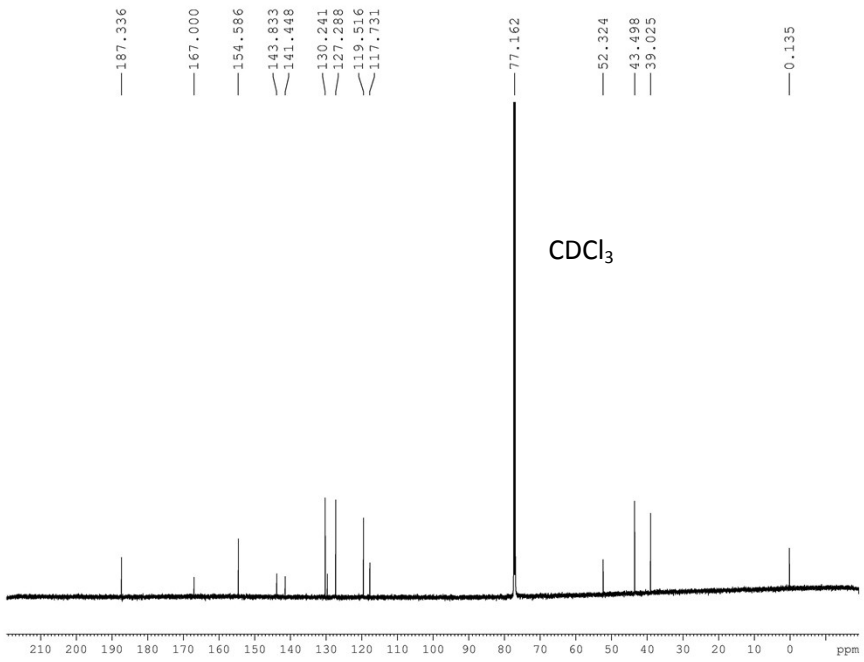


**Figure S11**. 1D $^{13}$C-NMR (600 MHz) of Compound **6** in $CDCl_3$.

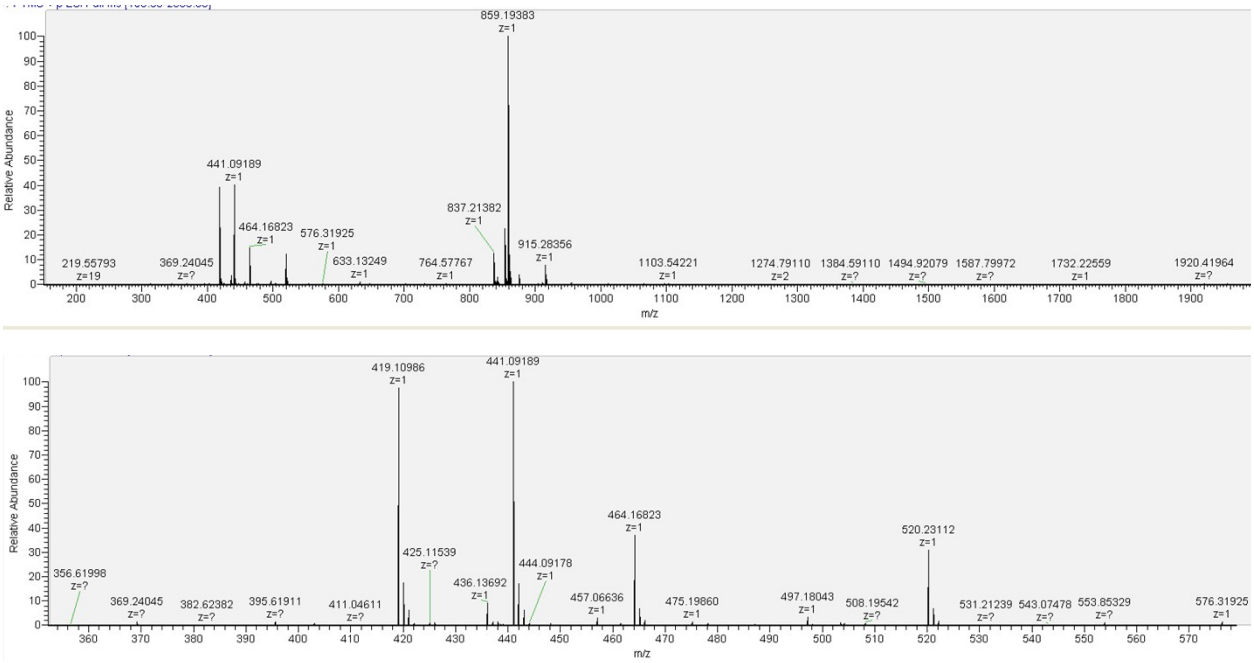


**Figure S12**. High resolution mass spectrum of Compound **6**.

**Synthesis of 7**. Compound **6** (0.30 g, 0.72 mmol, 1 equiv.) was dissolved in 5 mL of warm diphenyl ether and heated to 230°C for 3 hours. The reaction mixture was cooled to room temperature and diluted with 15 mL hexanes. The solution was purified by column chromatography (ethyl acetate/hexanes gradient from 0 to 50%) to obtain a white solid (0.25 g, 83%). $^{1}$H NMR ($CDCl_3$, 600 MHz): 8.084, 8.070 (d, 2H, CH), 7.768, 7.765 (d, 2H, CH), 7.663, 7.660 (d, 2H, CH), 7.650 (s, 1H, CH), 3.934 (s, 3H, $CH_3$), 3.013 (s, 6H, N-$CH_3$), 3.035 (s, 6H, N-$CH_3$). $^{13}$C NMR ($CDCl_3$, 600 MHz): 167.056, 166.371, 144.104, 141.550, 141.390, 135.328, 130.276, 130.210, 129.459, 127.460, 52.294, 37.113. MS (calculated): 419.11 [M+H], 441.09 [M+$Na^+$], 837.23 [2M+H], 859.21 [2M+$Na^+$]. HRMS (observed, ESI+): 419.11038 [M+H], 441.09259 [M+$Na^+$], 837.21406 [2M+H], 859.19353 [2M+$Na^+$].

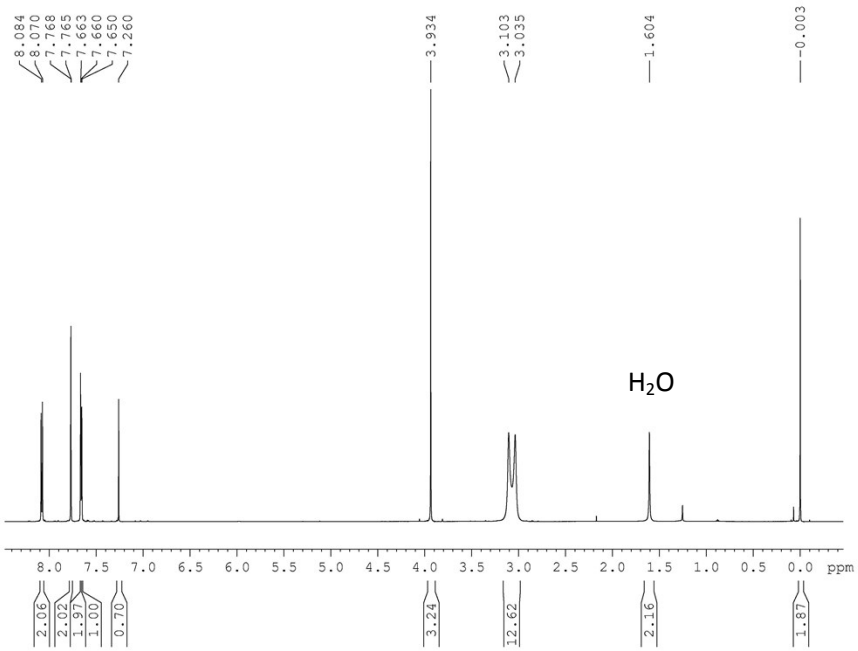


**Figure S13**. 1D $^{1}$H-NMR (600 MHz) of Compound **7** in $CDCl_3$.

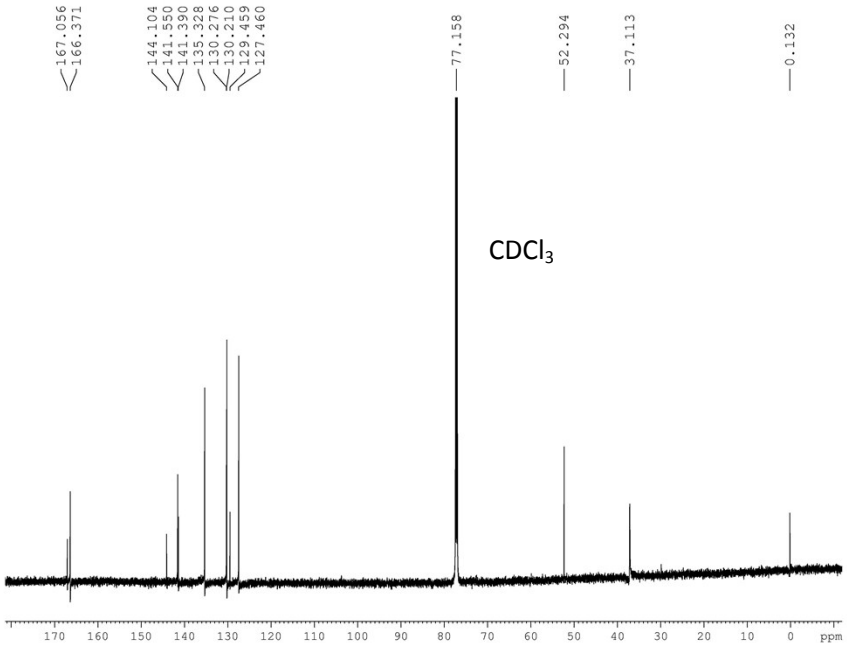


**Figure S14**. 1D $^{13}$C-NMR (600 MHz) of Compound **7** in $CDCl_3$.

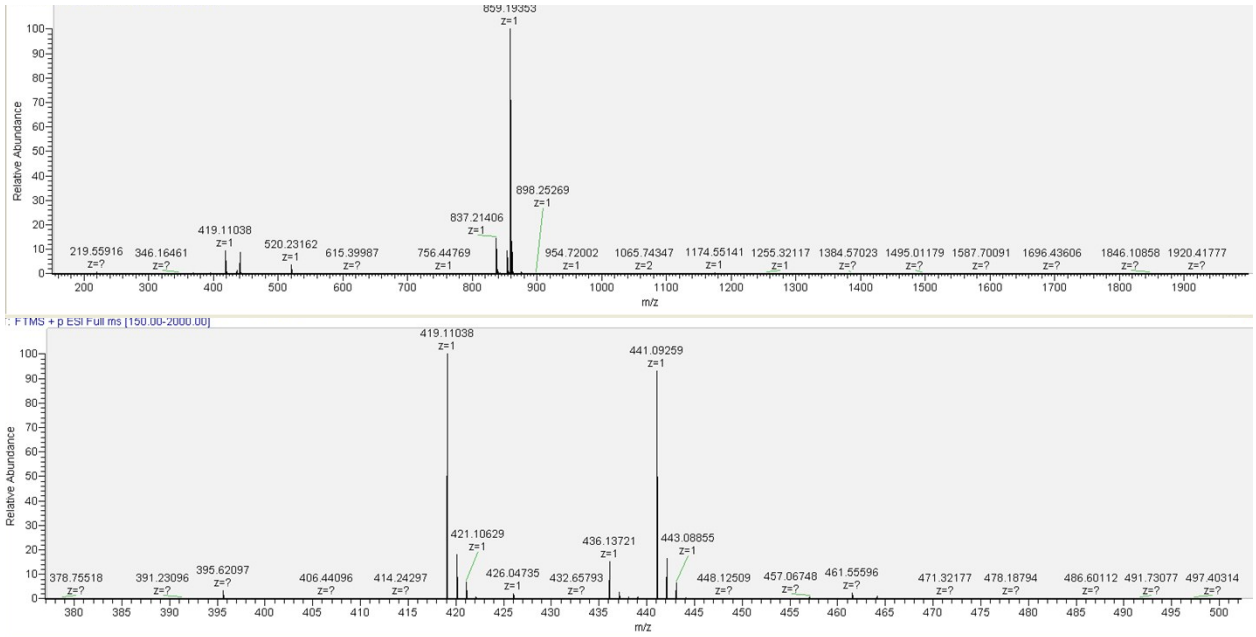


**Figure S15**. High resolution mass spectrum of Compound **7**.

**Synthesis of J**. Potassium hydroxide (0.80 g, 14 mmol, 33 equiv.) was dissolved in a solution of ethanol (2 mL) and water (4.5 mL), and the solution was degassed for 2 hours. To this solution was added compound **3** (0.18 g, 0.43 mmol, 1 equiv.). The reaction was refluxed for 3 hours and then cooled to room temperature. Ethanol was removed under reduced pressure, and 10% HCl (10 mL) was added. The precipitate was collected by vacuum filtration and dried under vacuum to give a white solid (0.102 g, 92%). $^{1}$H NMR ($CD_3OD$ 600 MHz): 8.093, 8.079 (d, 2H, CH), 7.684, 7.670 (d, 2H, CH), 7.343, 7.340 (d, 2H, CH), 7.234 (s, 1H, CH). $^{13}$C NMR ($CDCl_3$, 600 MHz): 169.560, 145.557, 142.835, 135.383, 131.365, 128.616, 128.040, 125.076. MS (calculated): 261.00 [M-H], HRMS (observed, ESI-): 261.00495.

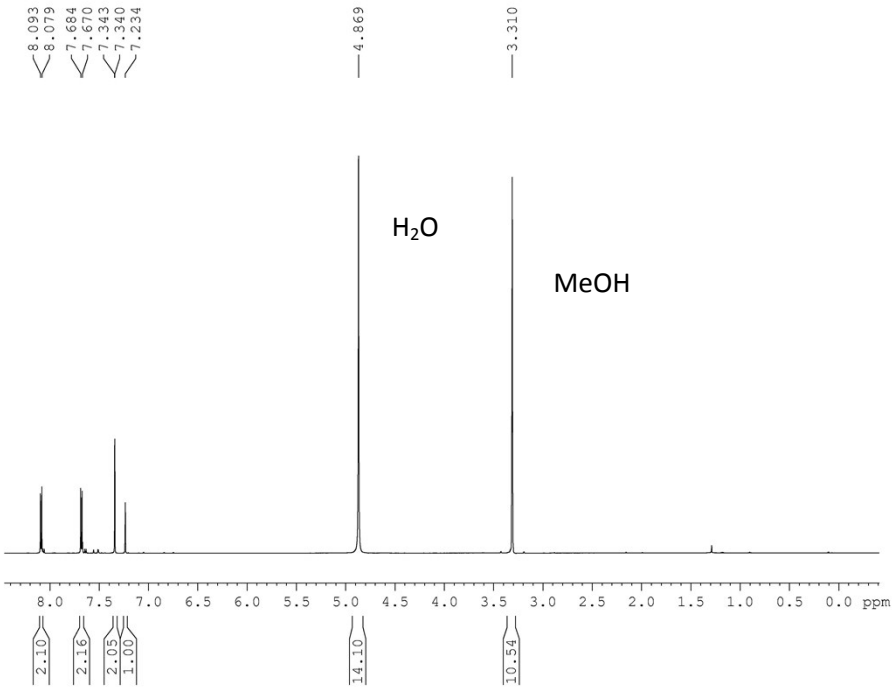


**Figure S16**. 1D $^{1}$H-NMR (600 MHz) of Monomer **J** in $CD_3OD$.

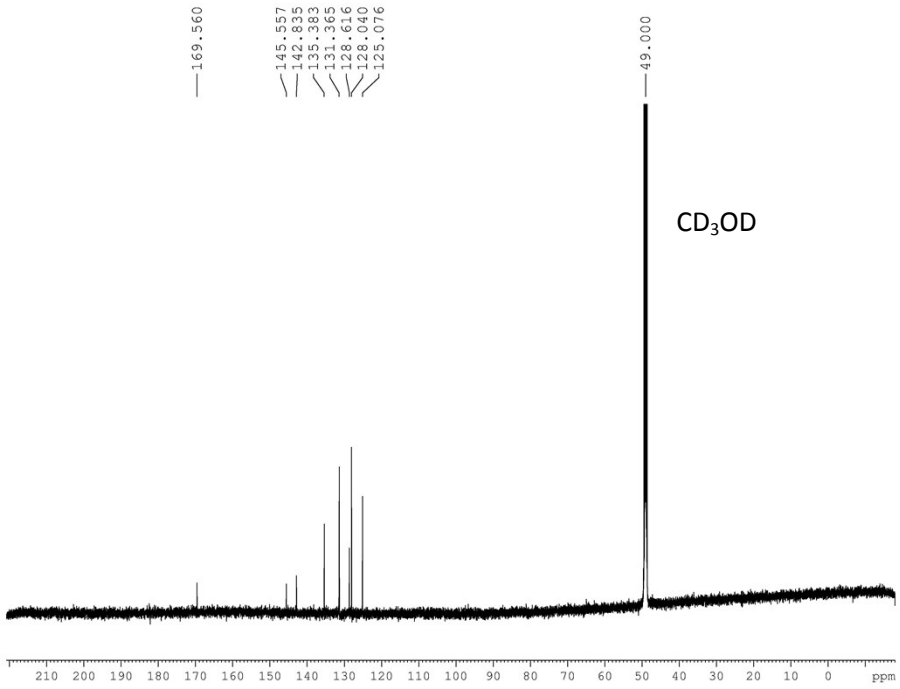


**Figure S17**. 1D $^{13}$C-NMR (600 MHz) of Monomer **J** in $CD_3OD$.

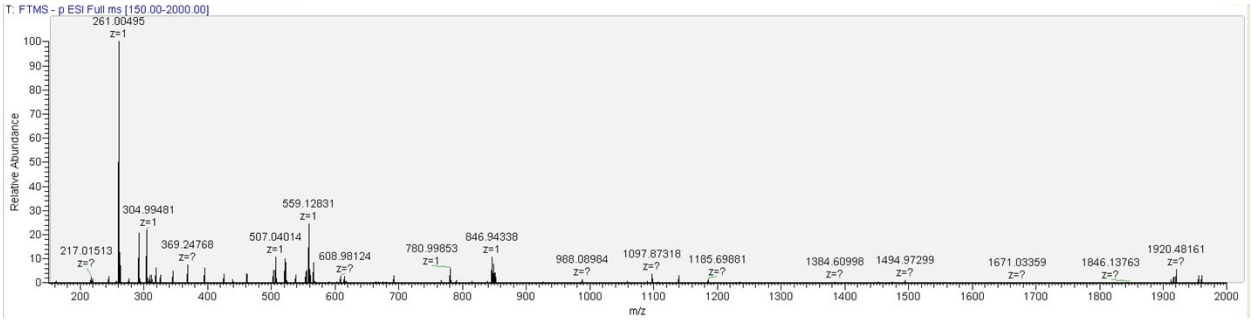


**Figure S18**. High resolution mass spectrum of Monomer **J**.

**Synthesis of $A_2I$ and $A_2J$**

DCLs were prepared on a preparative scale using butyltrimethylammonium bromide as a guest for templating the formation of the desired receptor. Libraries were prepared using 2.5 mM **A**, 2.5 mM biphenyl monomer (**I** or **J**), and 10 mM guest in 50 mM sodium borate buffer at pH 8.5. Equilibration was allowed to occur for at least 5 days, after which the desired receptor was purified by semi-preparative reversed-phase HPLC (solvent A: 10 mM $NH_4OAc$ in $H_2O$; solvent B: 10 mM $NH_4OAc$ in 9:1 $CH_3CN$:$H_2O$). For **$A_2I$**, a gradient from 10% B to 100% B in 1 hour was used for purification. For **$A_2J$**, the following gradient was used: 0% B to 35% B over 1 min, 35% B to 40% B over 5 min, 40% B to 55% B over 30 min, and 55% B to 100% B over 30 min. Collected fractions were lyophilized to give off-white solids.

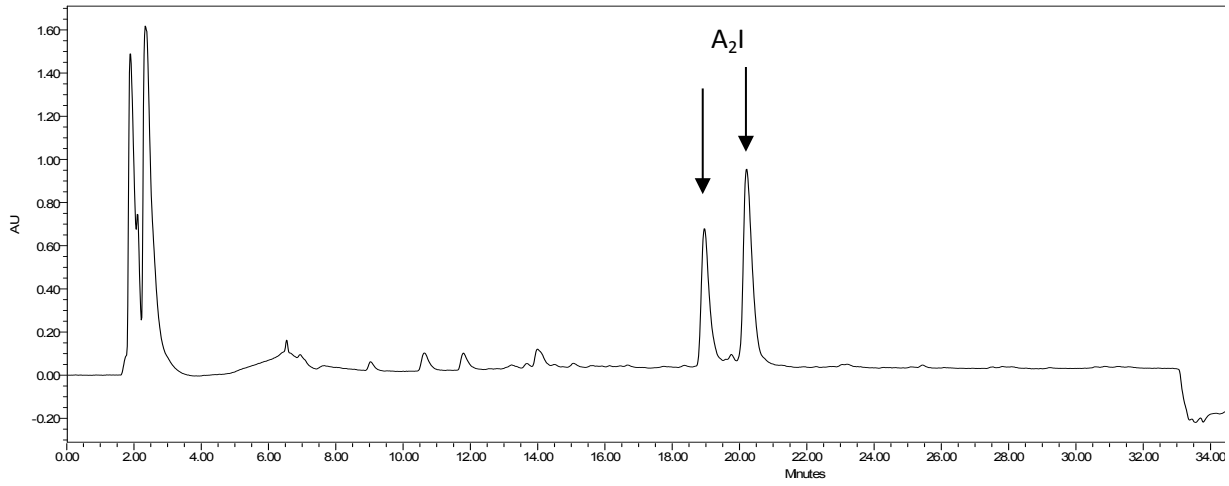


**Figure S19**. Semi-preparative reversed-phase HPLC traces of the purification of **$A_2I$** from a preparative scale DCL. Absorbance measured at 214 nm.

## $A_2I$-1

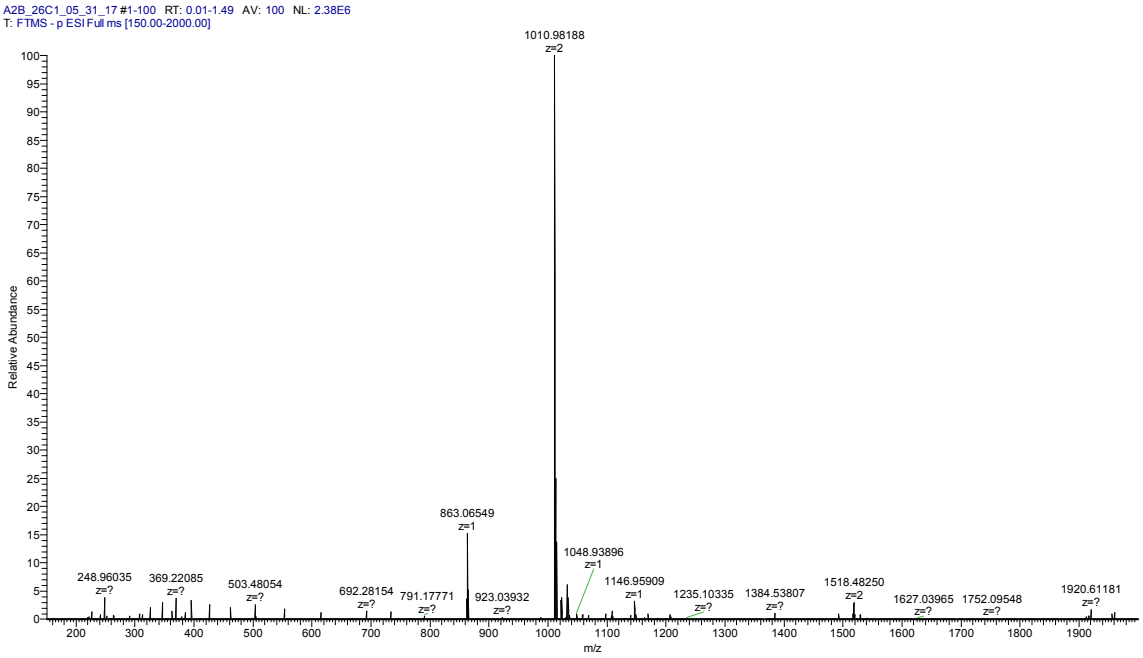


**Figure S20**. High resolution mass spectrum of **$A_2I$-1** (ESI -). MS calculated: 1010.98 [M-H]. MS observed: 1010.98188 [M-H].

## $A_2I$-2

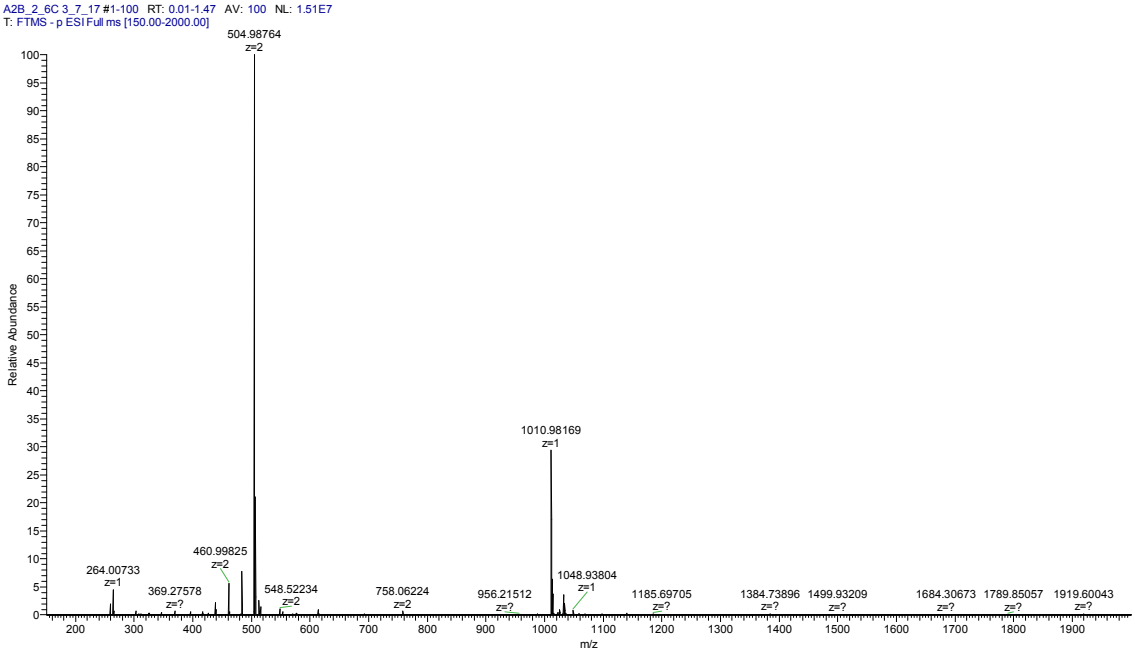


**Figure S21**. High resolution mass spectrum of **$A_2I$-2** (ESI -). MS calculated: 1010.98 [M-H], 504.99 [M-2H]. MS observed: 1010.98169 [M-H], 504.98764 [M-2H].

Background

(a)

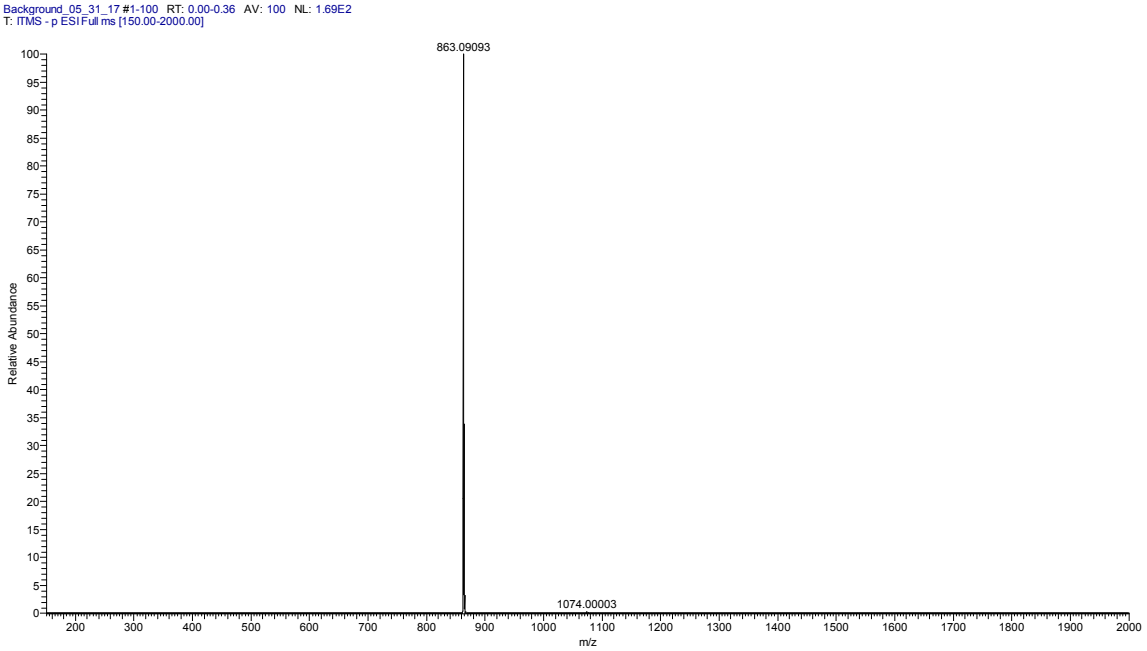


(b)

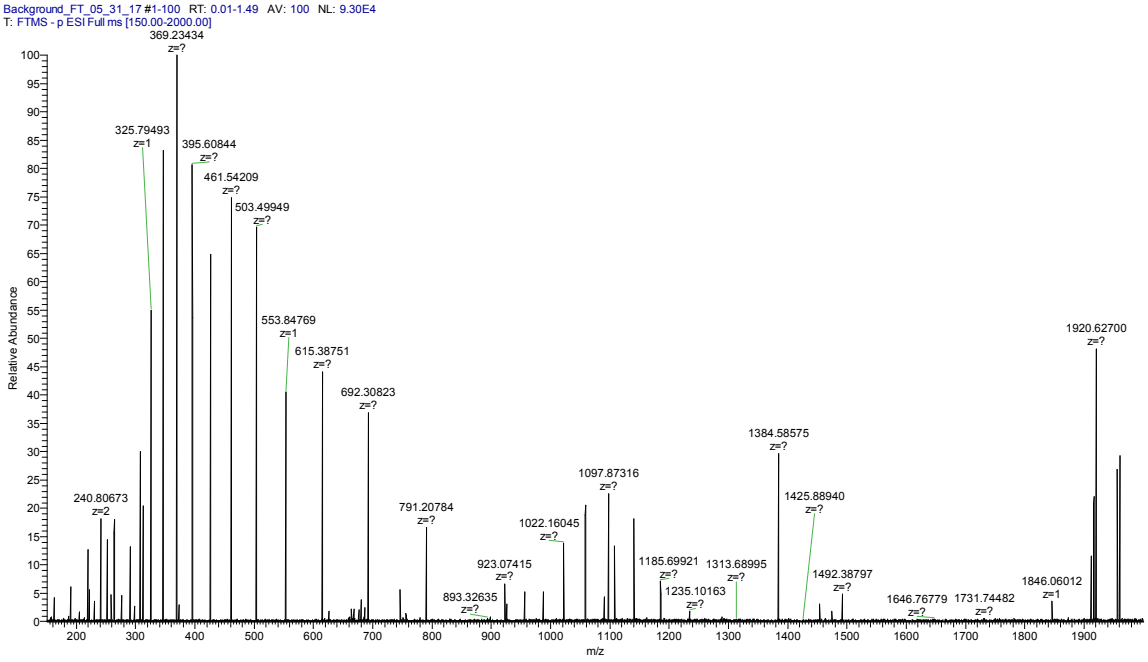


**Figure S22**. (a) Low resolution mass spectrum of background (ESI -). (b) High resolution mass spectrum of background (ESI -).

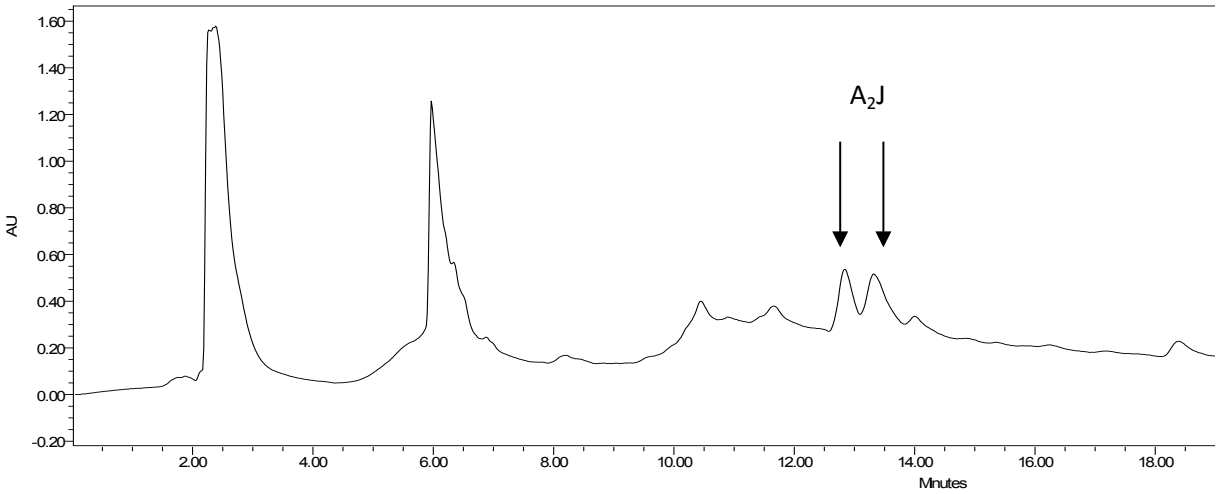


**Figure S23**. Semi-preparative reversed-phase HPLC traces of the purification of **$A_2$J** from a preparative scale DCL. Absorbance measured at 214 nm.

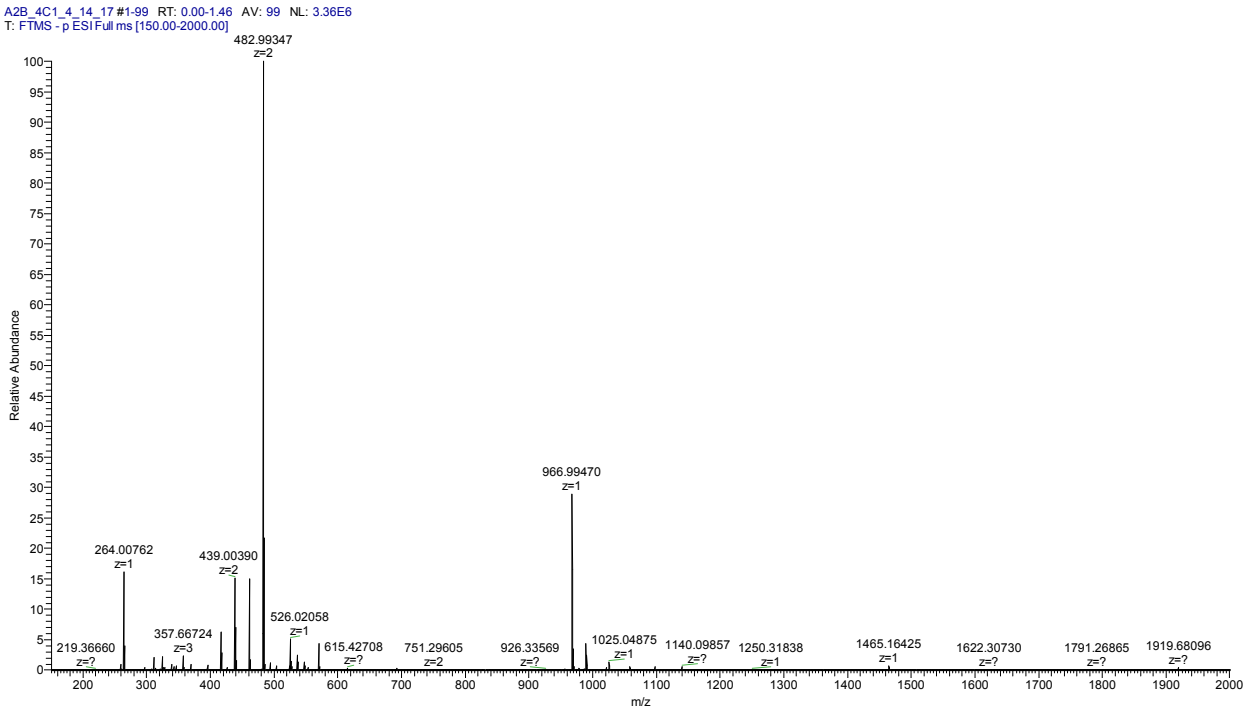


**Figure S24**. High resolution mass spectrum of **$A_2$J-1** (ESI -). MS calculated: 966.99 [M-H], 482.99 [M-2H]. MS observed: 966.99470 [M-H], 482.99347 [M-2H].

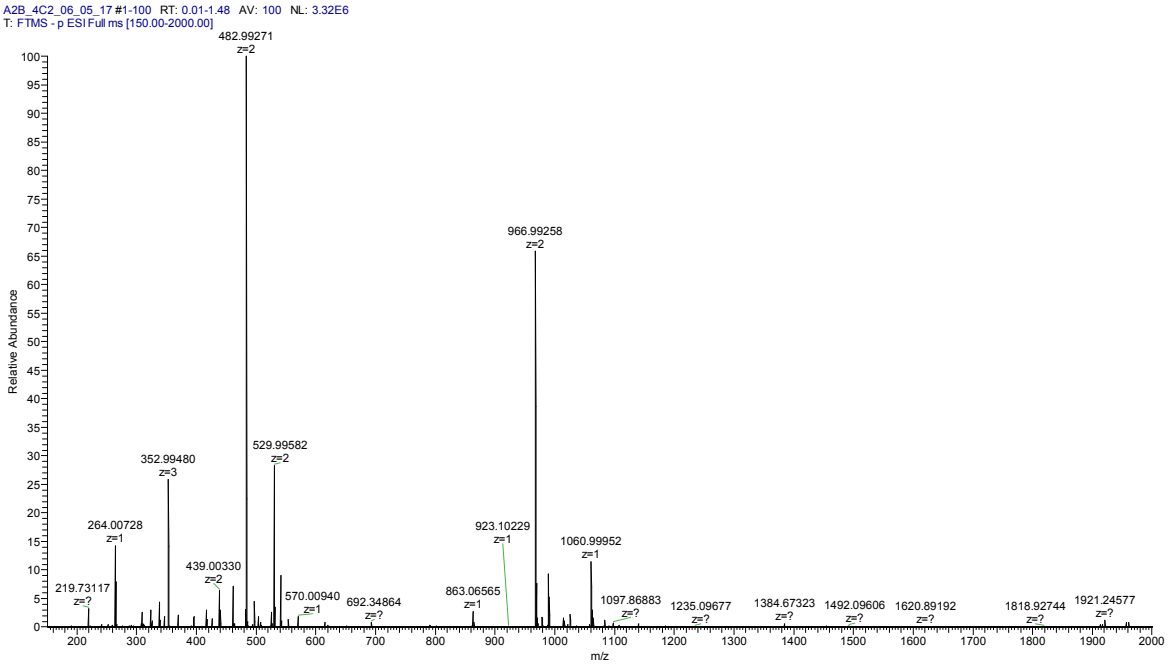


**Figure S25**. High resolution mass spectrum of **$A_2$J-2** (ESI -). MS calculated: 966.99 [M-H], 482.99 [M-2H]. MS observed: 966.99258 [M-H], 482.99271 [M-2H].

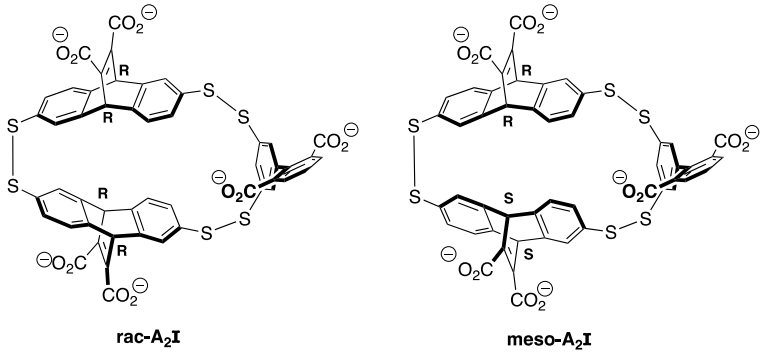


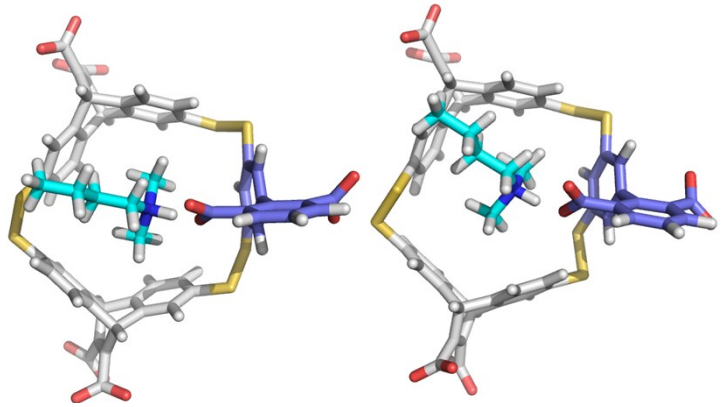

**Figure S26.** Chemdraw structure and computational models of *rac*- and *meso*-**$A_2$I**.

**NMR Characterization of $A_2I$ and $A_2J$**

Structural characterization of **$A_2I$-1**, **$A_2I$-2**, and **$A_2J$-2** was conducted in 50 mM sodium borate-d3 $D_2O$, pH 8.5 with 0.05 mM DSS (as a NMR standard) at room temperature using a Bruker 500 MHz instrument (40 $^oC$, 400 scans each, 3s pre-saturation and water suppression). The $^1H$ NMR spectrum of **$A_2J$-1** was taken in MeOD (40 $^oC$, 900 scans, 3s pre-saturation and water suppression).

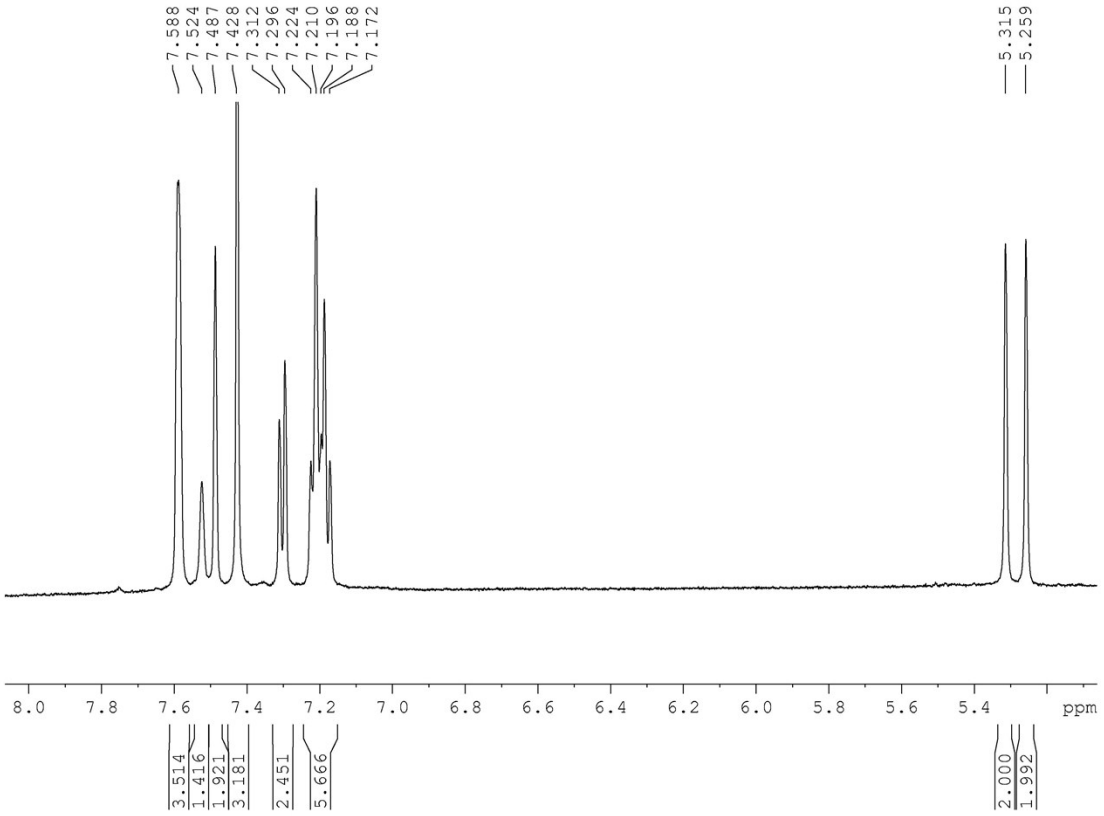


**Figure S27**. $^1H$ NMR spectrum of **$A_2I$-1** in 50 mM sodium borate-$d_3$ $D_2O$, pH 8.5 at room temperature. 7.588 (d, 4H, Ar-H), 7.524 (s, 1H, Ar-H), 7.487 (s, 2H, Ar-H), 7.428 (m, 3H, Ar-H), 7.294-7.312 (d, 2H, Ar-H), 7.172-7.224 (m, 6H, Ar-H), 5.315 (s, 2H, C-H), 5.259 (s, 2H, C-H).

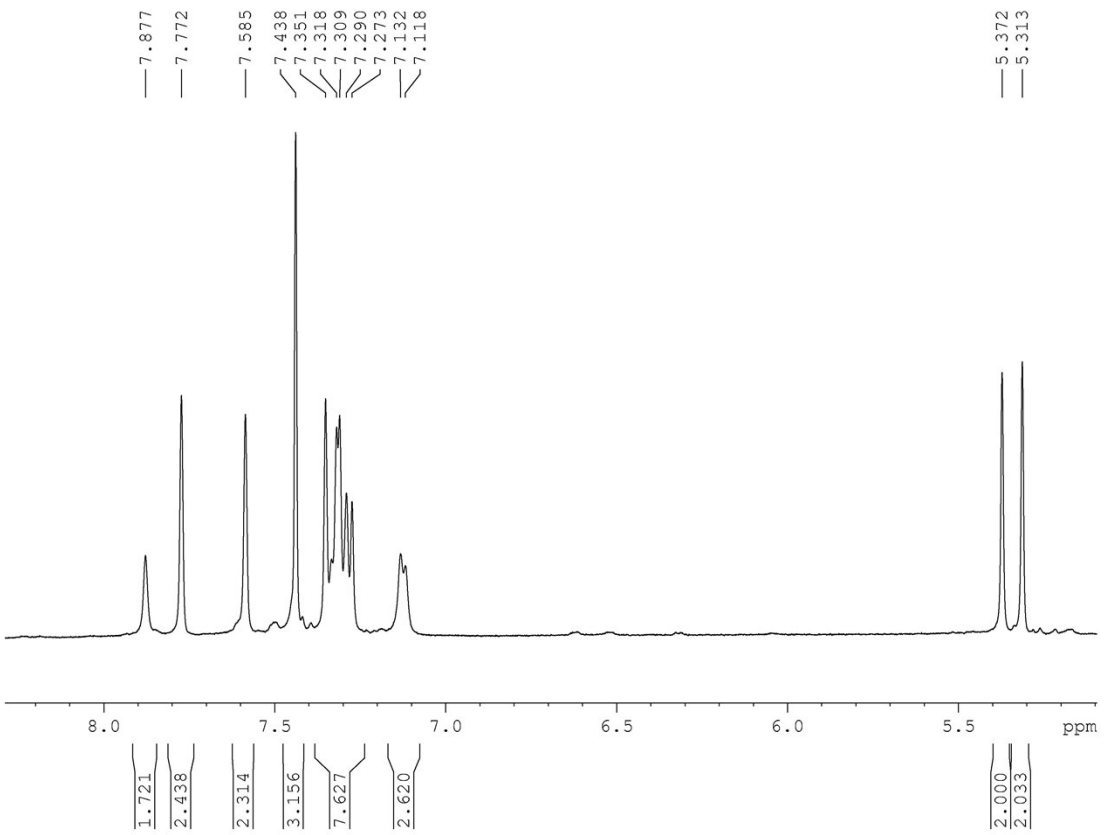


**Figure S28**. $^{1}$H NMR spectrum of **$A_2$I-2** in 50 mM sodium borate-$d_3$ $D_2O$, pH 8.5, 0.05 mM DSS (standard) at room temperature. 7.877 (s, 2H, Ar-H), 7.772 (s, 2H, Ar-H), 7.585 (s, 2H, Ar-H), 7.438 (m, 3H, Ar-H), 7.273-7.7.351 (m, 7H, Ar-H), 7.118-7.132 (d, 2H, Ar-H), 5.372 (s, 2H, C-H), 5.313 (s, 2H, C-H).

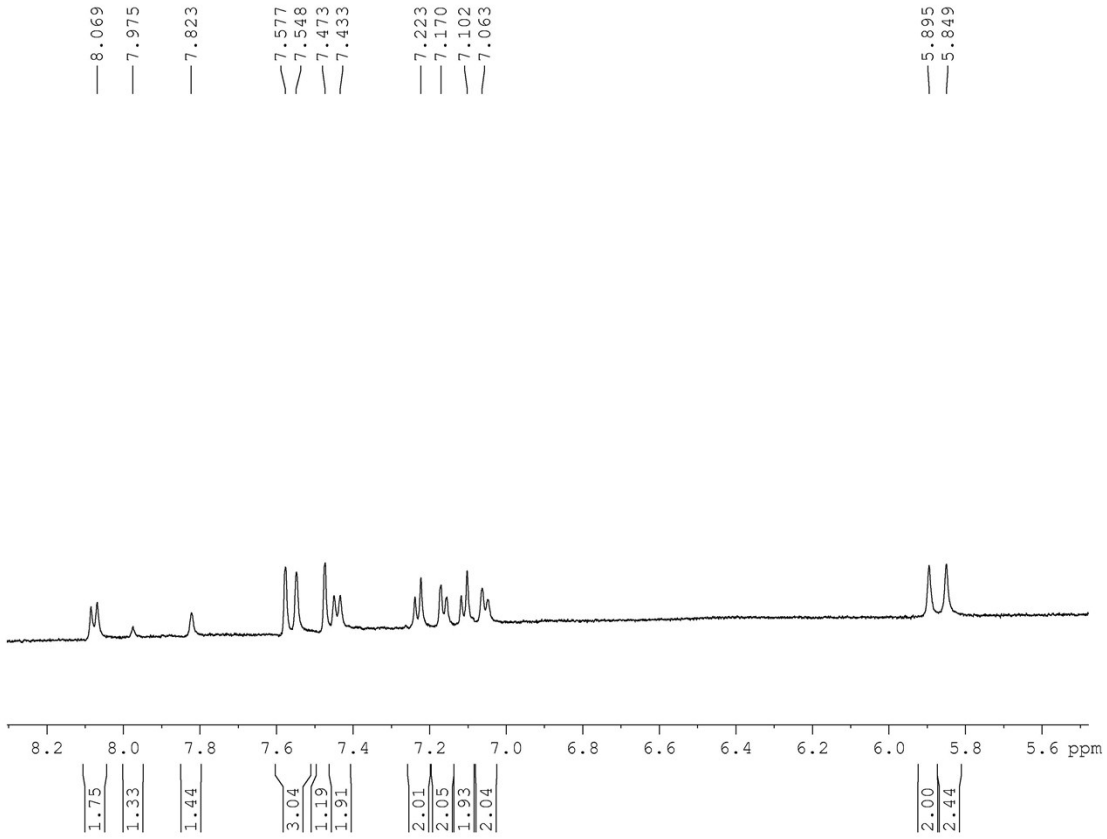


**Figure S29**. $^{1}$H NMR spectrum of **$A_2$J-1** in MeOD at 40 $^{o}$C. 8.069 (d, 2H, Ar-H), 7.975 (s, 1H, Ar-H), 7.823 (s, 2H, Ar-H), 7.548-7.577 (m, 3H, Ar-H), 7.473 (s, 1H, Ar-H), 7.433 (d, 2H, Ar-H), 7.223 (d, 2H, Ar-H), 7.170 (d, 2H, Ar-H), 7.102 (d, 2H, Ar-H), 7.063 (d, 2H, Ar-H), 5.895 (s, 2H, C-H), 5.849 (s, 2H, C-H).

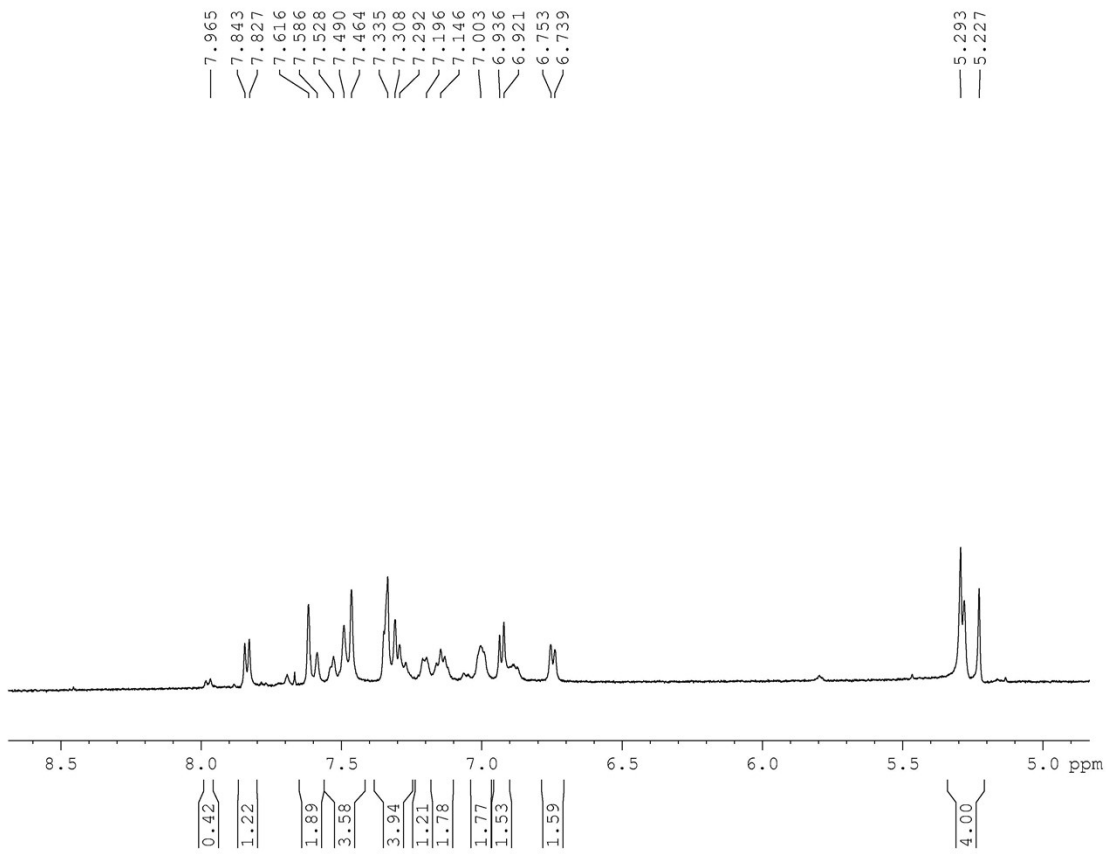


**Figure S30**. $^{1}$H NMR spectrum of **$A_2$J-2** in 50 mM sodium borate-$d_3$ $D_2O$, pH 8.5, 0.05 mM DSS (standard) at 40 $^{o}$C. Due to difficulty in purification, the second isomer could only be obtained in 83% purity, with the impurity presumably arising from HPLC peak overlap with the first isomer. 7.827-7.843 (d, 1H, Ar-H), 7.568-7.616 (m, 2H, Ar-H), 7.464-7.490 (m, 3H, Ar-H), 7.292-7.335 (m, 4 H, Ar-H), 7.196 (d, 1H, Ar-H), 7.146 (d, 2H, Ar-H), 7.003 (d, 2H, Ar-H), 6.921-6.936 (d, 2H, Ar-H), 6.739-6.753 (d, 2H, Ar-H), 5.227-5.293 (m, 4H, C-H).

**Dynamic Combinatorial Libraries**

DCLs were made from stock solutions of the monomers dissolved in 50 mM sodium borate at pH 8.5. Components of the library were mixed to give final monomer concentrations of 1 mM at a total volume of 500 µL. The concentration of methylated butylamine guest was equivalent to the total of concentration of monomer in the library. DCLs were allowed to undergo oxidation and disulfide exchange equilibration for a week. After equilibration, the library was filtered using a 0.22 µm PVDF syringe filter and was analyzed by analytical reversed phase HPLC (Atlantis T3 4.7 x 150 mm 5 µm C-18 column) using by monitoring UV absorbance at 280. An optimized gradient of mobile phases A and B (A: 100% $H_2O$, 10 mM $NH_4OAc$; B: 90% $CH_3CN$, 10% $H_2O$, 10 mM $NH_4OAc$) was used for DCL analysis: (100% A for 1 min; 0 to 20% B over 9 min; 20 to 70% B over 50 min; flush in 100% B for 5 min; flush in 100% A for 5 min).

Analysis of DCLs by LCMS was carried out using an Agilent Rapid Resolution LC-MSD instrument with an online degasser, binary pump, autosampler, heated column compartment, and diode array detector. Separations were achieved using a mobile phase of mobile phases A ($H_2O$, 5 mM $NH_4OAc$) and B (95% $CH_3CN$, 5% $H_2O$, 5 mM $NH_4OAc$) at pH 5.5 on a Zorbax Extend C18 column (4.6 Å 2.1 x 50 mm, 1.8 micron). Negative ion electrospray ionization MS analysis was performed with a single quad mass spectrometer. Data were analyzed using the Agilent ChemStation software. Optimized gradient for A and J library: 3 to 20% B for 1 min; 20 to 40% B for 17 min; 40 to 50% B for 4 min; flush in 100% B for 4 min; flush in 100% A for 4 min. Optimized gradient for A and I library: 3 to 5% B for 1 min; 5 to 40% B for 17 min; 40 to 50% B for 4 min; flush in 100% B for 4 min; flush in 100% A for 4 min.

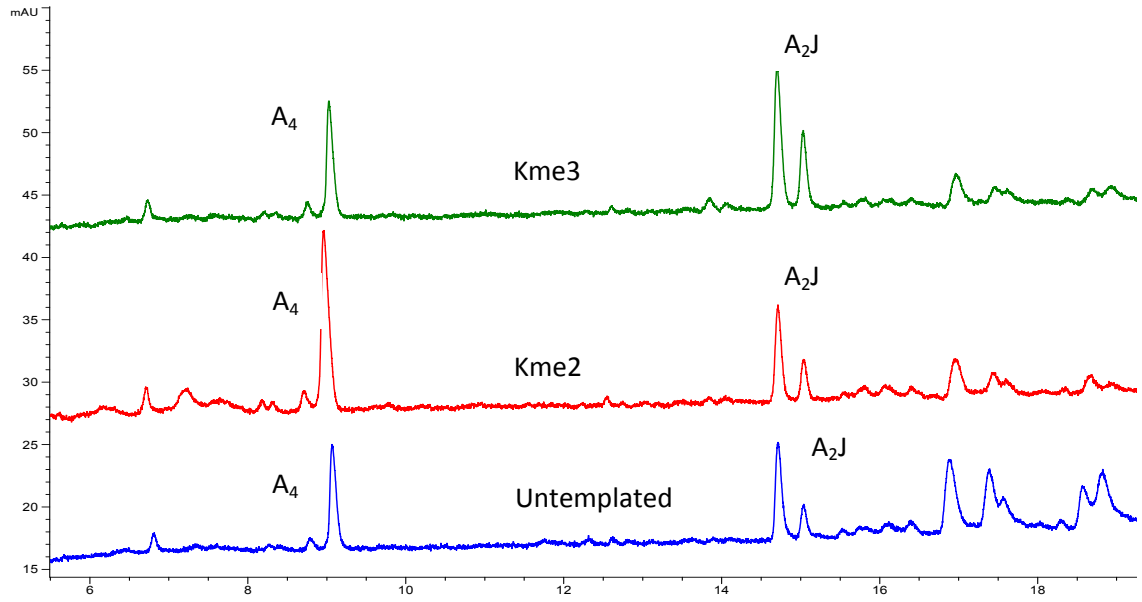


**Figure S31**. Overlaid HPLC traces of DCLs after 7 days containing 1 mM **A**, 1 mM **J**, and 2 mM guest (absorbance at 280 nm). **$A_2$J** is amplified in the presence of Kme2 and Kme3.

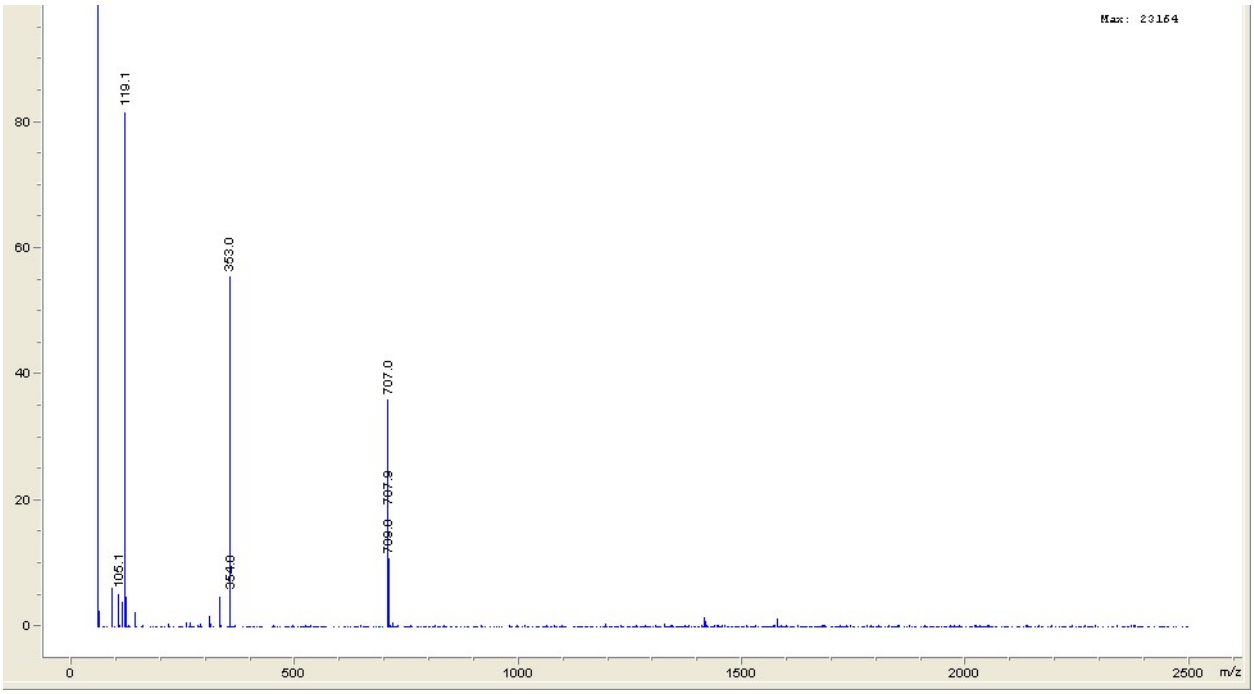


**Figure S32**. LCMS spectrum of peak near 9.1 min corresponding to $\mathbf{A_4}$ (ESI -). MS calculated: 707.0 [M-2H], 353.0 [M-4H]. MS observed: 707.0 [M-2H], 353.0 [M-4H].

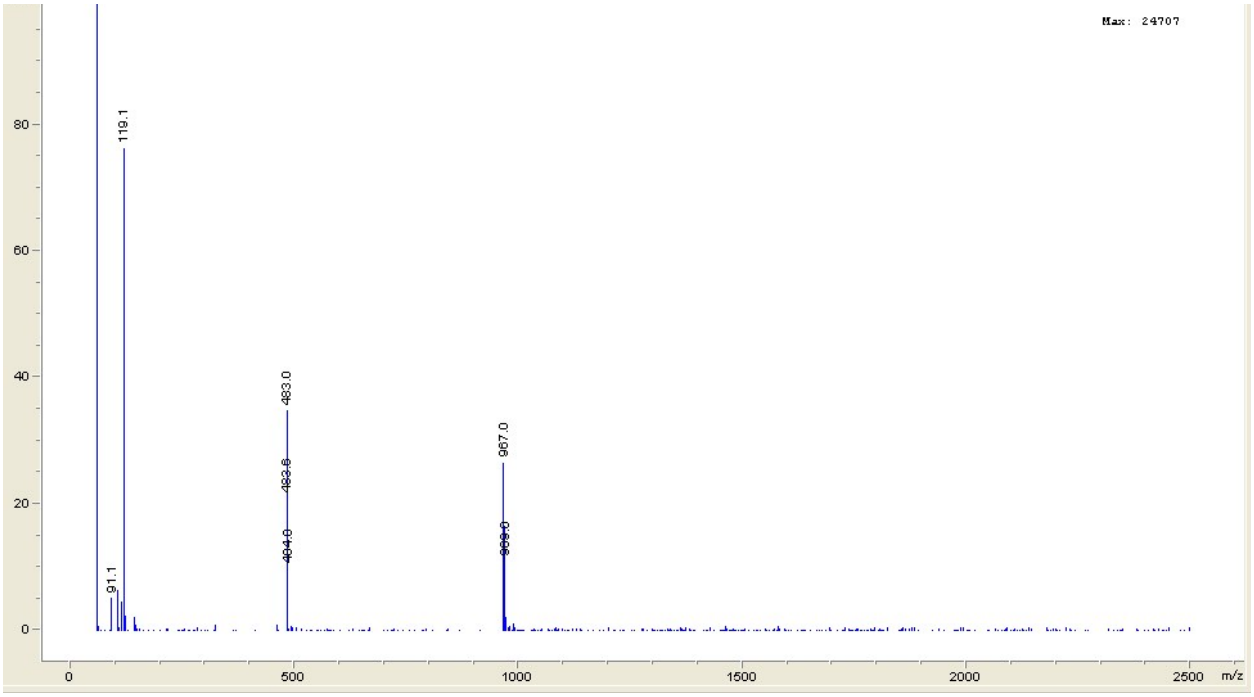


**Figure S33**. LCMS spectrum of peak near 14.7 min corresponding to $\mathbf{A_2J\text{-}1}$ (ESI -). MS calculated: 967.0 [M-H], 483.0 [M-2H]. MS observed: 967.0 [M-H], 483.0 [M-2H].

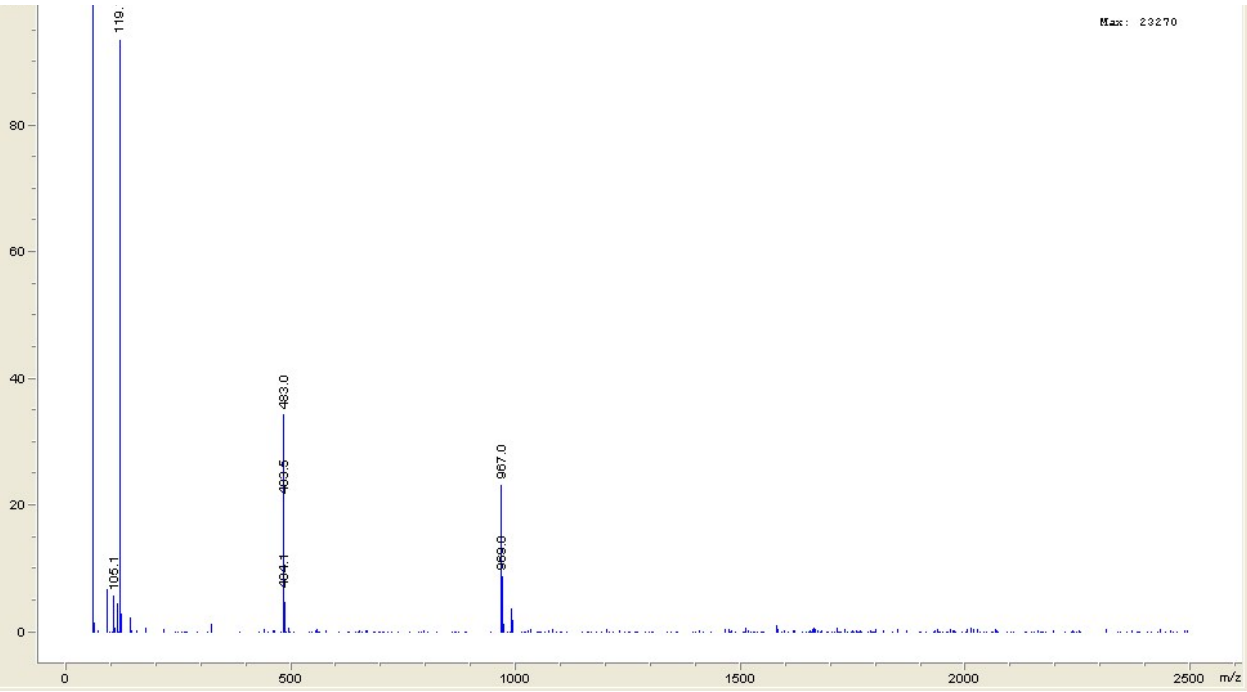


**Figure S34**. LCMS spectrum of peak near 15.0 min corresponding to **$A_2$J-2** (ESI -). MS calculated: 967.0 [M-H], 483.0 [M-2H]. MS observed: 967.0 [M-H], 483.0 [M-2H].

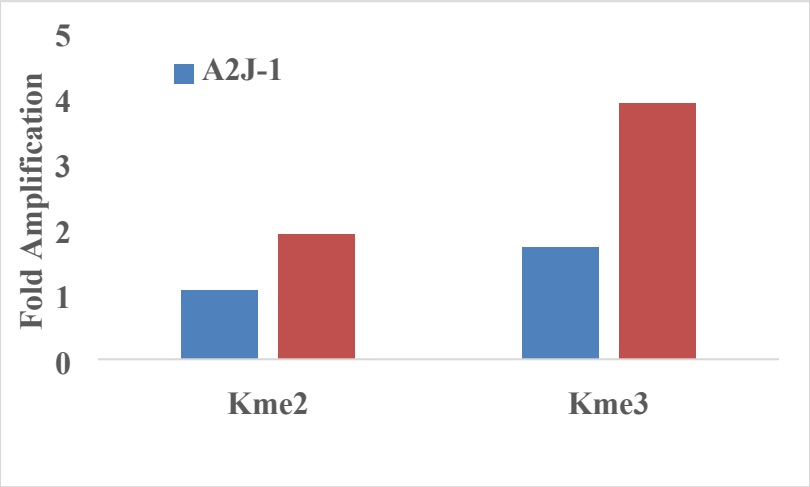


**Figure S35**. Amplification of **$A_2$J-1** and **$A_{2J}$-2** in the presence of Kmex mimics. Fold amplification is defined as the peak area of the guest-templated library divided by the peak area of the untemplated library determined from the HPLC trace at 280 nm.

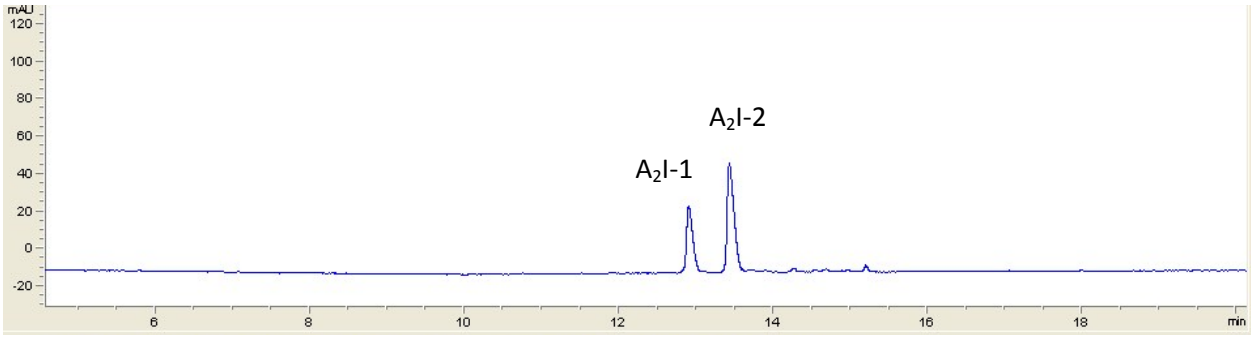


**Figure S36**. LCMS UV trace of DCL after 7 days containing 1 mM **A**, 1 mM **I**, and 2 mM Kme2 guest (absorbance at 280 nm). **$A_2$I-1** and **$A_2$I-2** are amplified in the presence of the Kme2 guest.

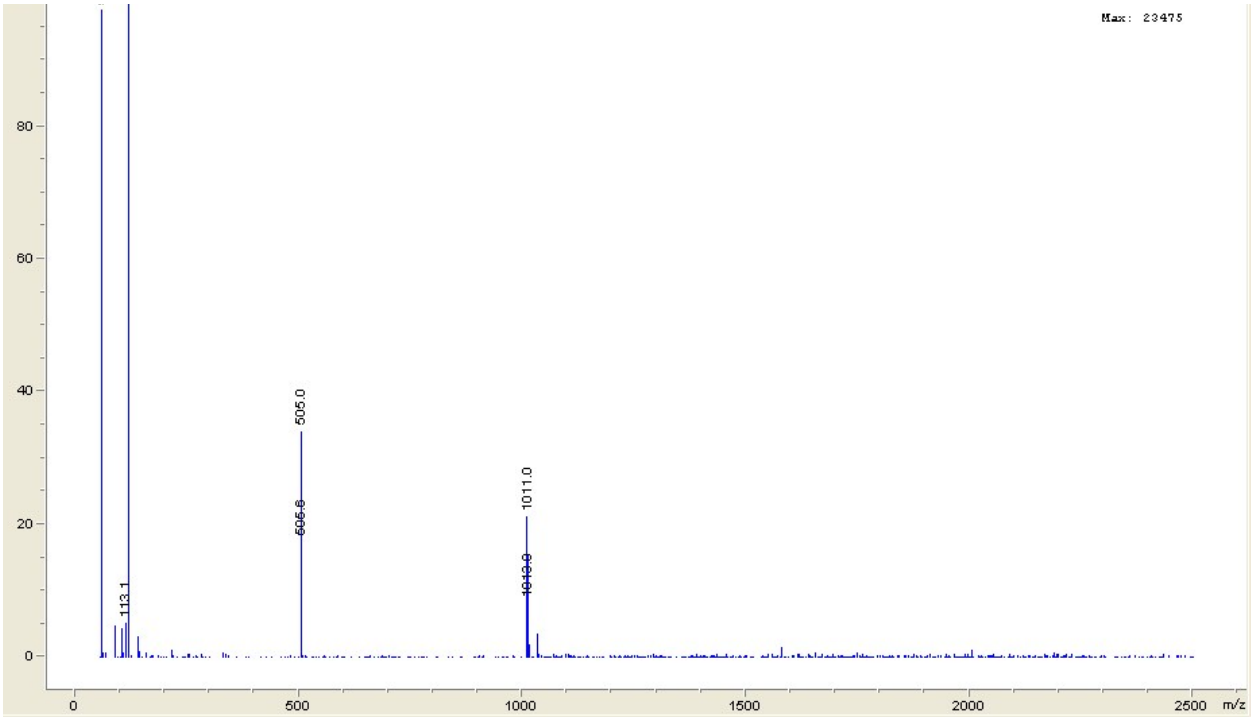


**Figure S37**. LCMS spectrum of peak near 12.9 min corresponding to **$A_2$I-1** (ESI -). MS calculated: 1011.0 [M-H], 505.0 [M-2H]. MS observed: 1011.0 [M-H], 505.0 [M-2H].

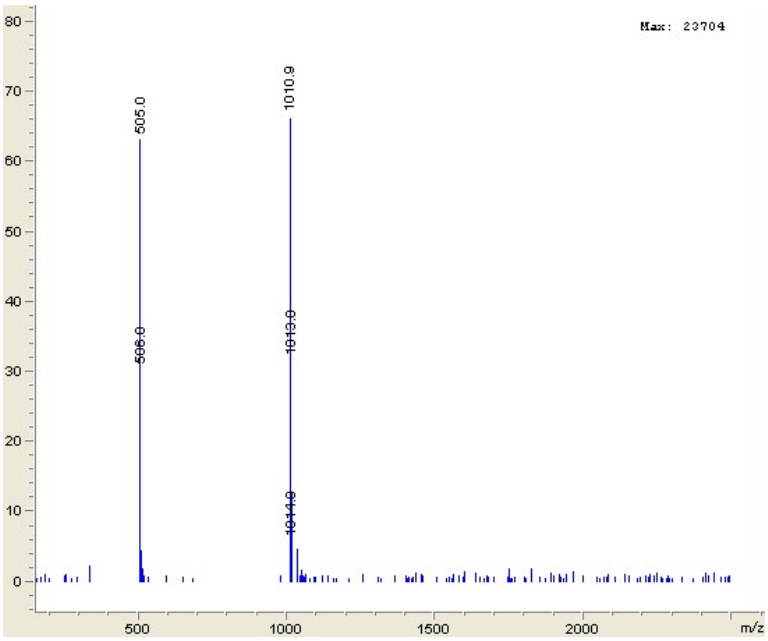


**Figure S38**. LCMS spectrum of peak near 13.4 min corresponding to **$A_2$I-2** (ESI -). MS calculated: 1011.0 [M-H], 505.0 [M-2H]. MS observed: 1010.9 [M-H], 505.0 [M-2H].

**Peptide Synthesis**

Peptides were synthesized on a 0.6 mmol scale via solid-phase peptide synthesis in a peptide synthesis flask using Fmoc protected amino acids. Coupling reagents were HOBt/HBTU in DMF (4 equiv each), with coupling times of 60 min, followed by rinsing with DMF, MeOH, and $CH_2Cl_2$. Deprotection was performed with 20% piperidine in DMF. All peptides were acylated at the N-terminus with a solution of 5% acetic anhydride and 6% 2,6-lutidine in DMF. Cleavage was performed using a cocktail of 95% TFA/2.5% triisopropylsilane/2.5% $H_2O$ for 3 hours. Peptides were purified by semi-preparative reverse-phase HPLC on a C18 column at a flow rate of 4 mL/min. Peptides were purified with a linear gradient of A and B (A: 95% $H_2O$/5% $CH_3CN$ with 0.1% TFA, B: 95% $CH_3CN$/5% $H_2O$ with 0.1 % TFA).

Methylated peptides were synthesized with 2 equivalents of Fmoc-Lys$(Me)_2$-OH HCl or Fmoc-Lys(Me,Boc)-OH purchased from EMP Millipore and coupled for 5 hours. The trimethyllysine containing peptides were synthesized by reacting corresponding dimethylated peptides (0.06 mmol scale) prior to cleavage from the resin with MTBD (7-Methyl-1,5,7-triazabicyclo[4.4.0]dec-5-ene, 10 equiv.) and methyl iodide (10 equiv.) in DMF (5 mL) for 5 hours with bubbling nitrogen in a peptide flask. After washing the resin with DMF and $CH_2Cl_2$ and drying, the peptide was cleaved as normal.

Peptides:

H3K9: Ac-WGGGQTARKSTG-$NH_2$

H3K9me: Ac-WGGGQTARKmeSTG -$NH_2$

H3K9$me_2$: Ac-WGGGQTARKme2STG-$NH_2$

H3K9$me_3$: Ac-WGGGQTARKme3STG-$NH_2$

Kme2GGY: Ac-Kme2GGY-$NH_2$

Kme3GGY: Ac-Kme3GGY-$NH_2$

## H3K9

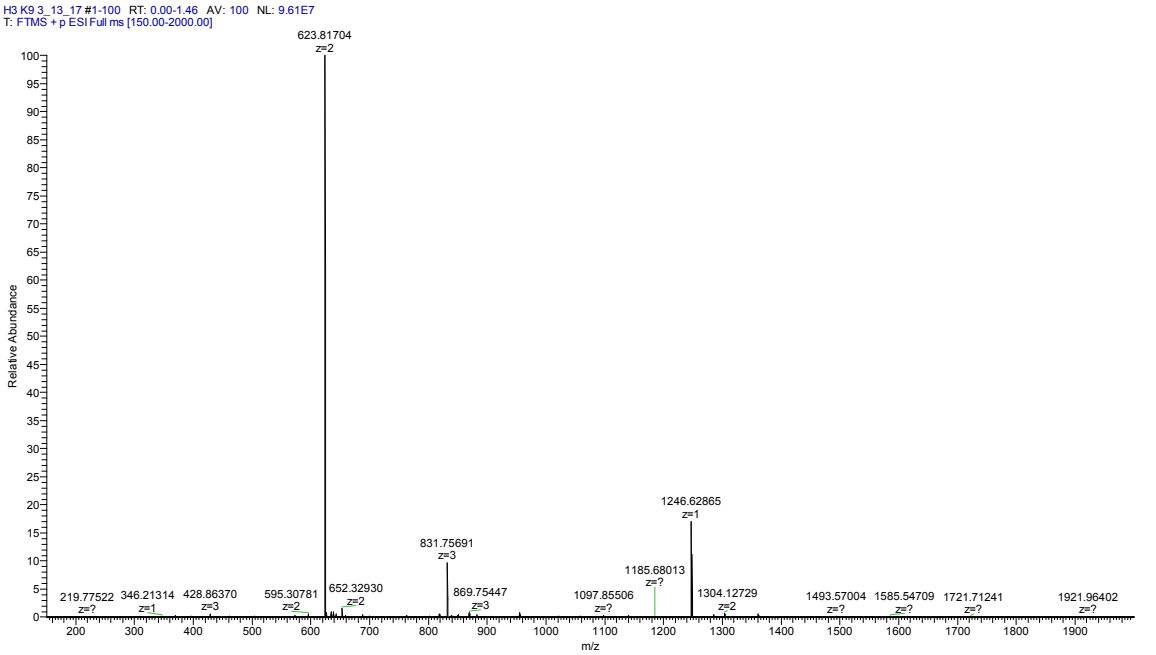


**Figure S39**. High resolution mass spectrum of H3K9 (ESI +). MS calculated: 1246.63 [M+H], 623.82 [M+2H]. MS observed: 1246.62865 [M+H], 623.81704 [M+2H].

## H3K9me

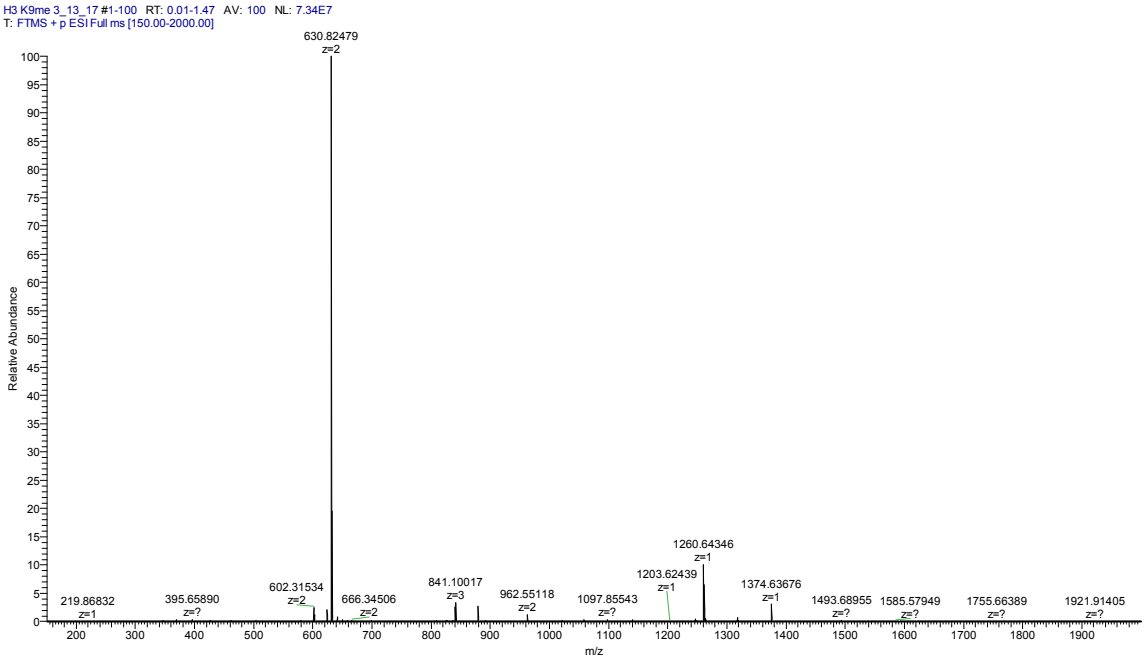


**Figure S40**. High resolution mass spectrum of H3K9me (ESI +). MS calculated: 1260.64 [M+H], 630.83 [M+2H]. MS observed: 1260.64346 [M+H], 630.82479 [M+2H].

## H3K9me2

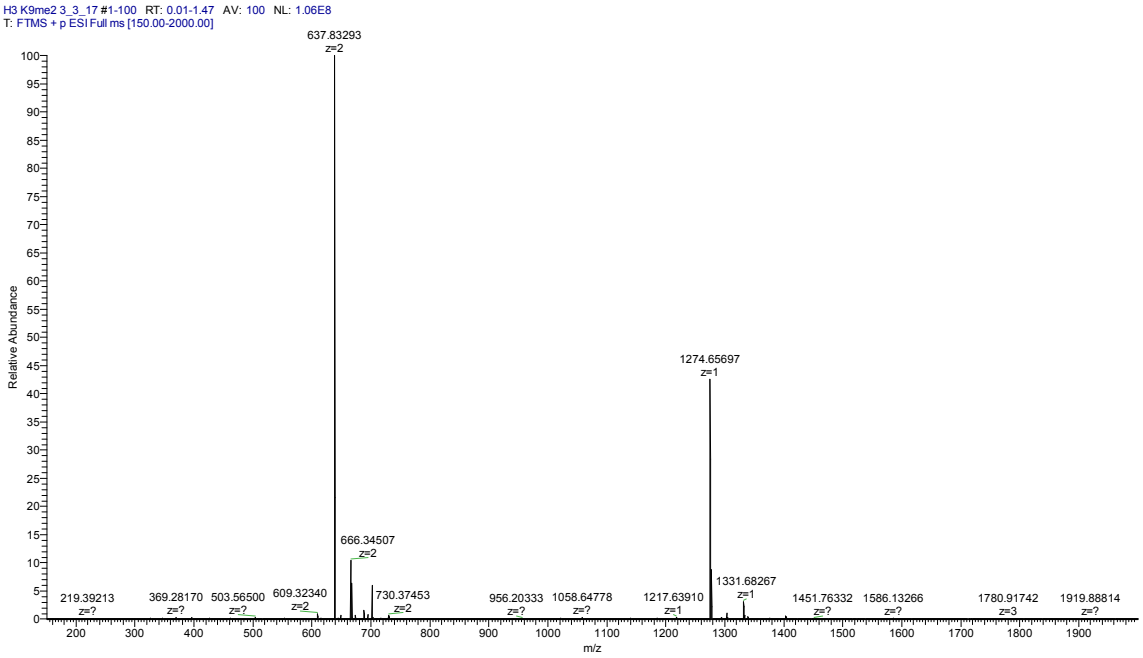


**Figure S41**. High resolution mass spectrum of H3K9me2 (ESI +). MS calculated: 1274.66 [M+H], 637.83 [M+2H]. MS observed: 1274.65697 [M+H], 637.83293 [M+2H].

## H3K9me3

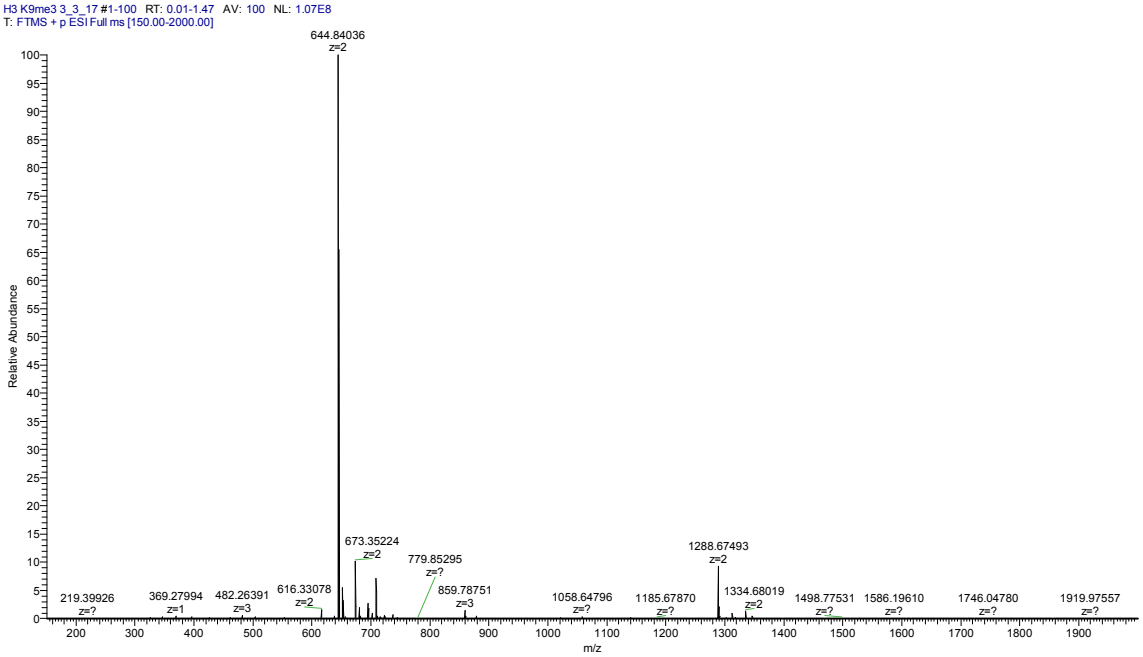


**Figure S42**. High resolution mass spectrum of H3K9me3 (ESI +). MS calculated: 1288.68 [M+H], 644.84036 [M+2H]. MS observed: 1288.67493 [M+H], 644.84 [M+2H].

## Kme2GGY

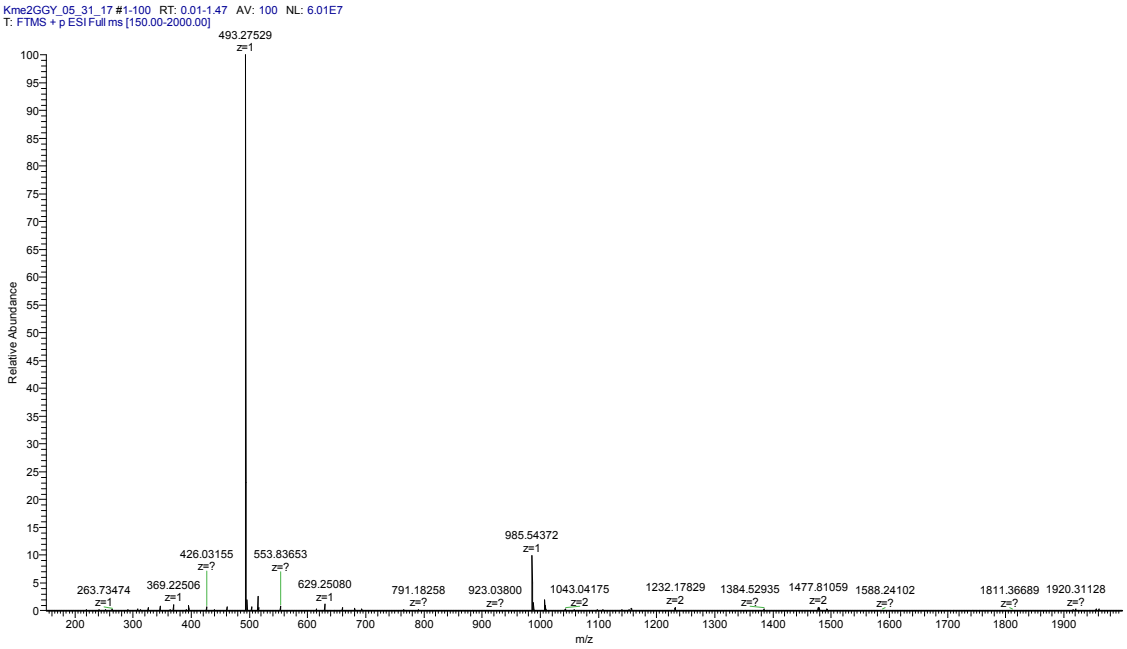


**Figure S43**. High resolution mass spectrum of Kme2GGY (ESI +). MS calculated: 492.28 [M+H], 985.55 [2M+H]. MS observed: 493.27529 [M+H], 985.54372 [2M+H].

## Kme3GGY

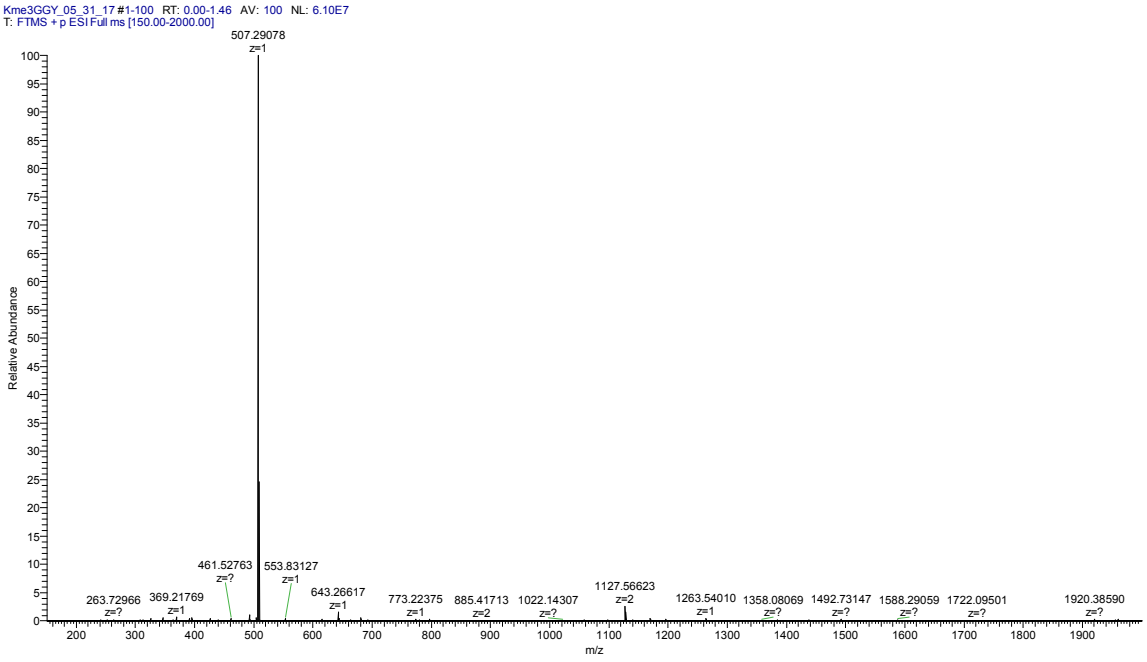


**Figure S44**. High resolution mass spectrum of Kme3GGY (ESI +). MS calculated: 507.29 [M+H]. MS observed: 507.29078 [M+H].

**Extinction Coefficient Determination for $A_2I$ and $A_2J$.**

Receptors were purified using reversed phase-HPLC with 10 mM $NH_4OAc$ as the mobile phase additive. After purification, they were lyophilized for five days to remove volatile $NH_4OAc$ salts. The dried compound was then dissolved in anhydrous methanol and filtered using a 0.33 µm filter to remove any remaining salts. Methanol was evaporated and the receptors were further dried under vacuum. The mass was accurately determined, and a stock solution of receptor (1.07 mM for **$A_2I$** and 0.607 mM for **$A_2J$**) in 10 mM sodium borate buffer, pH 8.5 was prepared. The stock solution was serially diluted (80:20, receptor: buffer) to give 10 to 12 concentrations. The absorbance at 315 nm or 300 nm was measured for each concentration, which was then plotted against the concentration. The extinction coefficient of the receptors was determined from the slope of the line of regression using Beer's law and was found to be 401.5 $M^{-1}cm^{-1}$ for **$A_2I$** and 1,400 $M^{-1}cm^{-1}$ for **$A_2J$**.

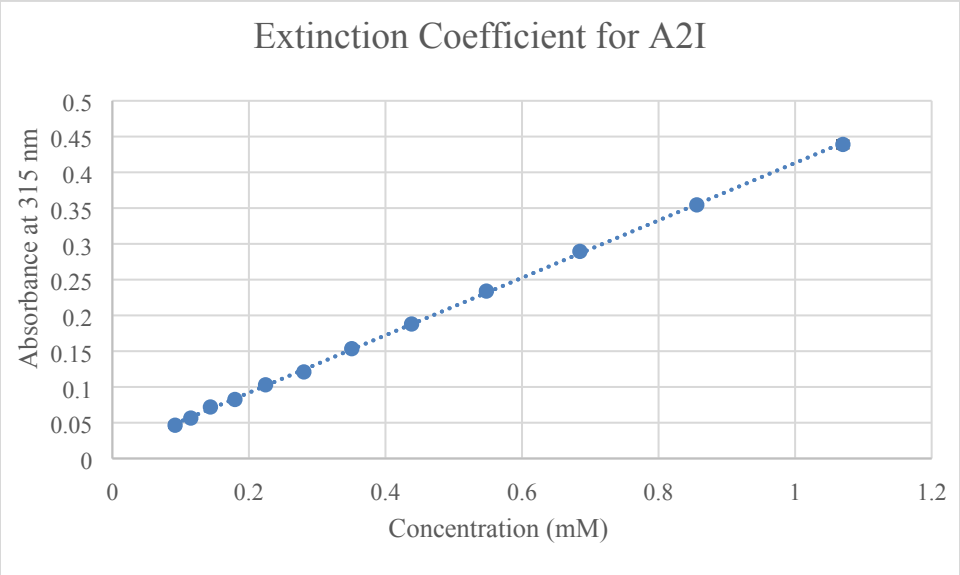


**Figure S45**. Extinction coefficient determination of **$A_2I$** from the slope of the line of regression.

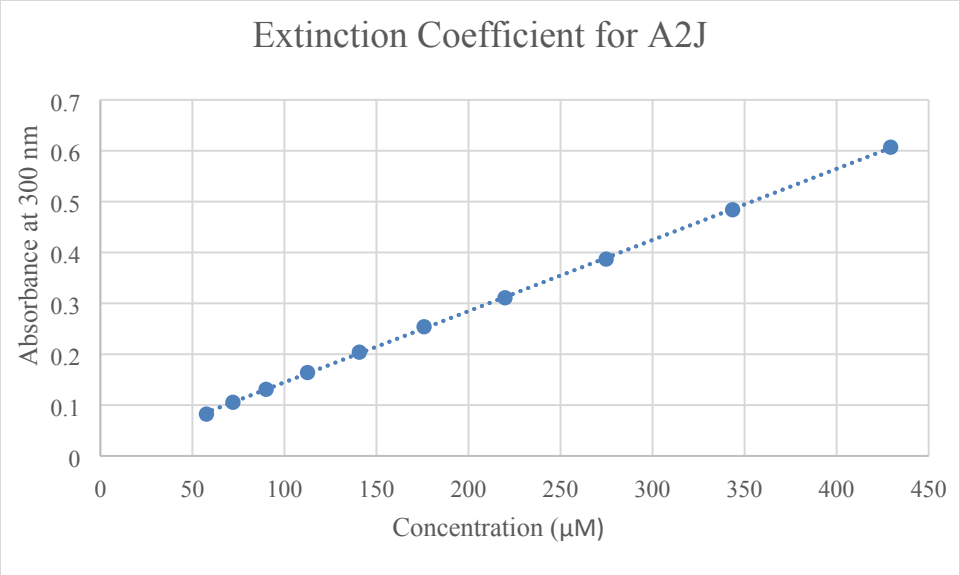


**Figure S46**. Extinction coefficient determination of $\mathbf{A_2J}$ from the slope of the line of regression.

**NMR Analysis of Binding to Kme2 and Kme3**

NMR binding experiments were conducted to characterize the mode of binding of **$A_2$I-2** to a Kme2GGY and Kme3GGY peptide. Experiments were carried out in 50 mM sodium borate-d3 $D_2O$, pH 8.5 with 0.05 mM DSS (as an internal standard) at room temperature and 40 $^oC$ using a Bruker 500 MHz instrument (400 scans each, 3s pre-saturation and water suppression). suppression). Stock solutions of receptor and peptide were prepared in the NMR buffer (the concentrations of each were determined using a NanoDrop™). Samples were prepared by measuring out aliquots from the stock and diluting with buffer to the appropriate concentration.

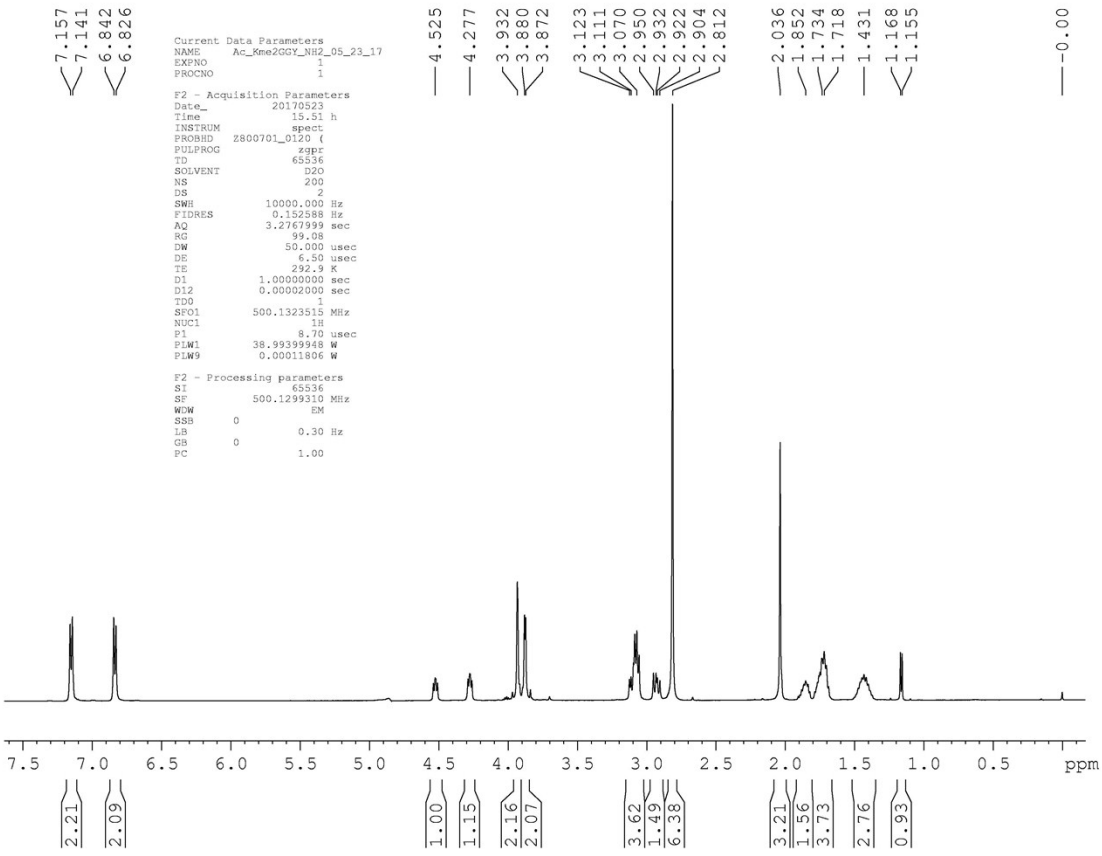


**Figure S47**. $^1H$ NMR spectrum of Kme2GGY (5.6 mM) alone in 50 mM sodium borate-$d_3$ $D_2O$, pH 8.5, 0.05 mM DSS (standard) at room temperature.

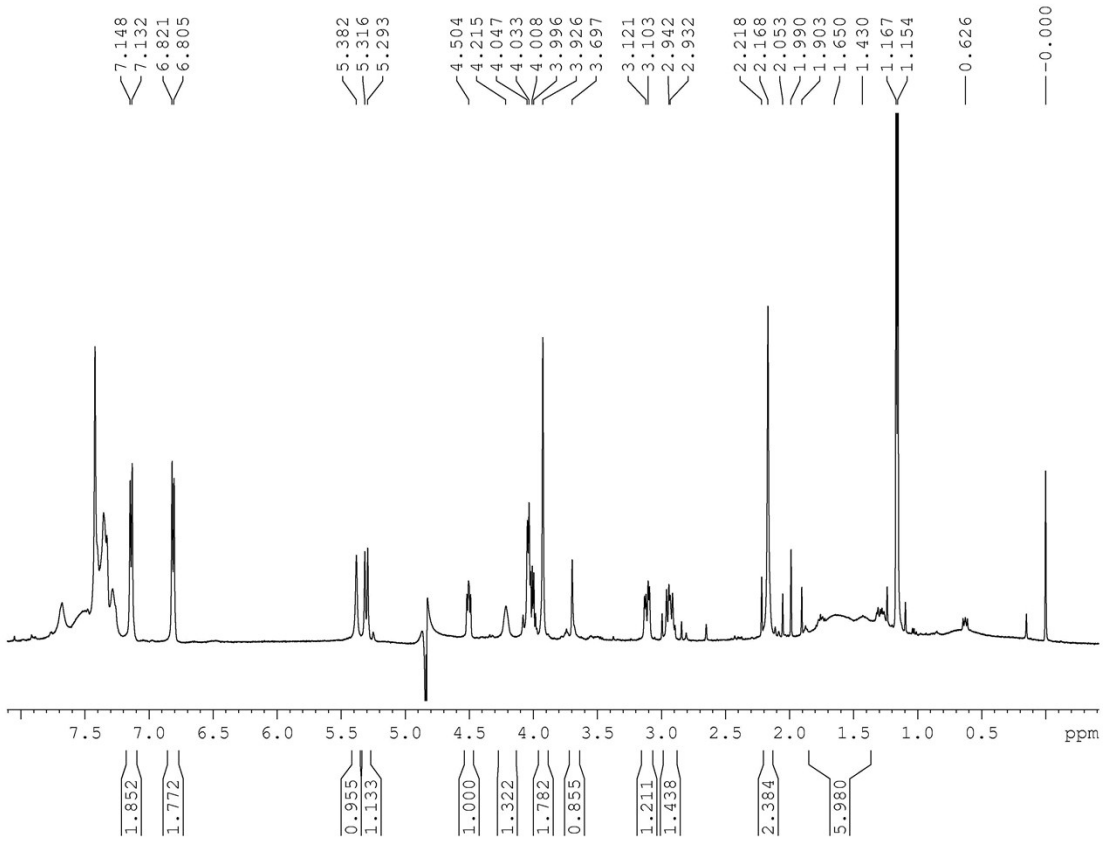


**Figure S48**. $^{1}$H NMR spectrum of **$A_2$I-2** (0.75 mM) with Kme2GGY (0.70 mM) in 50 mM sodium borate-$d_3$ $D_2O$, pH 8.5 at room temperature.

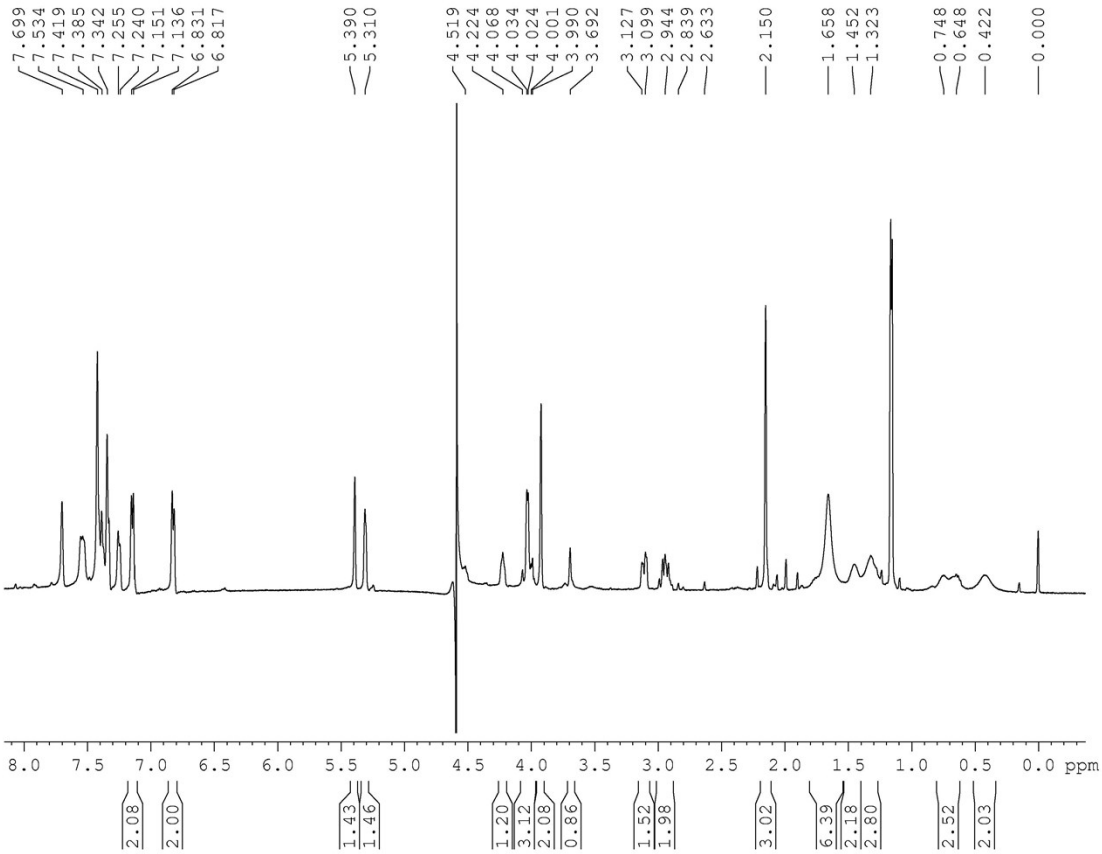


**Figure S49**. $^{1}$H NMR spectrum of **$A_2$I-2** (0.75 mM) with Kme2GGY (0.70 mM) in 50 mM sodium borate-$d_3$ $D_2O$, pH 8.5 at 40 $^{o}$C.

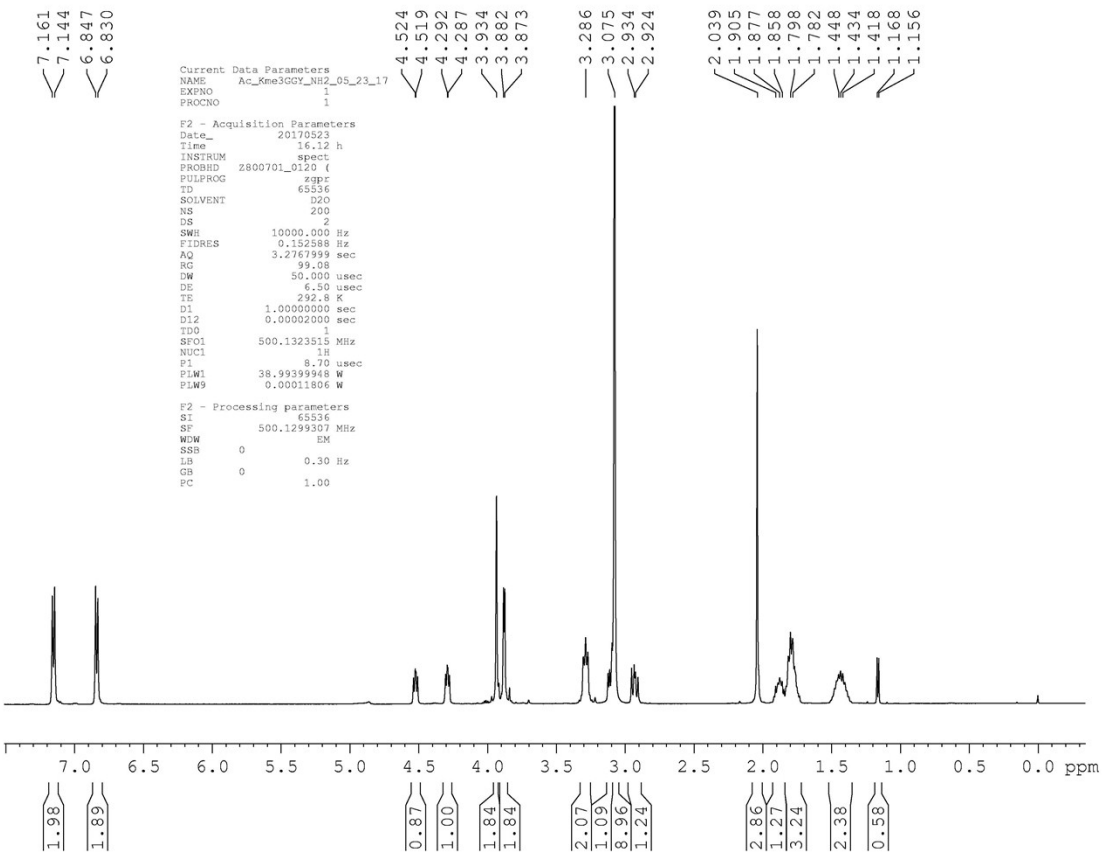


**Figure S50**. $^{1}$H NMR spectrum of Kme3GGY (7.6 mM) alone in 50 mM sodium borate-$d_3$ $D_2O$, pH 8.5, 0.05 mM DSS (standard) at room temperature.

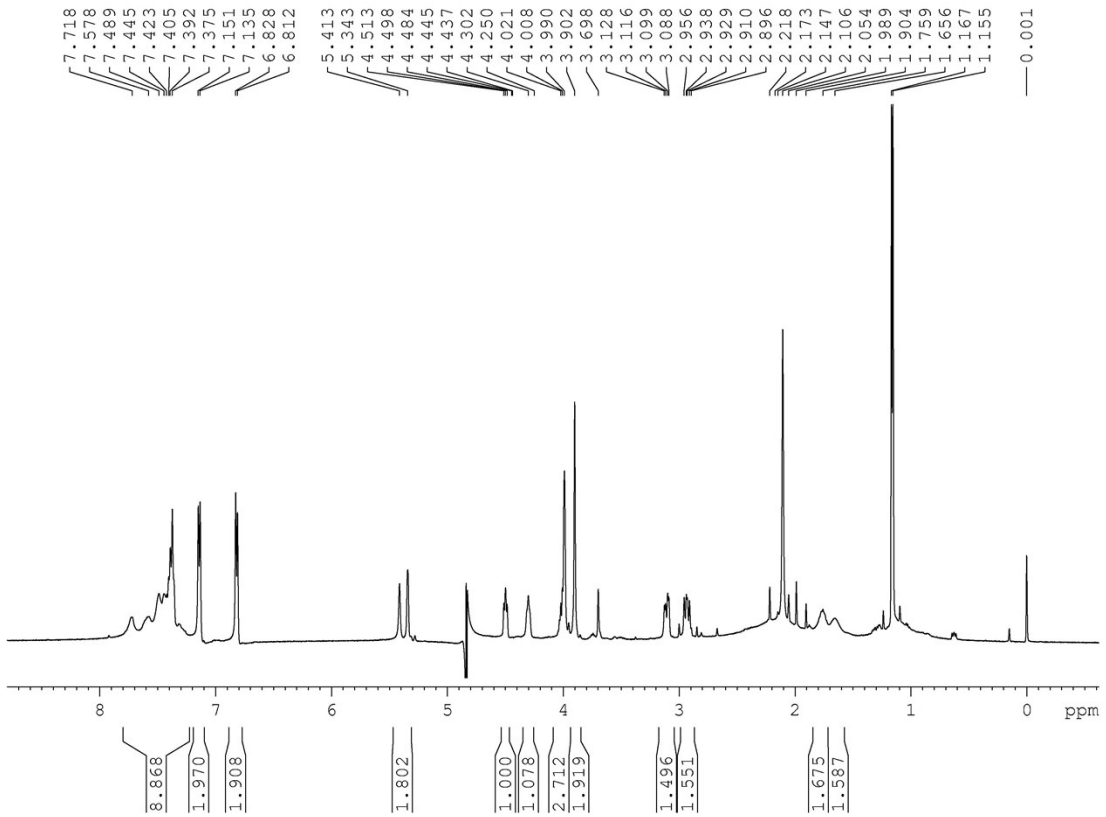


**Figure S51**. $^{1}H$ NMR spectrum of **$A_2$I-2** (0.75 mM) with Kme3GGY (0.70 mM) in 50 mM sodium borate-$d_3$ $D_2O$, pH 8.5 at room temperature.

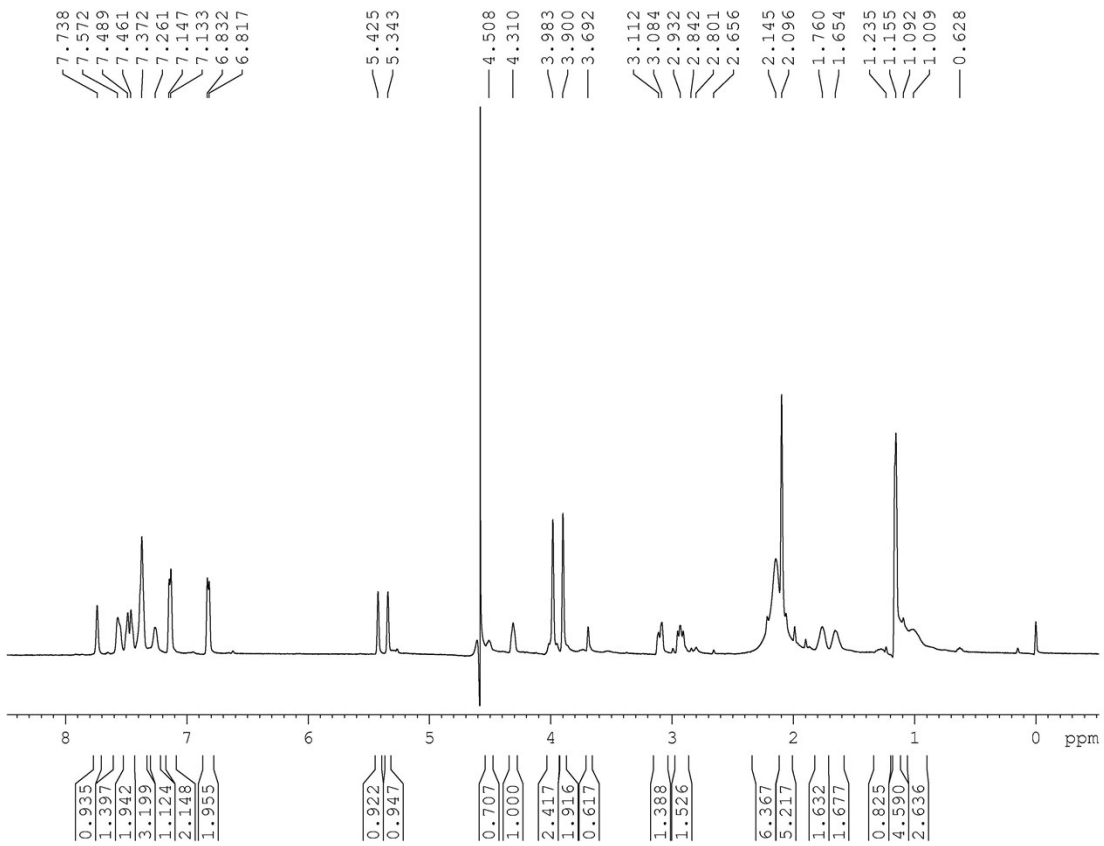


**Figure S52**. $^{1}$H NMR spectrum of **$A_2$I-2** (0.75 mM) with Kme3GGY (0.70 mM) in 50 mM sodium borate-$d_3$ $D_2O$, pH 8.5 at 40 $^{o}$C.

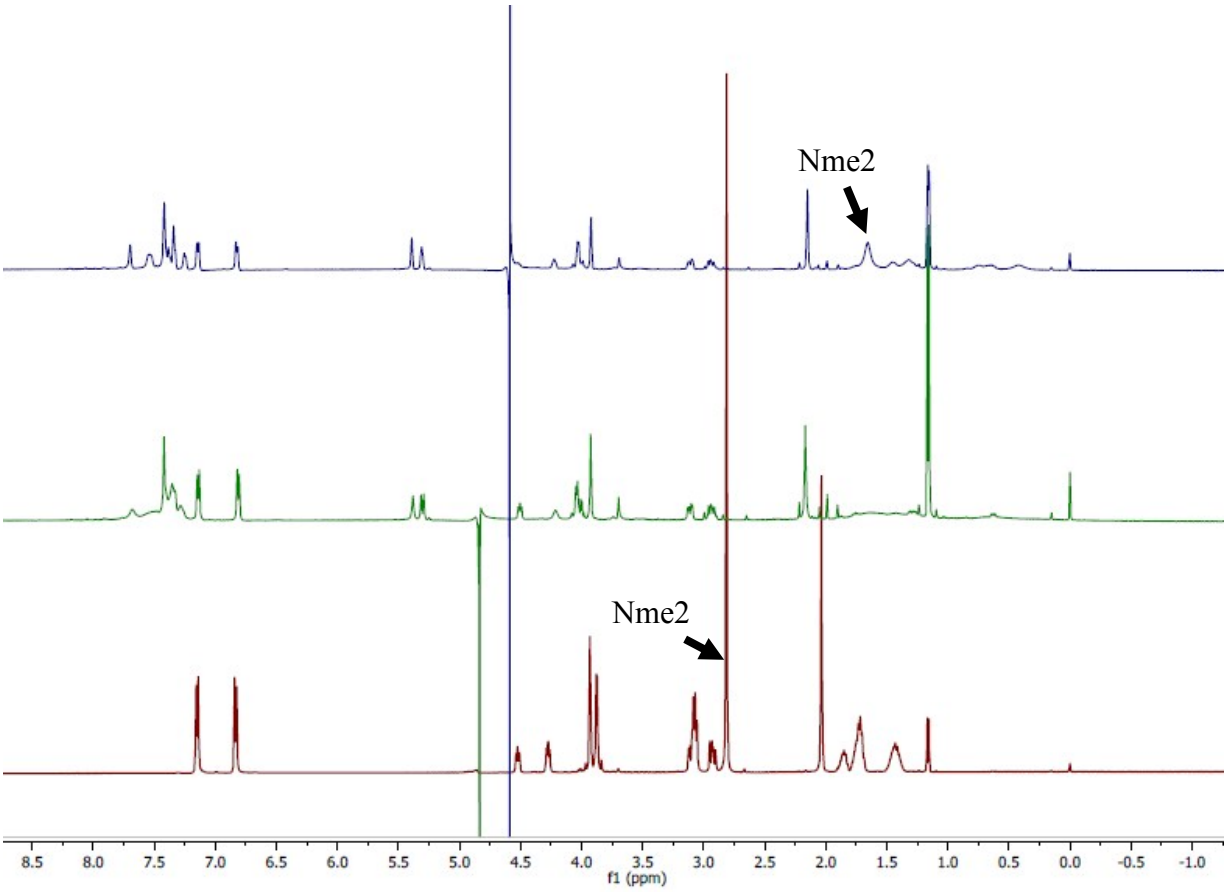


**Figure S53**. NMR analysis of **$A_2$I-2** binding to Kme2GGY. Red: $^1$H NMR spectrum of Kme2GGY (5.6 mM) alone in 50 mM sodium borate-$d_3$ $D_2O$, pH 8.5, 0.05 mM DSS (standard) at room temperature. Green: $^1$H NMR spectrum of **$A_2$I-2** (0.75 mM) with Kme2GGY (0.70 mM) in 50 mM sodium borate-$d_3$ $D_2O$, pH 8.5 at room temperature. Blue: $^1$H NMR spectrum of **$A_2$I-2** (0.75 mM) with Kme2GGY (0.70 mM) in 50 mM sodium borate-$d_3$ $D_2O$, pH 8.5 at 40 $^o$C.

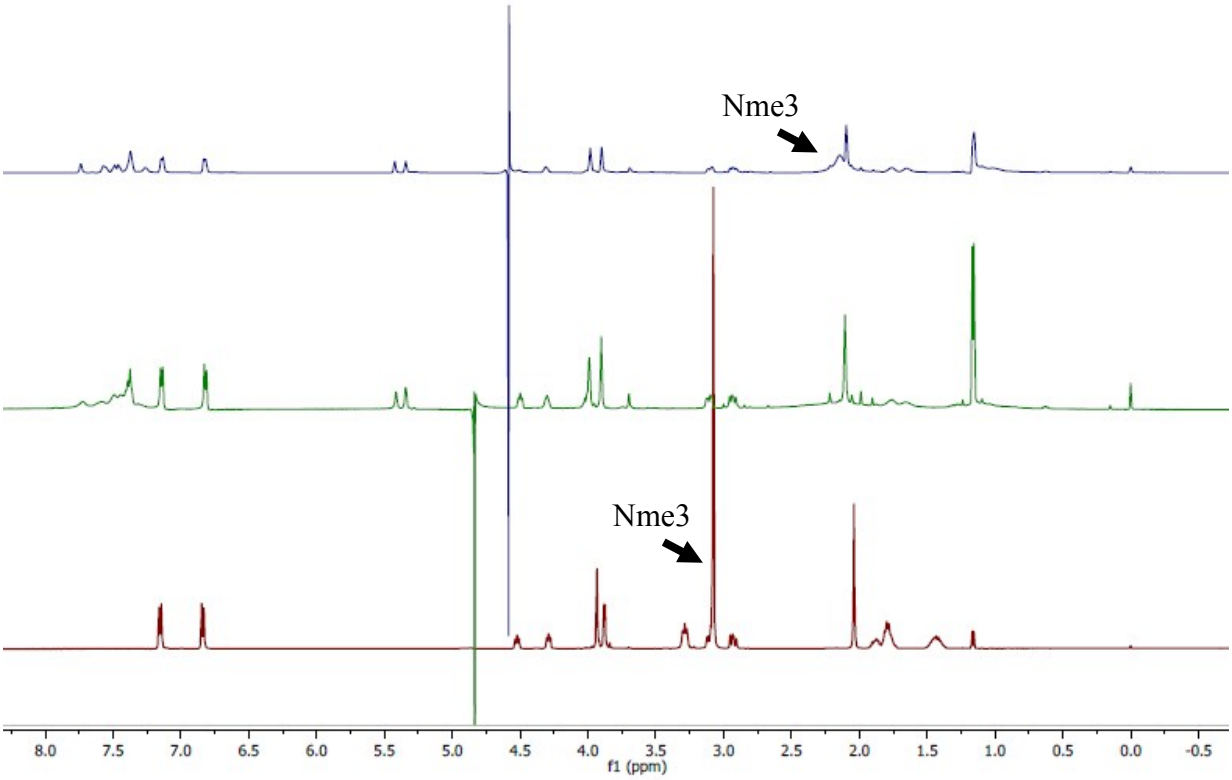


**Figure S54**. NMR analysis of **$A_2$I-2** binding to Kme3GGY. Red: $^1$H NMR spectrum of Kme3GGY (7.6 mM) alone in 50 mM sodium borate-$d_3$ $D_2O$, pH 8.5, 0.05 mM DSS (standard) at room temperature. Green: $^1$H NMR spectrum of **$A_2$I-2** (0.75 mM) with Kme3GGY (0.70 mM) in 50 mM sodium borate-$d_3$ $D_2O$, pH 8.5 at room temperature. Blue: $^1$H NMR spectrum of **$A_2$I-2** (0.75 mM) with Kme3GGY (0.70 mM) in 50 mM sodium borate-$d_3$ $D_2O$, pH 8.5 at 40 $^o$C.

**Isothermal Titration Calorimetry**

ITC binding experiments were conducted using a Microcal AutoITC200. Titrations were performed at 25 °C in 10 mM sodium borate buffer at pH 8.5. The concentration of receptor was determined by measuring the UV-Vis at 300 nm or 315 nm, using a NanoDrop2000 with a xenon flash lamp, 2048 element linear silicon CCD array detector, and 1 mm path length. Solutions of 0.2–1.3 mM of peptide were titrated into a 20–91 μM solution of receptor, using 2.0 μL increments every 3 min. Heats of dilution were taken as the last 3-4 points and subtracted before fitting. Binding curves were prepared with Origin 7 software using 1-site binding models.

It should be noted that while a 1-site binding model is used to fit the ITC data, N-values that deviate from 1 are observed in many situations. These deviations in N-value can be attributed to the error in the concentration determination of the receptors that arises from the difficulty in determining accurate extinction coefficients by mass. Efforts to fit any of the data to a 2-site binding model were not successful. Furthermore, NMR is consistent with 1-site binding.

**Table S1**. Summary of ITC data from using a one-site binding model. Values represent an average of 3 measurements. Errors are from standard deviation from three separate runs.

| Entry | Receptor | Peptide | Charge | $K_d$[b] | SF[d] | ΔG[c] | ΔH[c] | TΔS[c] |
|---|---|---|---|---|---|---|---|---|
| 1[a] | $A_2B$ | H3 K9me3 | +2 | 2.6 ± 0.1 | - | -7.63 ± 0.03 | - | - |
| 2[a] | $A_2B$ | H3 K9me2 | +2 | 6.3 ± 0.3 | 2.4 | -7.10 ± 0.07 | - | - |
| 3[a] | $A_2B$ | H3 K9me | +2 | 13.9 ± 0.1 | 5.4 | -6.64 ± 0.01 | - | - |
| 4[a] | $A_2B$ | H3 K9 | +2 | 22 ± 1 | 8.3 | -6.38 ± 0.02 | - | - |
| 5 | $A_2I$-2 | H3 K9me3 | +2 | 0.22 ± 0.03 [c] | - | -9.11 ± 0.09 | -11.11 ± 0.05 | -2.0 ± 0.07 |
| 6 | $A_2I$-2 | H3 K9me2 | +2 | 0.20 ± 0.01 | 0.9 | -9.11 ± 0.09 | -11.11 ± 0.05 | -2.0 ± 0.02 |
| 7 | $A_2I$-2 | H3 K9me | +2 | 1.00 ± 0.04 | 4.5 | -8.18 ± 0.04 | -10.18 ± 0.04 | -2.0 ± 0.01 |
| 8 | $A_2I$-2 | H3 K9 | +2 | 1.79 ± 0.1 [c] | 8 | -7.88 ± 0.1 | -9.88 ± 0.04 | -2.0 ± 0.1 |
| 9 | $A_2I$-1 | H3 K9me3 | +2 | 0.13 ± 0.005 | - | -9.39 ± 0.04 | -12.29 ± 0.04 | -2.9 ± 0.02 |
| 10 | $A_2I$-1 | H3 K9me2 | +2 | 0.18 ± 0.04 | 1.4 | -9.19 ± 0.2 | -11.39 ± 0.08 | -2.2 ± 0.2 |
| 11 | $A_2I$-1 | H3 K9me | +2 | 1.23 ± 0.04 [c] | 9.5 | -8.03 ± 0.06 | -8.83 ± 0.03 | -0.8 ± 0.05 |
| 12 | $A_2I$-1 | H3 K9 | +2 | 2.09 ± 0.15 [c] | 16 | -7.78 ± 0.2 | -8.48 ± 0.06 | -0.7 ± 0.2 |
| 13 | $A_2I$-2 | Kme3GGY | +1 | 4.30 ± 0.33 | - | -7.32 ± 0.1 | -8.72 ± 0.1 | -1.40 ± 0.05 |
| 14 | $A_2I$-2 | Kme2GGY | +1 | 3.32 ± 0.20 | 0.8 | -7.48 ± 0.1 | -8.96 ± 0.1 | -1.48 ± 0.08 |
| 15 | $A_2J$-1 | H3 K9me3 | +2 | 2.61 ± 0.23 | - | -7.62 ± 0.8 | - | - |
| 16 | $A_2J$-1 | H3 K9me2 | +2 | 5.21 ± 0.44 | 2.0 | -7.21 ± 0.7 | - | - |
| 17 | $A_2J$-1 | H3 K9me | +2 | 6.36 ± 0.64 | 2.4 | -7.09 ± 0.7 | - | - |
| 18 | $A_2J$-1 | H3 K9 | +2 | 7.02 ± 0.75 | 2.7 | -7.03 ± 0.7 | - | - |
| 19 | $A_2J$-2 | H3 K9me3 | +2 | 2.25 ± 0.18 | - | -7.70 ± 0.7 | - | - |
| 20 | $A_2J$-2 | H3 K9me2 | +2 | 6.74 ± 0.62 | 3.0 | -7.05 ± 0.7 | - | - |
| 21 | $A_2J$-2 | H3 K9me | +2 | 8.37 ± 1.0 | 3.7 | -6.93 ± 0.7 | - | - |
| 22 | $A_2J$-2 | H3 K9 | +2 | 10.60 ± 1.1 | 4.7 | -6.79 ± 0.7 | - | - |

[a] Conditions: 25 $^oC$ in 10 mM sodium borate buffer, pH 8.5. [b] Errors are averages of the error in the fit as determined by the Origin 7 software. [c] Errors are from averages of the runs. [d] The selectivity factor is calculated as the $K_d$ of Kmex (where x = 0-2) divided by the $K_d$ of Kme3.

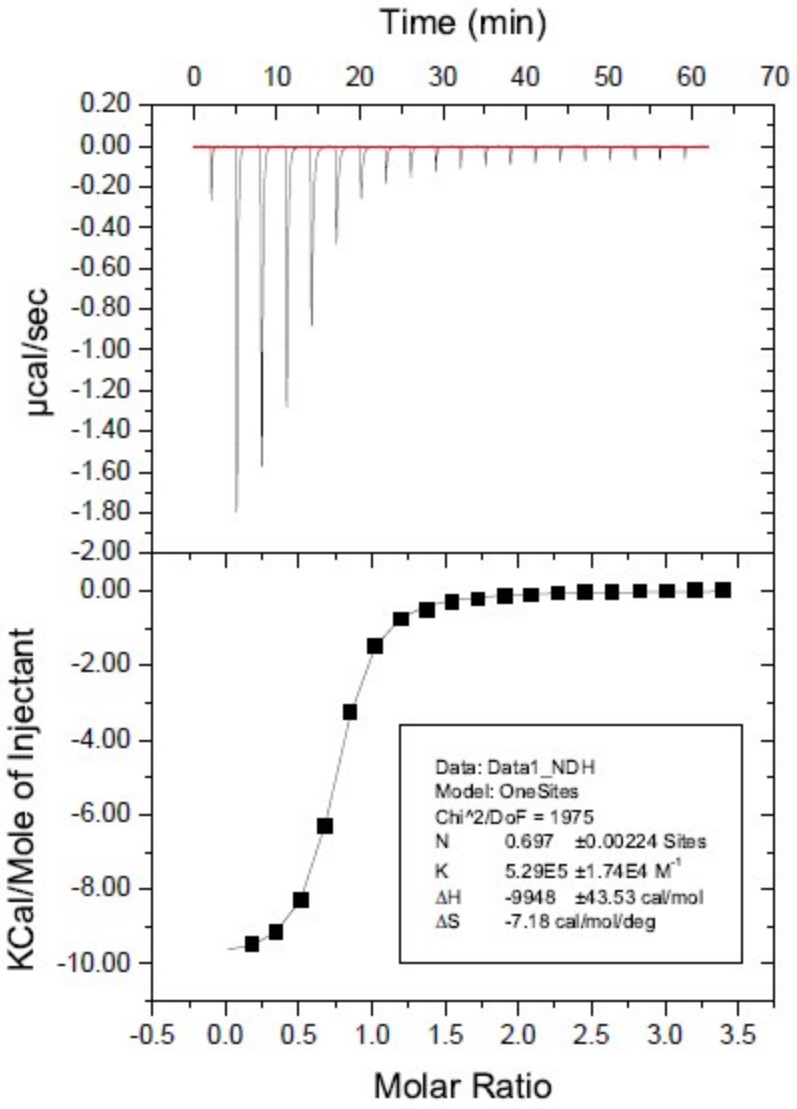


**Figure S52**. One trial of three of H3K9 (Ac-WGGGQTARKSTG-$NH_2$) (1.33 mM) titrated into **$A_2$I-2** (79 µM) at 25 °C in 10 mM sodium borate buffer pH 8.5 (Run 1).

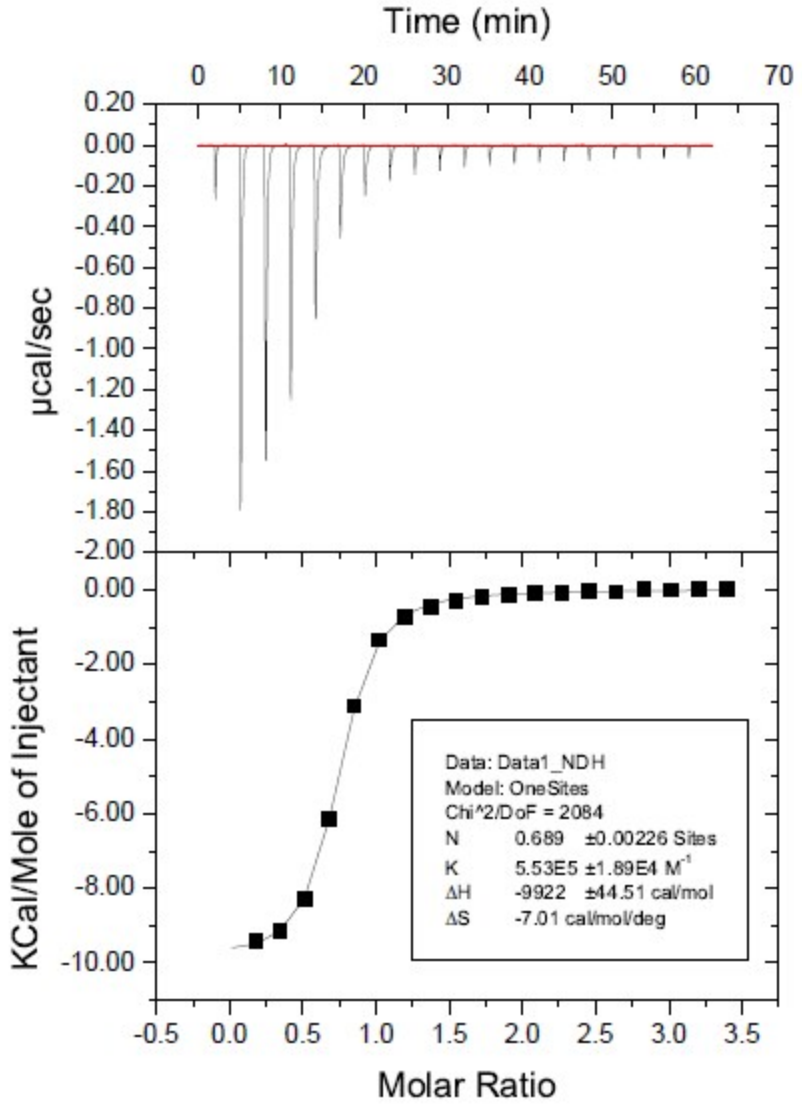


**Figure S53**. One trial of three of H3K9 (Ac-WGGGQTARKSTG-$NH_2$) (1.33 mM) titrated into **$A_2$I-2** (79 µM) at 25 °C in 10 mM sodium borate buffer pH 8.5 (Run 2).

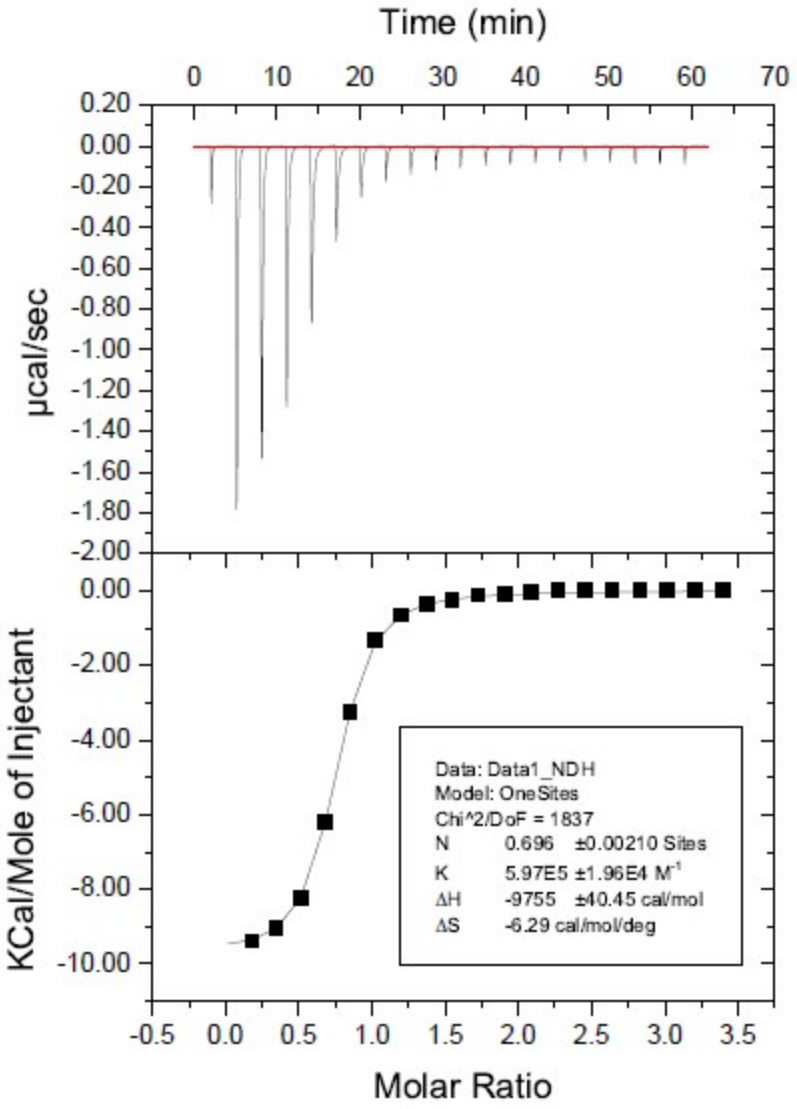


**Figure S54**. One trial of three of H3K9 (Ac-WGGGQTARKSTG-$NH_2$) (1.33 mM) titrated into **$A_2$I-2** (79 µM) at 25 °C in 10 mM sodium borate buffer pH 8.5 (Run 3).

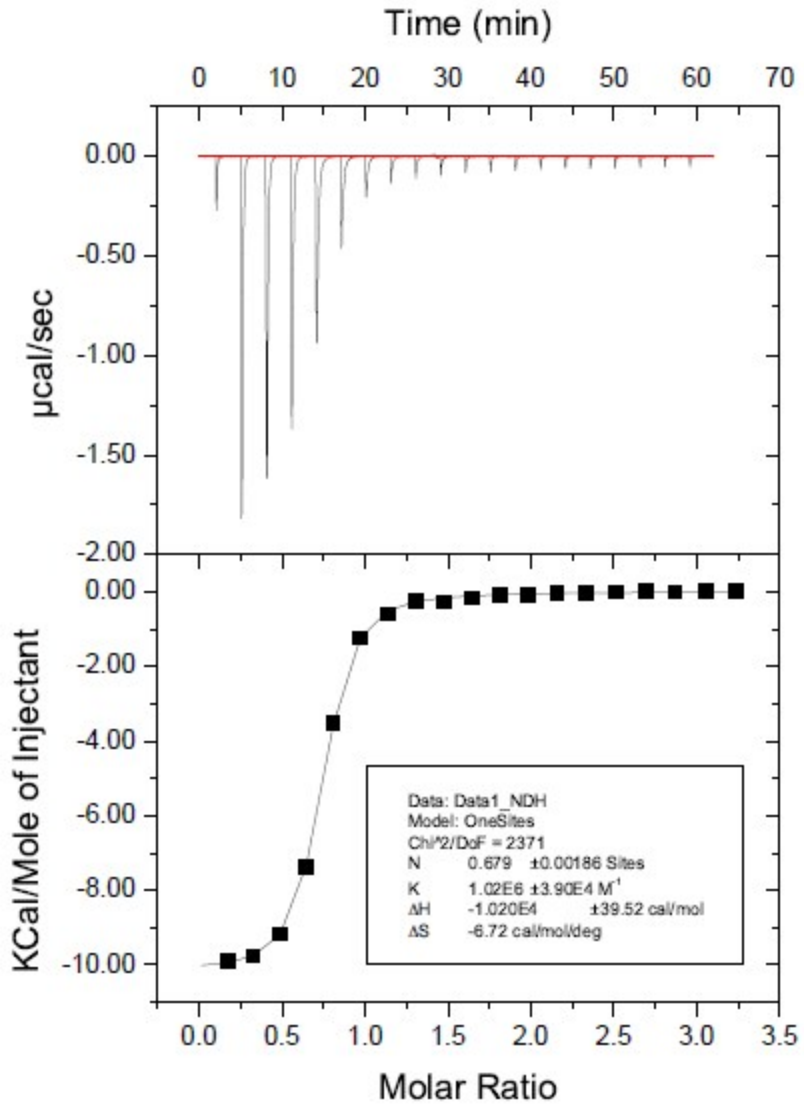


**Figure S55**. One trial of three of H3K9me (Ac-WGGGQTARKmeSTG-$NH_2$) (1.26 mM) titrated into **$A_2$I-2** (79 µM) at 25 °C in 10 mM sodium borate buffer pH 8.5 (Run 1).

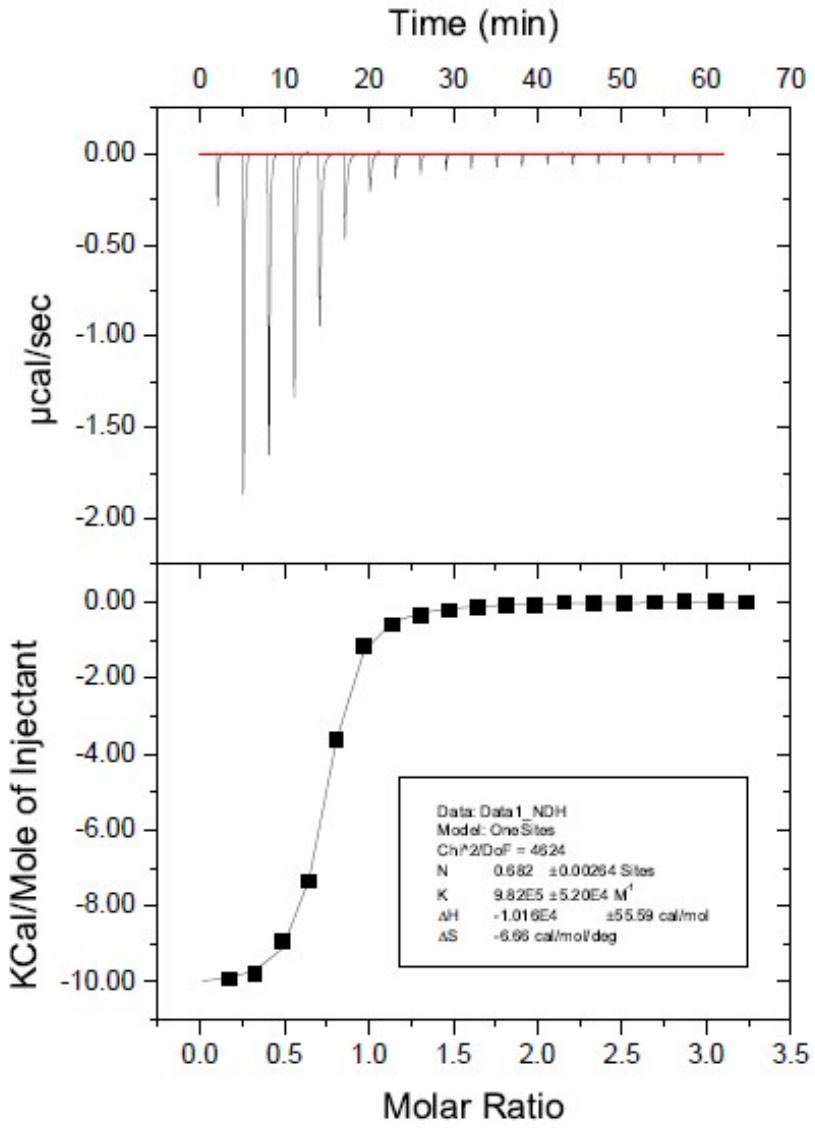


**Figure S56**. One trial of three of H3K9me (Ac-WGGGQTARKmeSTG-$NH_2$) (1.26 mM) titrated into **$A_2$I-2** (79 µM) at 25 °C in 10 mM sodium borate buffer pH 8.5 (Run 2).

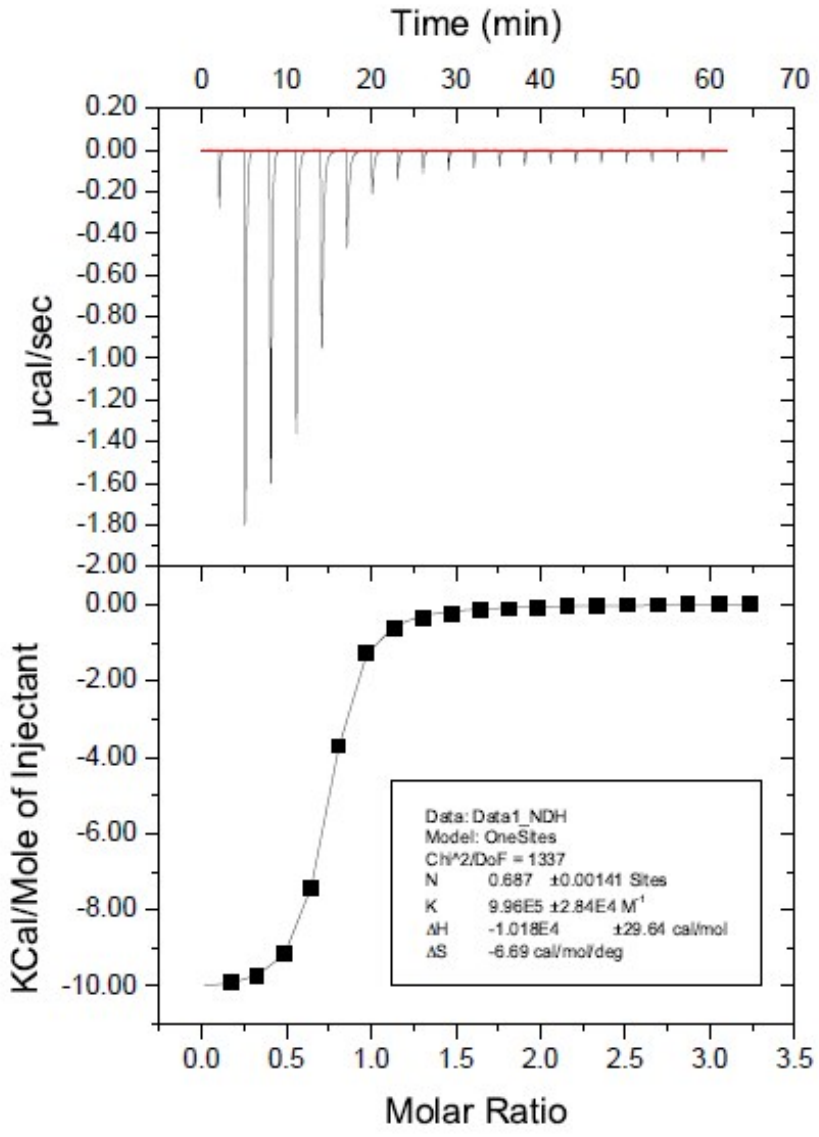


**Figure S57**. One trial of three of H3K9me (Ac-WGGGQTARKmeSTG-$NH_2$) (1.26 mM) titrated into **$A_2$I-2** (79 µM) at 25 °C in 10 mM sodium borate buffer pH 8.5 (Run 3).

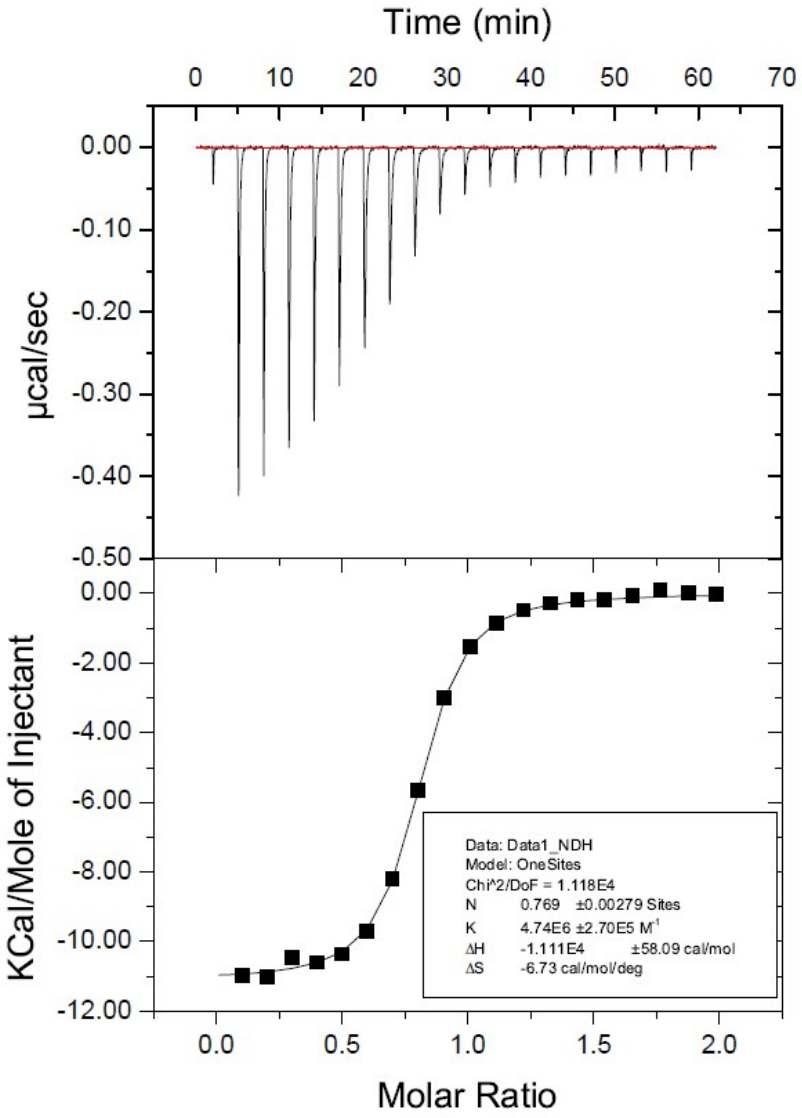


**Figure S58**. One trial of three of H3K9me$_2$ (Ac-WGGGQTARKme2STG-NH$_2$) (197 µM) titrated into **A$_2$I-2** (20 µM) at 25 $^{o}$C in 10 mM sodium borate buffer pH 8.5 (Run 1).

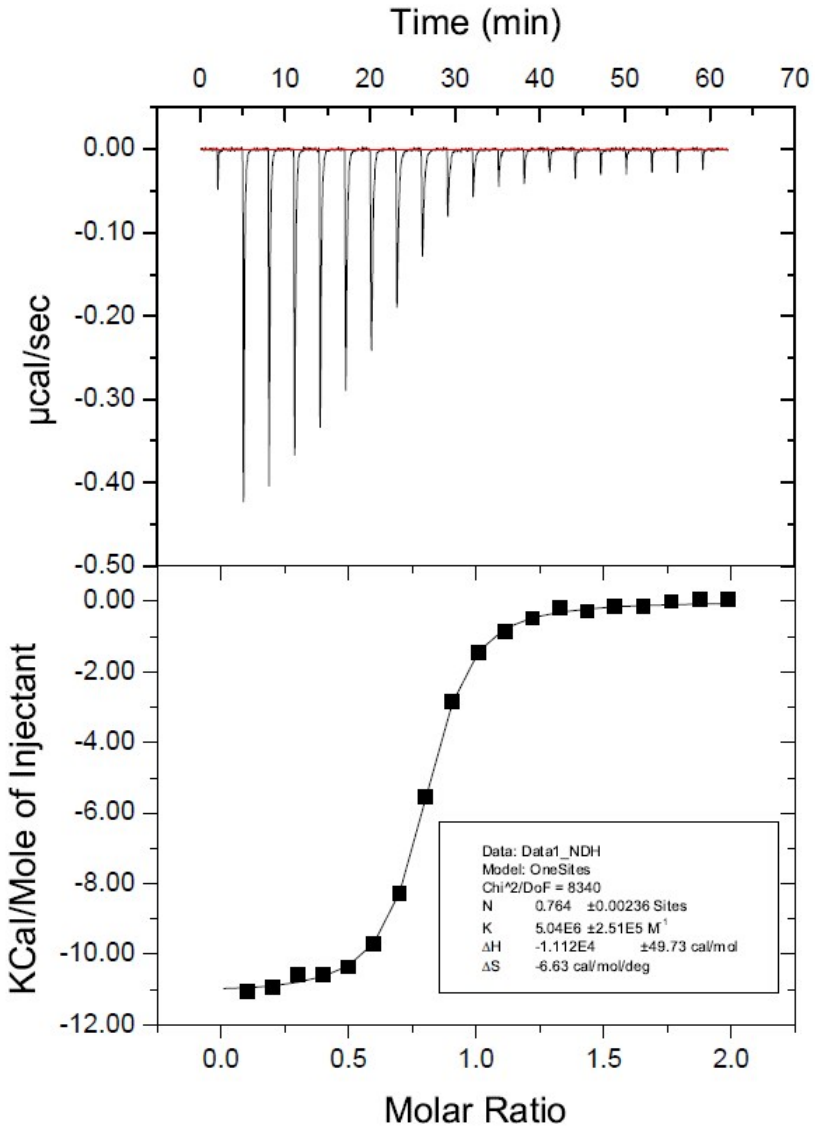


**Figure S59**. One trial of three of H3K9me$_2$ (Ac-WGGGQTARKme2STG-NH$_2$) (197 µM) titrated into **A$_2$I-2** (20 µM) at 25 °C in 10 mM sodium borate buffer pH 8.5 (Run 2).

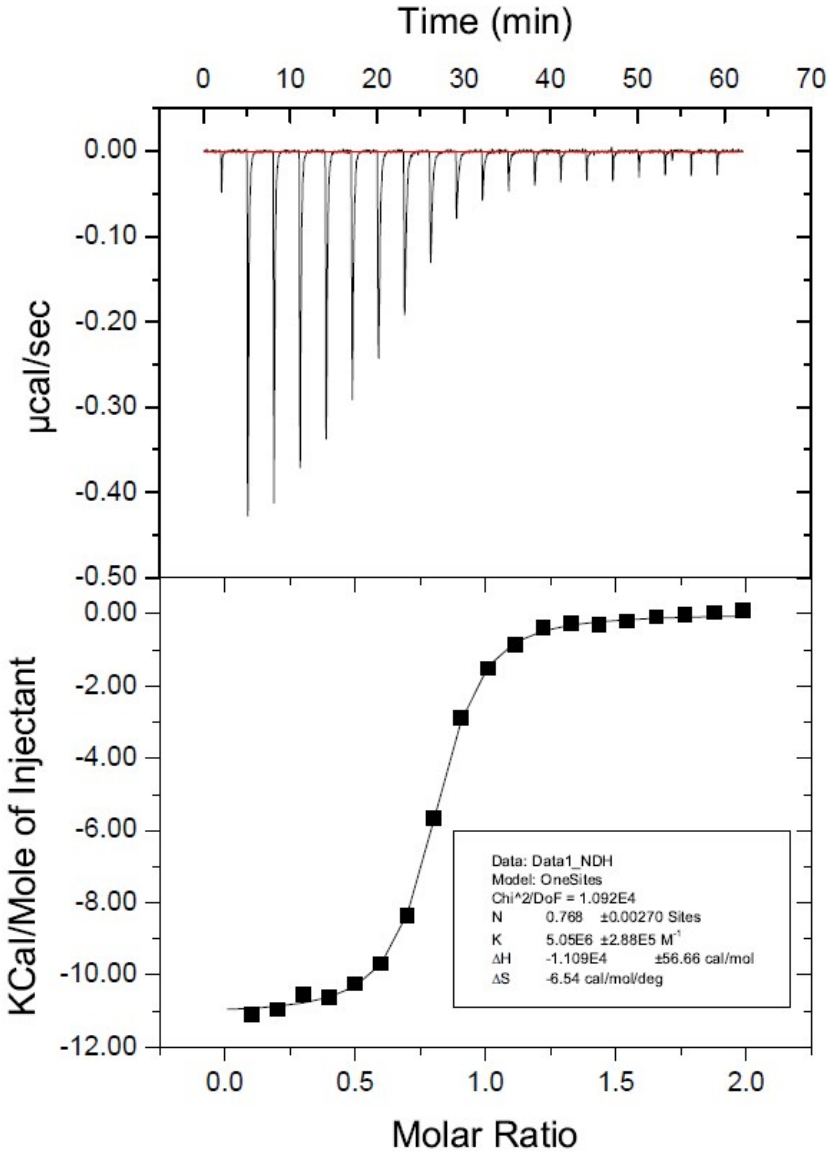


**Figure S60**. One trial of three of H3K9me$_2$ (Ac-WGGGQTARKme2STG-NH$_2$) (197 µM) titrated into **A$_2$I-2** (20 µM) at 25 $^{o}$C in 10 mM sodium borate buffer pH 8.5 (Run 3).

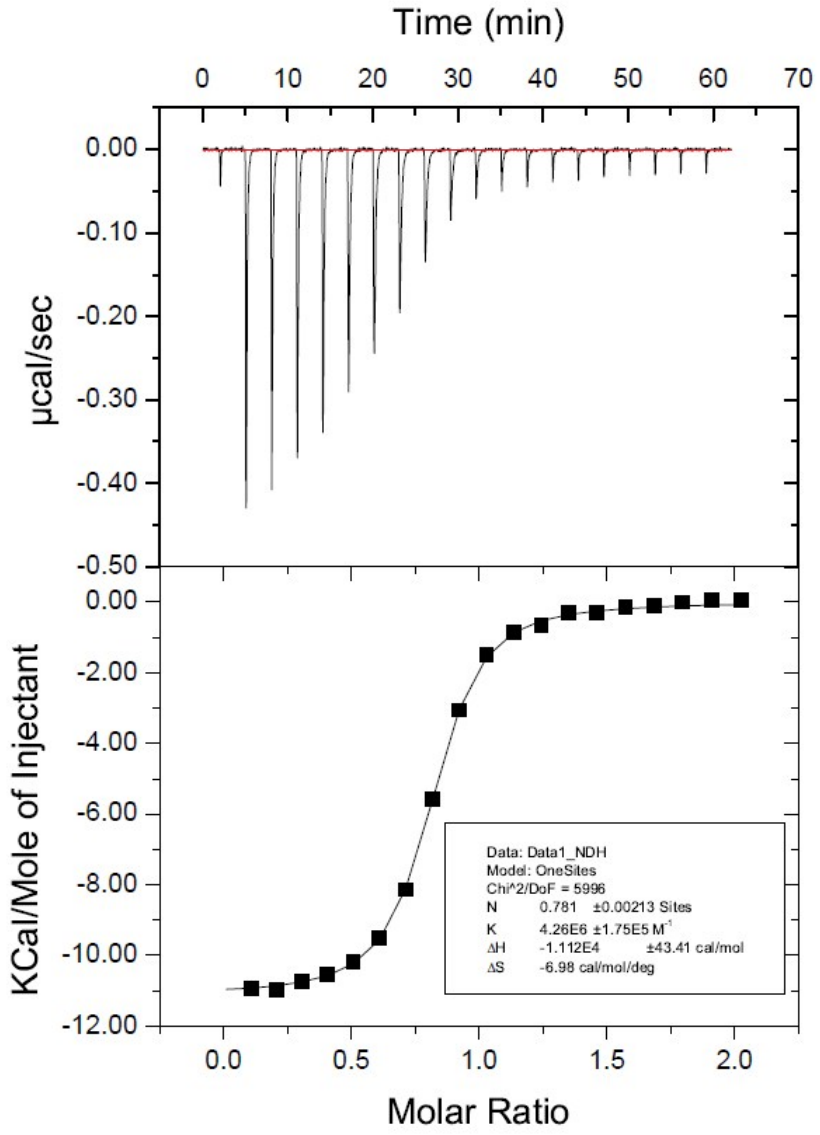


**Figure S61**. One trial of three of H3K9me$_3$ (Ac-WGGGQTARKme3STG-NH$_2$) (200 µM) titrated into **A$_2$I-2** (20 µM) at 25 $^{o}$C in 10 mM sodium borate buffer pH 8.5 (Run 1).

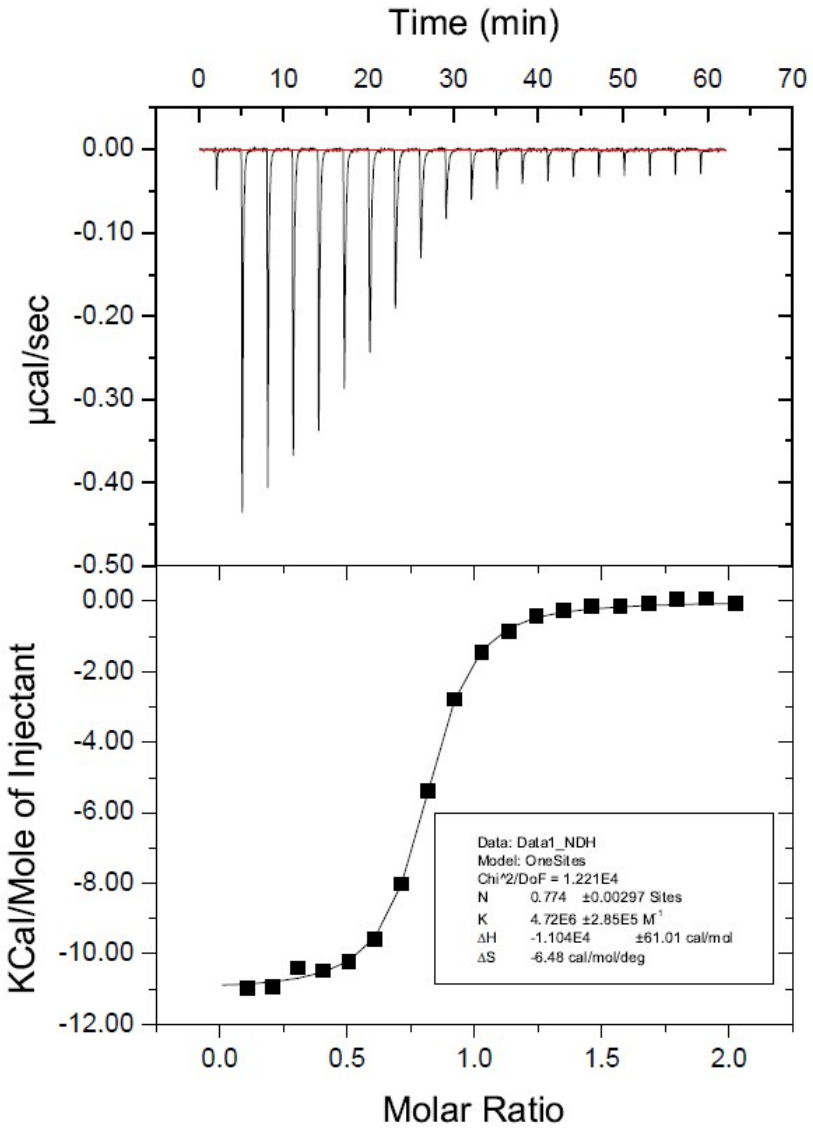


**Figure S62**. One trial of four of H3K9me$_3$ (Ac-WGGGQTARKme3STG-NH$_2$) (200 µM) titrated into **$A_2$I-2** (20 µM) at 25 °C in 10 mM sodium borate buffer pH 8.5 (Run 2).

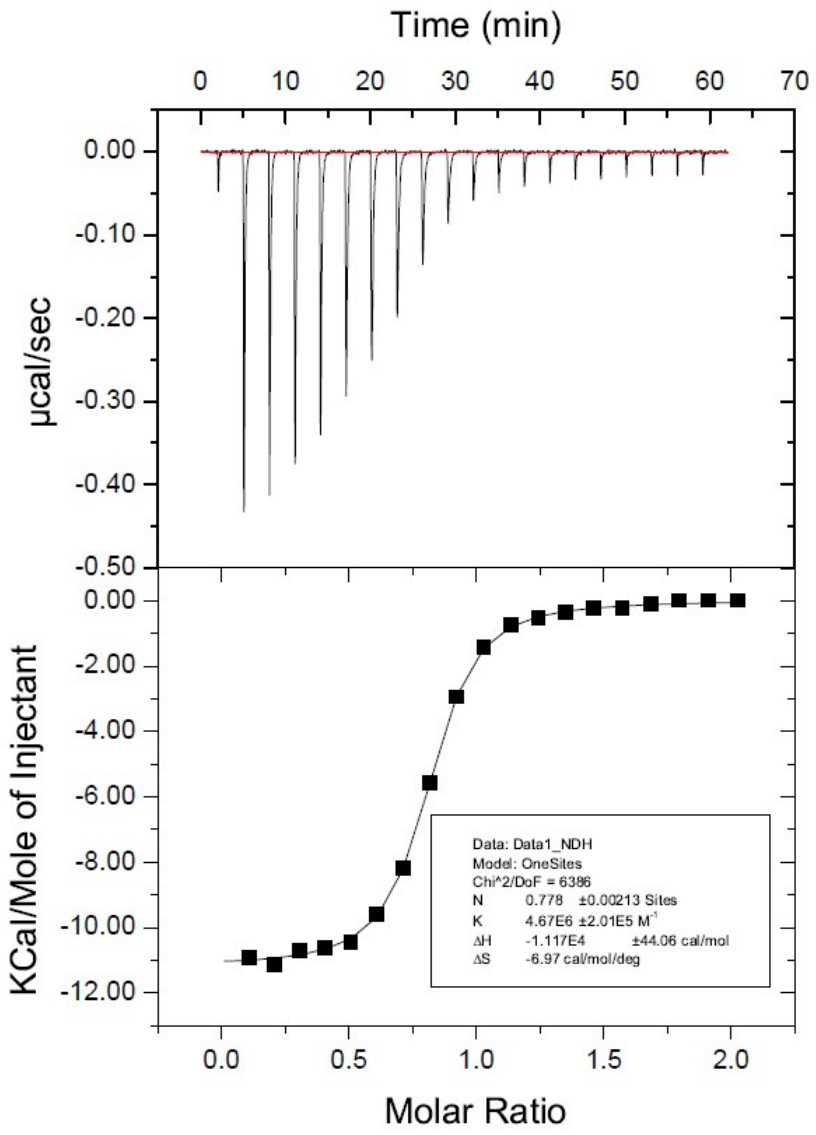


**Figure S63**. One trial of four of H3K9me$_3$ (Ac-WGGGQTARKme3STG-NH$_2$) (200 µM) titrated into **$A_2$I-2** (20 µM) at 25 °C in 10 mM sodium borate buffer pH 8.5 (Run 3).

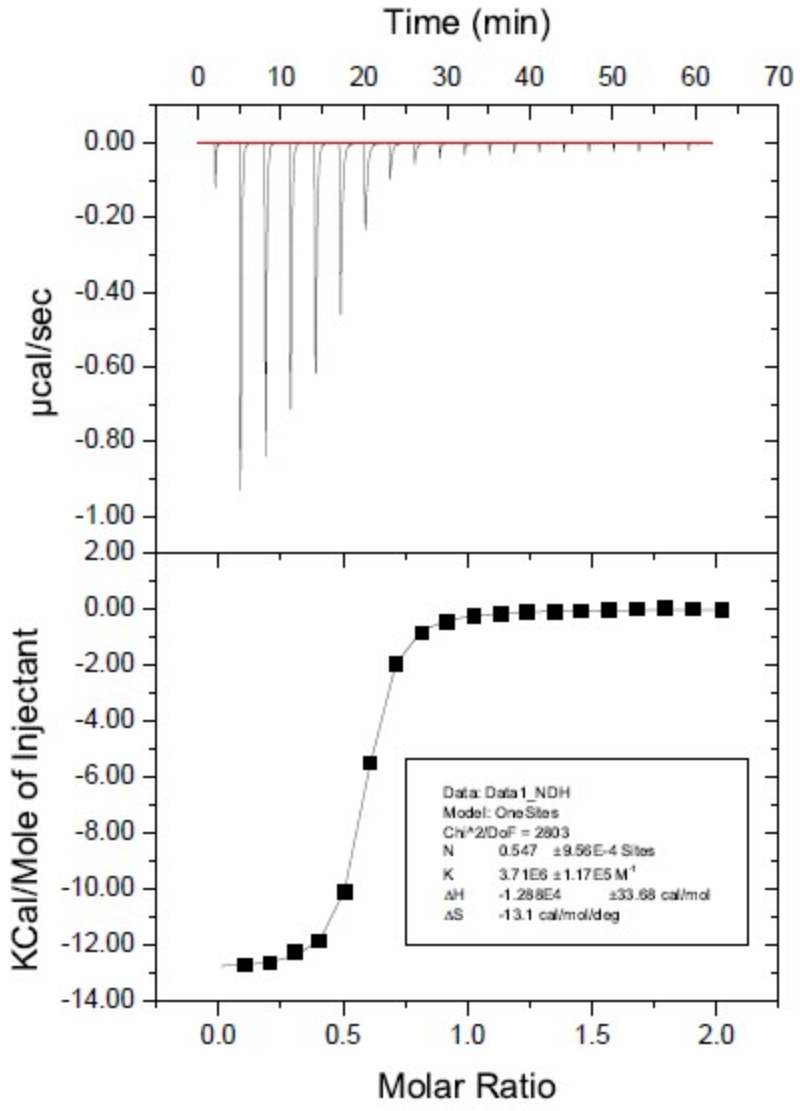


**Figure S64**. One trial of four of H3K9me$_3$ (Ac-WGGGQTARKme3STG-NH$_2$) (225 µM) titrated into **A$_2$I-2** (23 µM) at 25 $^{o}$C in 10 mM sodium borate buffer pH 8.5 (Run 4).

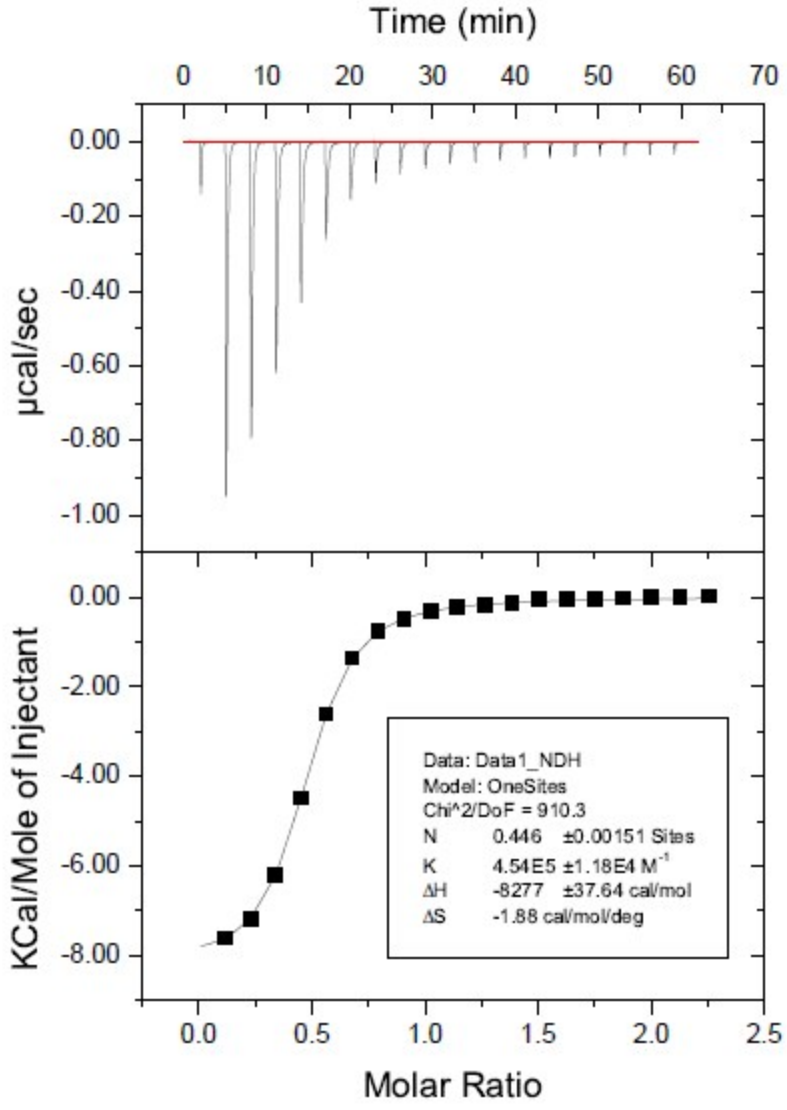


**Figure S65**. One trial of four of H3K9 (Ac-WGGGQTARKSTG-$NH_2$) (900 µM) titrated into **$A_2$I-1** (81 µM) at 25 °C in 10 mM sodium borate buffer pH 8.5 (Run 1).

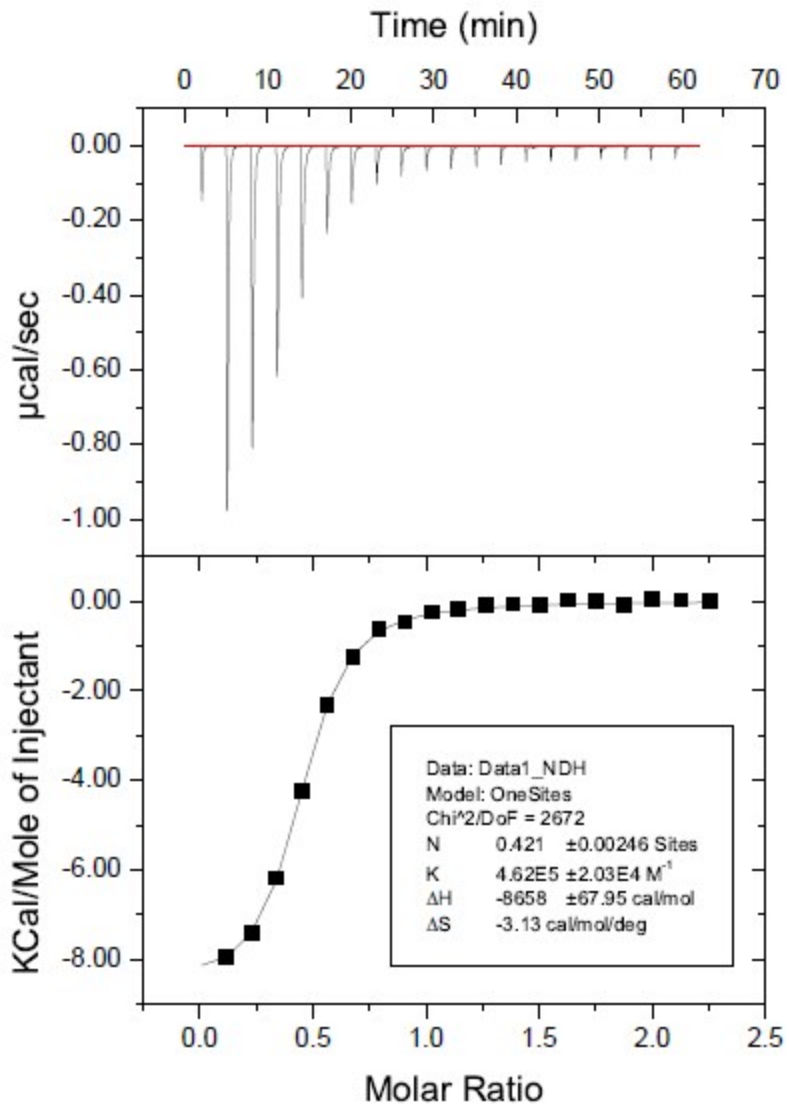


**Figure S66**. One trial of four of H3K9 (Ac-WGGGQTARKSTG-$NH_2$) (900 µM) titrated into **$A_2$I-1** (81 µM) at 25 °C in 10 mM sodium borate buffer pH 8.5 (Run 2).

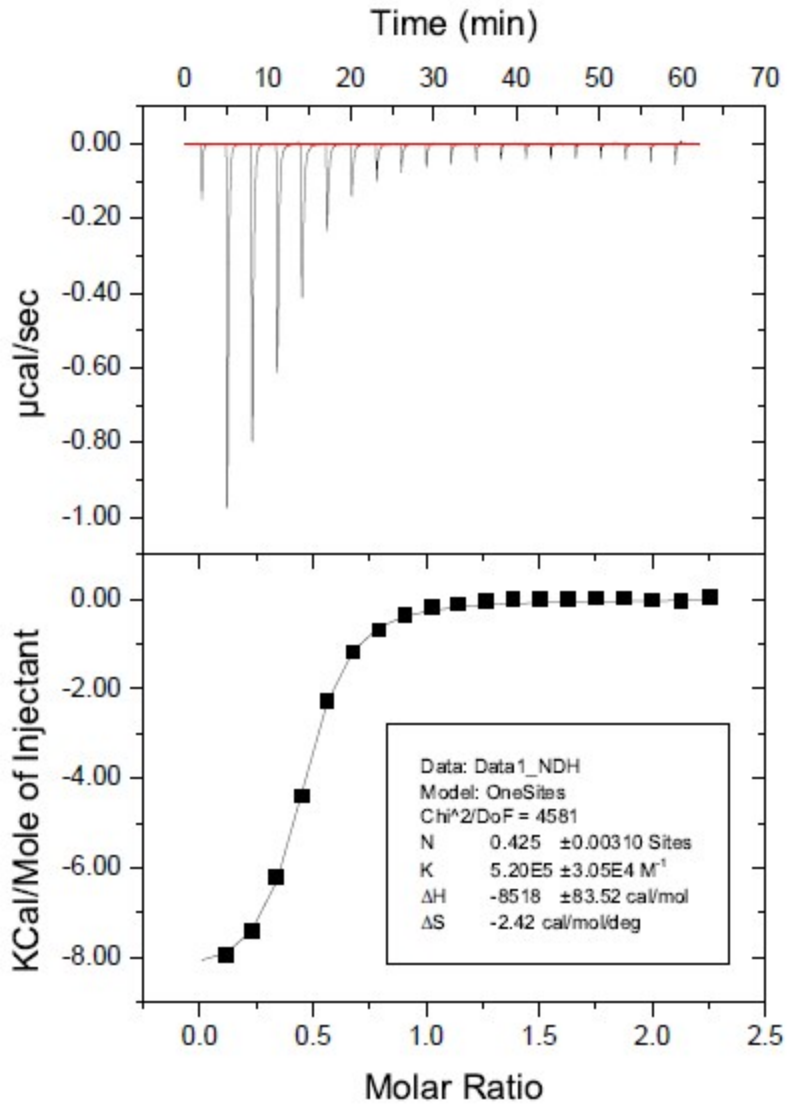


**Figure S67**. One trial of four of H3K9 (Ac-WGGGQTARKSTG-$NH_2$) (900 µM) titrated into **$A_2$I-1** (81 µM) at 25 °C in 10 mM sodium borate buffer pH 8.5 (Run 3).

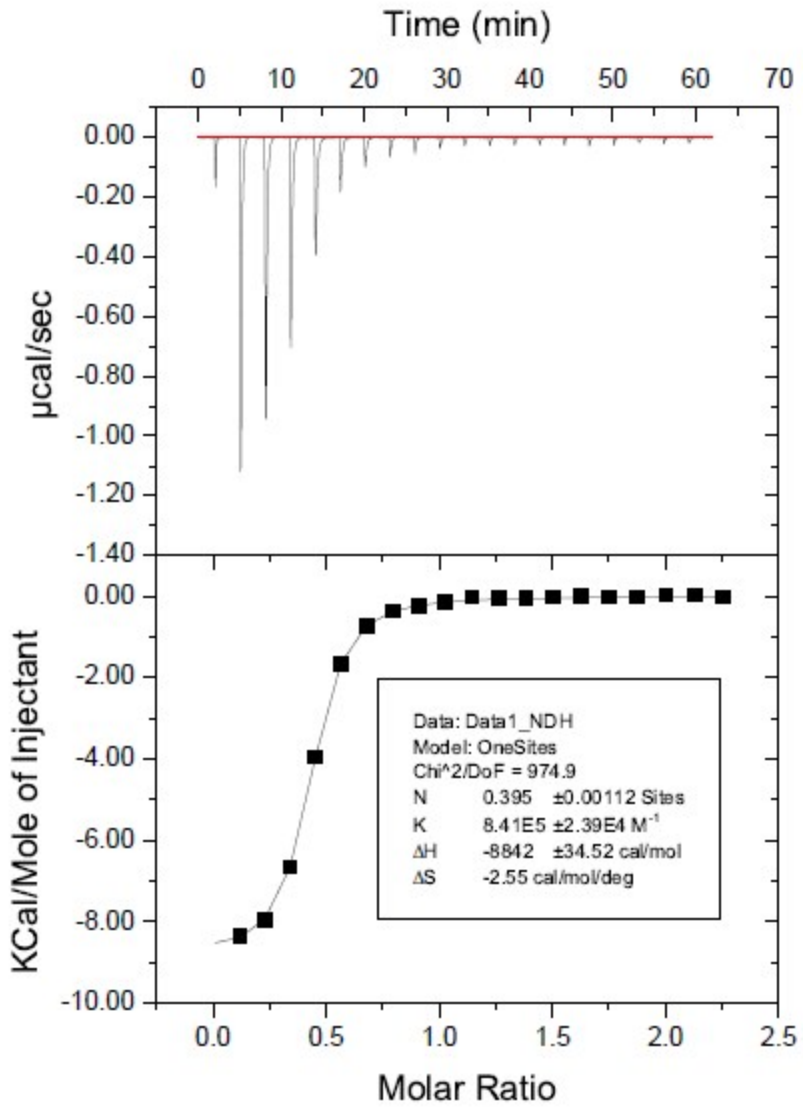


**Figure S68**. One trial of three of H3K9me (Ac-WGGGQTARKmeSTG-$NH_2$) (900 µM) titrated into **$A_2$I-1** (81 µM) at 25 °C in 10 mM sodium borate buffer pH 8.5 (Run 1).

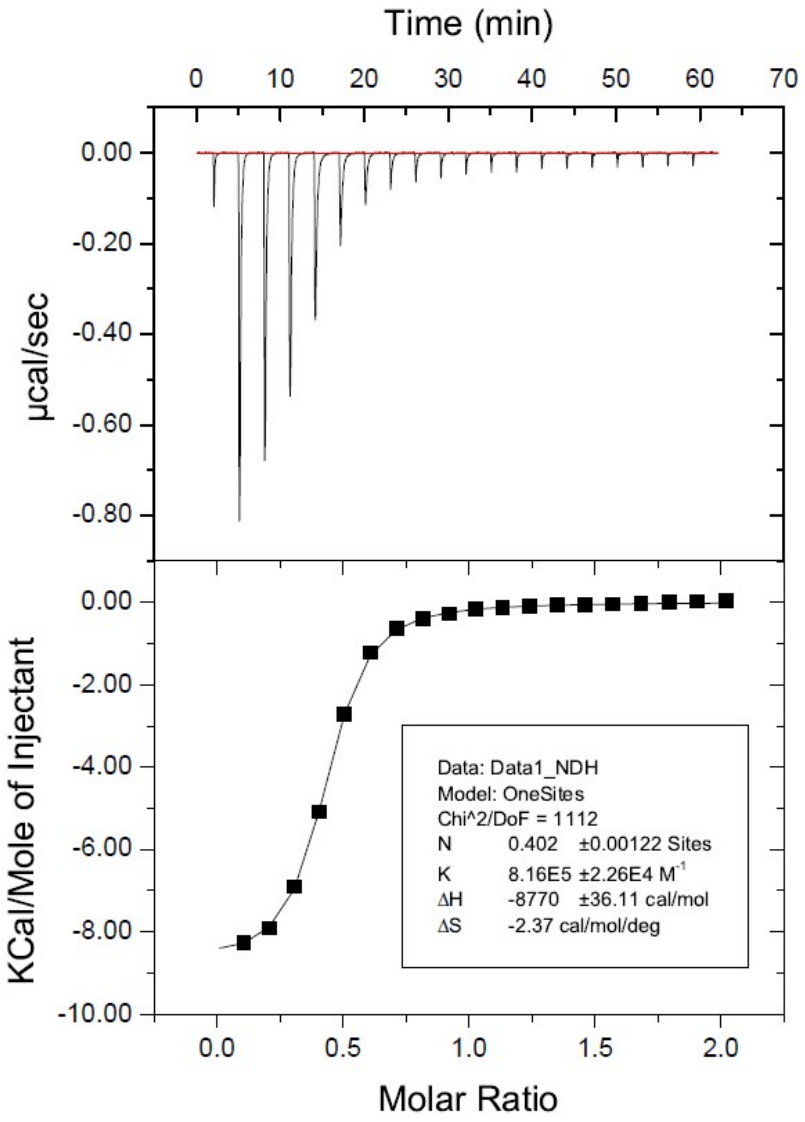


**Figure S69**. One trial of three of H3K9me (Ac-WGGGQTARKmeSTG-$NH_2$) (700 µM) titrated into **$A_2$I-1** (70 µM) at 25 °C in 10 mM sodium borate buffer pH 8.5 (Run 2).

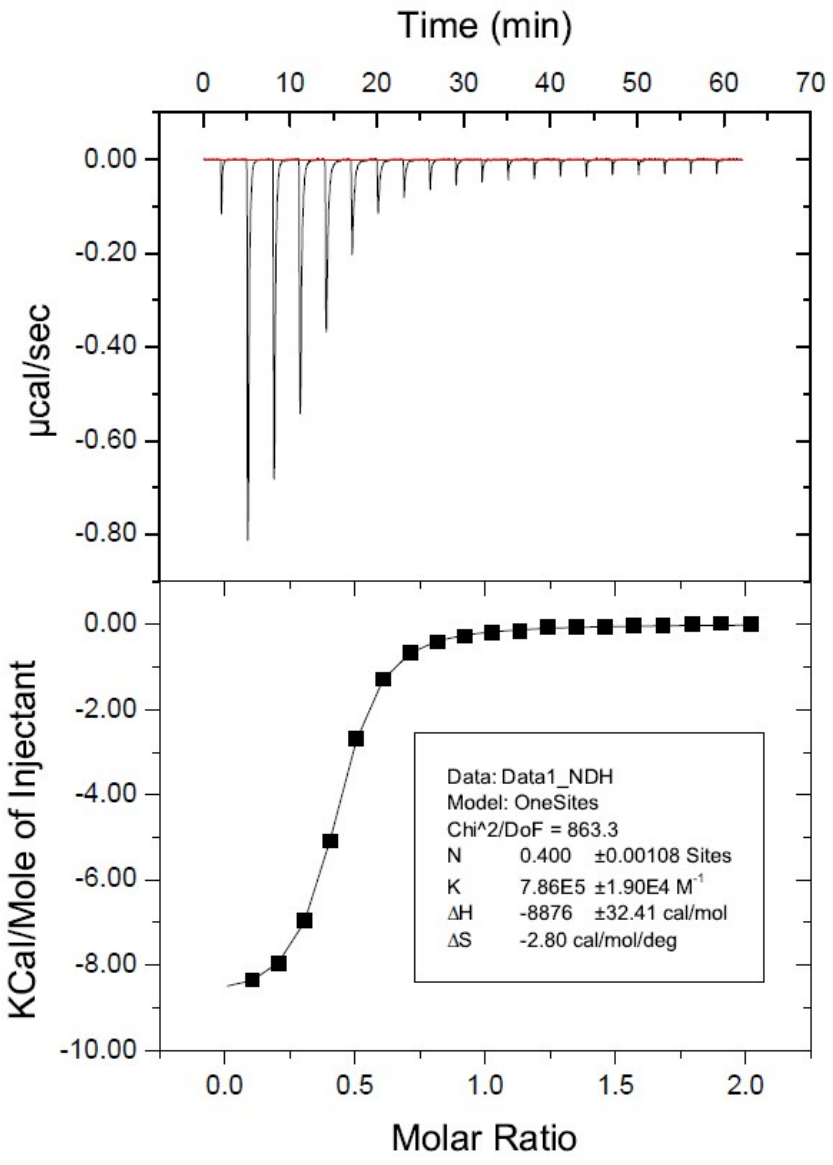


**Figure S70**. One trial of three of H3K9me (Ac-WGGGQTARKmeSTG-$NH_2$) (700 µM) titrated into **$A_2$I-1** (70 µM) at 25 °C in 10 mM sodium borate buffer pH 8.5 (Run 3).

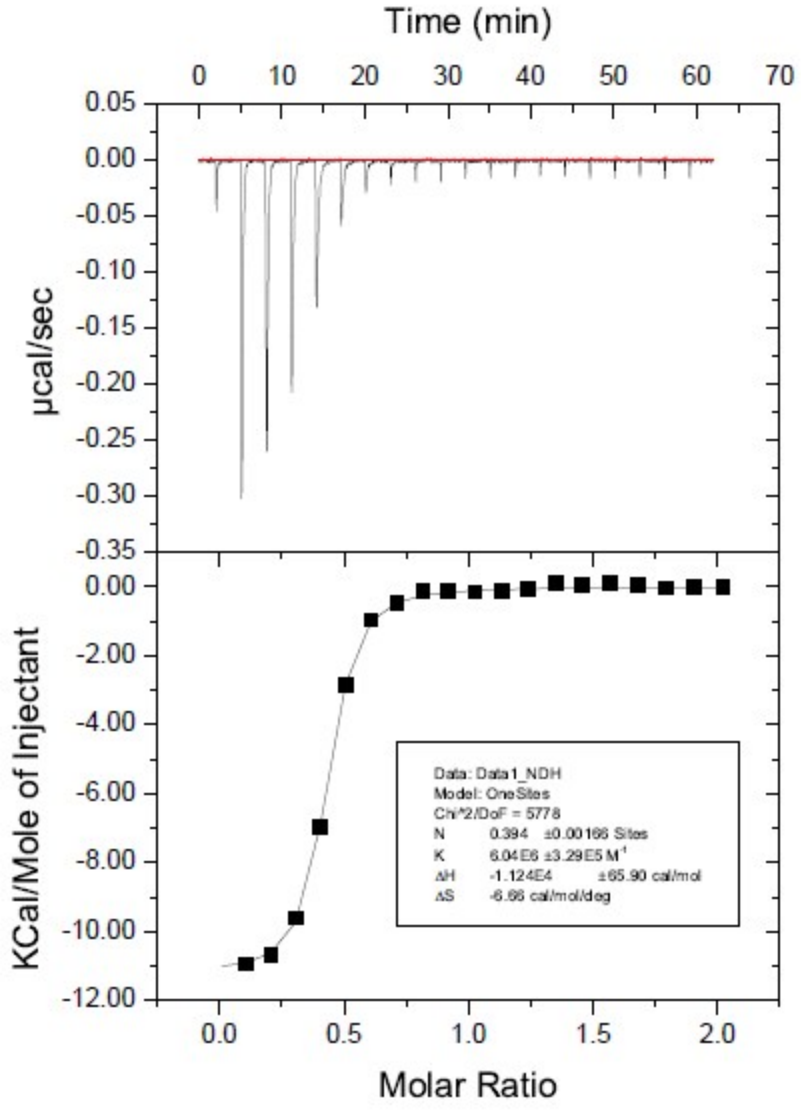


**Figure S71**. One trial of two of H3K9me$_2$ (Ac-WGGGQTARKme2STG-NH$_2$) (200 µM) titrated into **$A_2$I-1** (20 µM) at 25 °C in 10 mM sodium borate buffer pH 8.5 (Run 1).

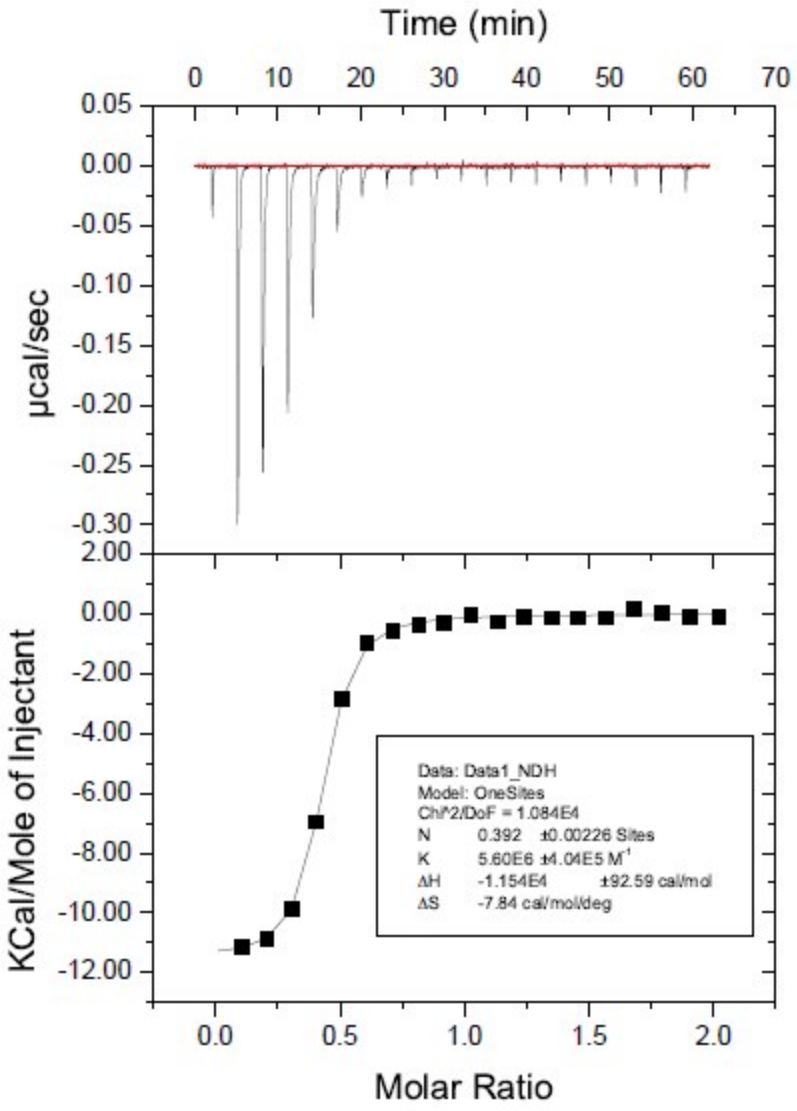


**Figure S72**. One trial of two of H3K9me$_2$ (Ac-WGGGQTARKme2STG-NH$_2$) (200 µM) titrated into **$A_2$I-1** (20 µM) at 25 °C in 10 mM sodium borate buffer pH 8.5 (Run 2).

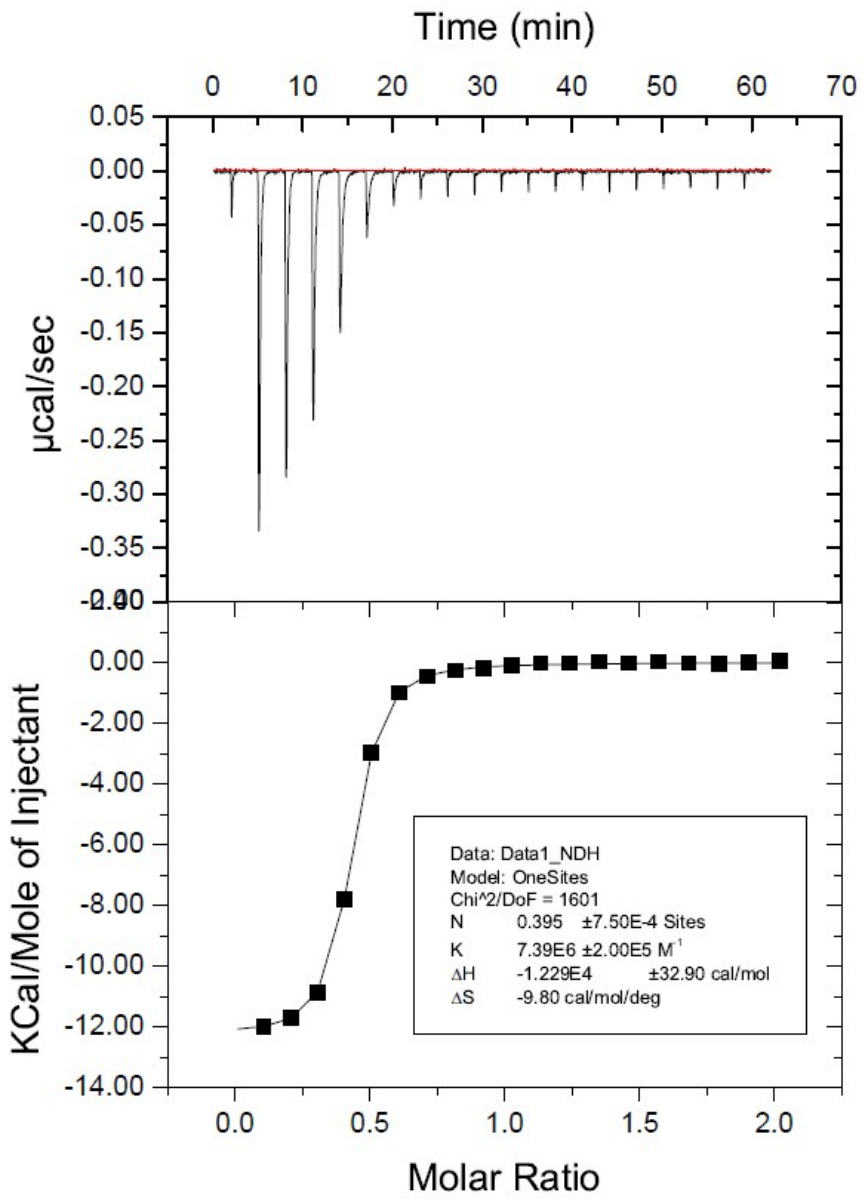


**Figure S73**. One trial of two of H3K9me$_3$ (Ac-WGGGQTARKme3STG-NH$_2$) (200 µM) titrated into **$A_2$I-1** (20 µM) at 25 °C in 10 mM sodium borate buffer pH 8.5. (Run 1).

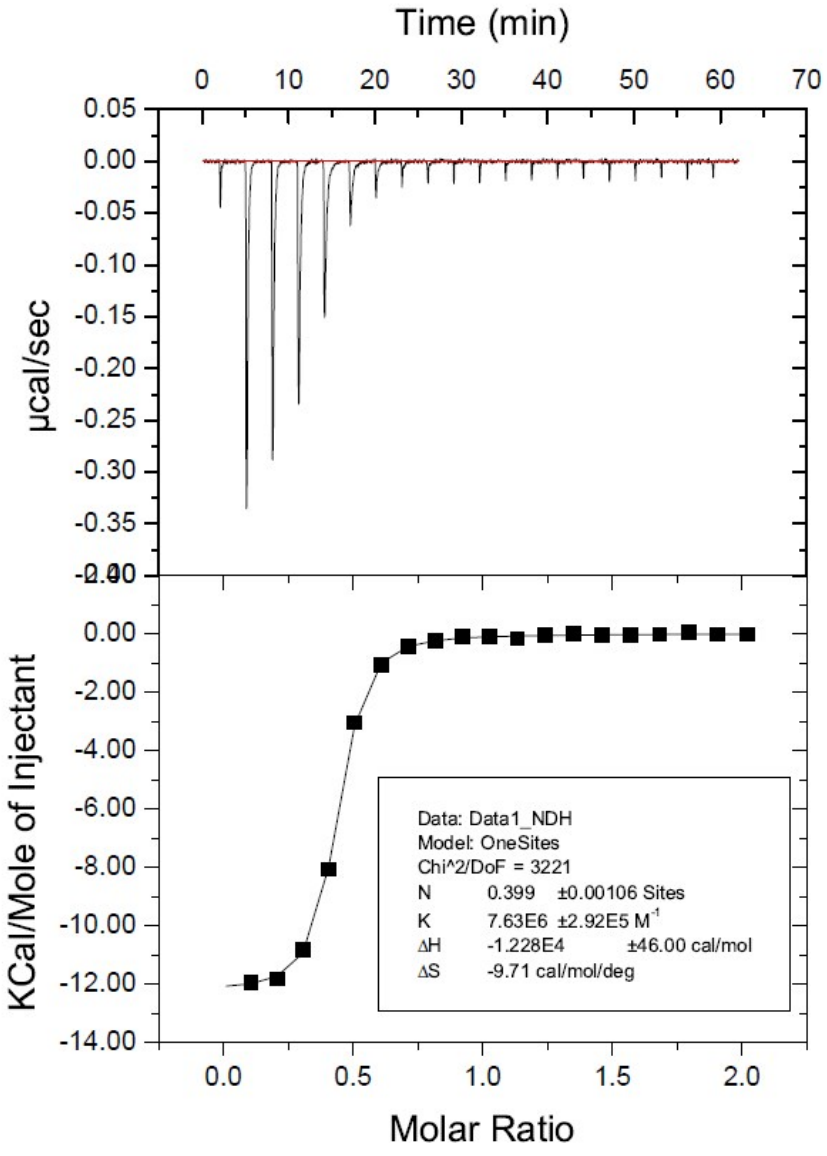


**Figure S74**. One trial of two of H3K9me$_3$ (Ac-WGGGQTARKme3STG-NH$_2$) (200 µM) titrated into **$A_2$I-1** (20 µM) at 25 °C in 10 mM sodium borate buffer pH 8.5. (Run 2).

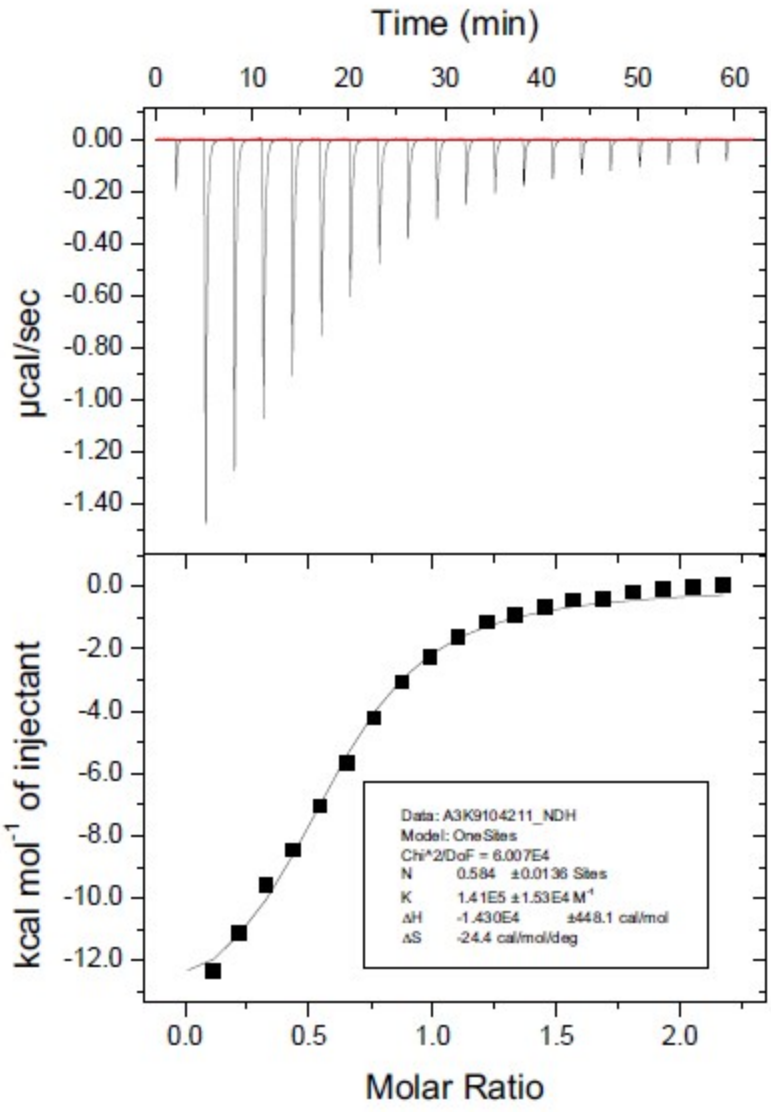


**Figure S75**. One trial of two of H3K9 (Ac-WGGGQTARKSTG-$NH_2$) (817 µM) titrated into **$A_2$J-1** (76 µM) at 25 °C in 10 mM sodium borate buffer pH 8.5. (Run 1).

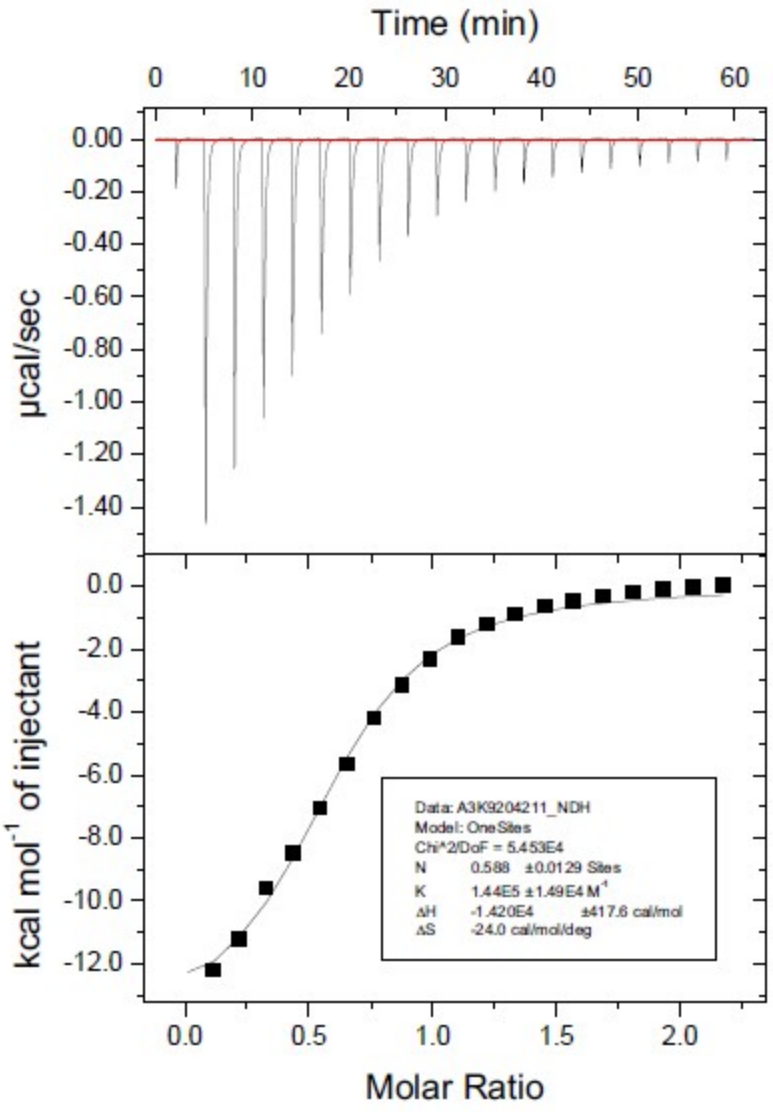


**Figure S76**. One trial of two of H3K9 (Ac-WGGGQTARKSTG-$NH_2$) (817 µM) titrated into **$A_2$J-1** (76 µM) at 25 °C in 10 mM sodium borate buffer pH 8.5. (Run 2).

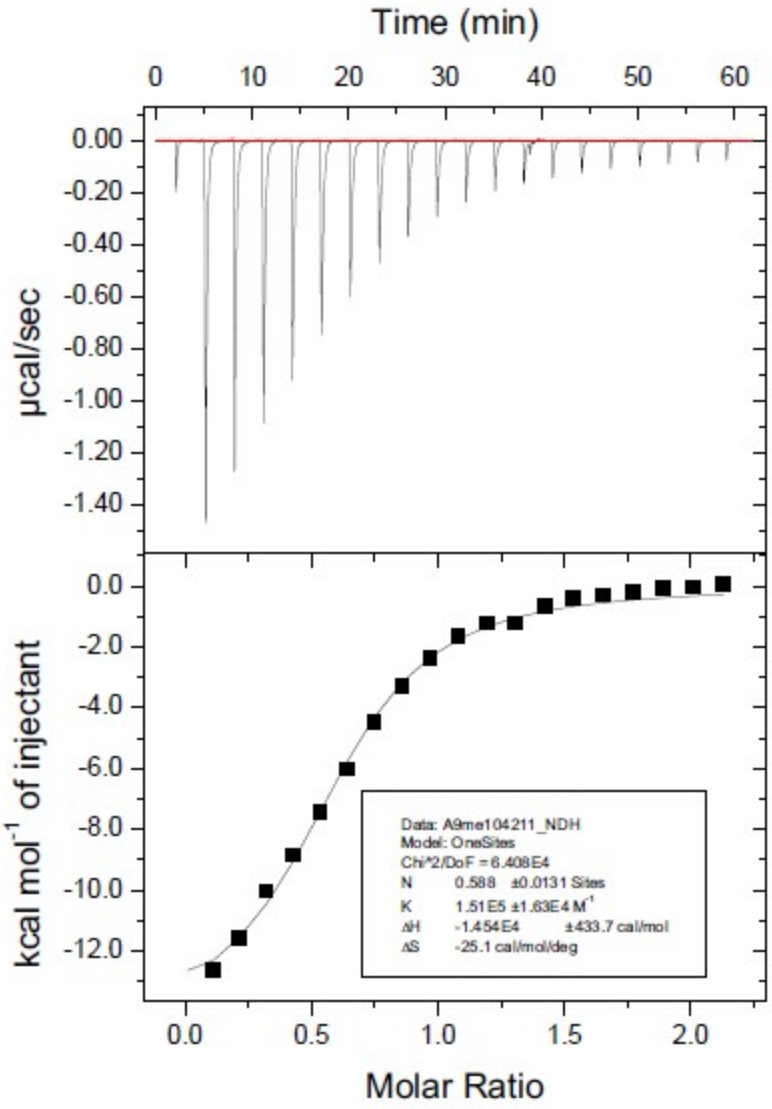


**Figure S77**. One trial of two of H3K9me (Ac-WGGGQTARKmeSTG-$NH_2$) (800 µM) titrated into **$A_2$J-1** (76 µM) at 25 °C in 10 mM sodium borate buffer pH 8.5. (Run 1).

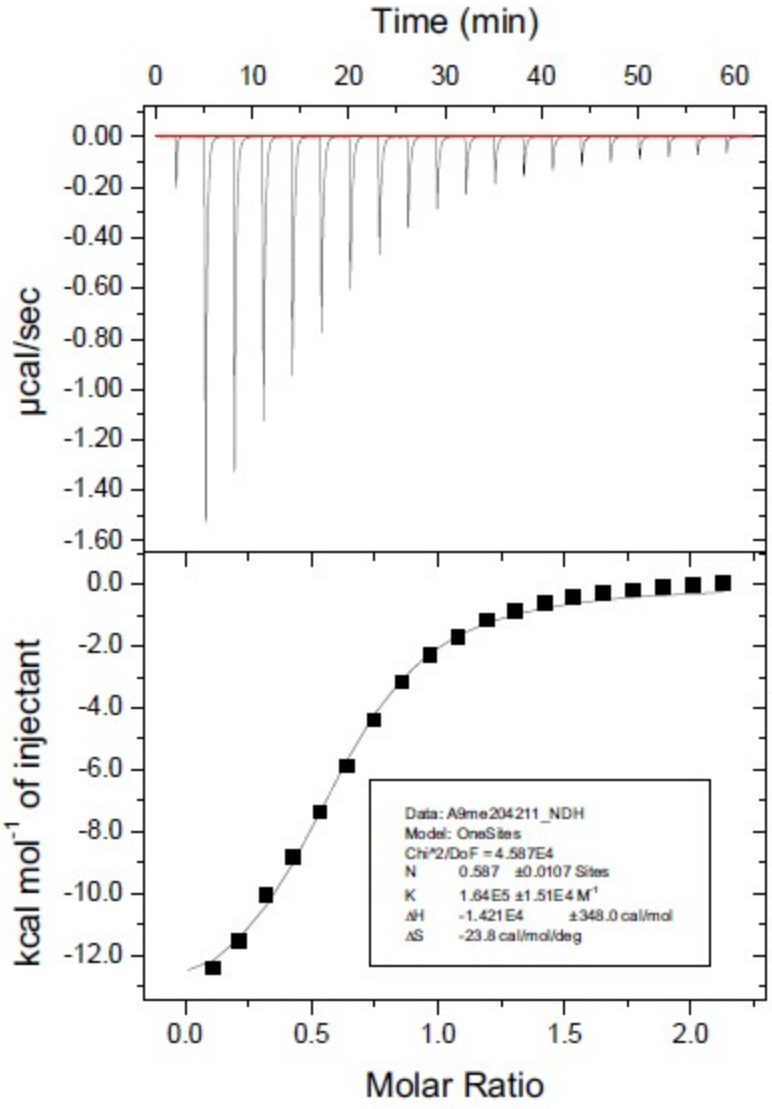


**Figure S78**. One trial of two of H3K9me (Ac-WGGGQTARKmeSTG-$NH_2$) (800 µM) titrated into **$A_2$J-1** (76 µM) at 25 °C in 10 mM sodium borate buffer pH 8.5. (Run 2).

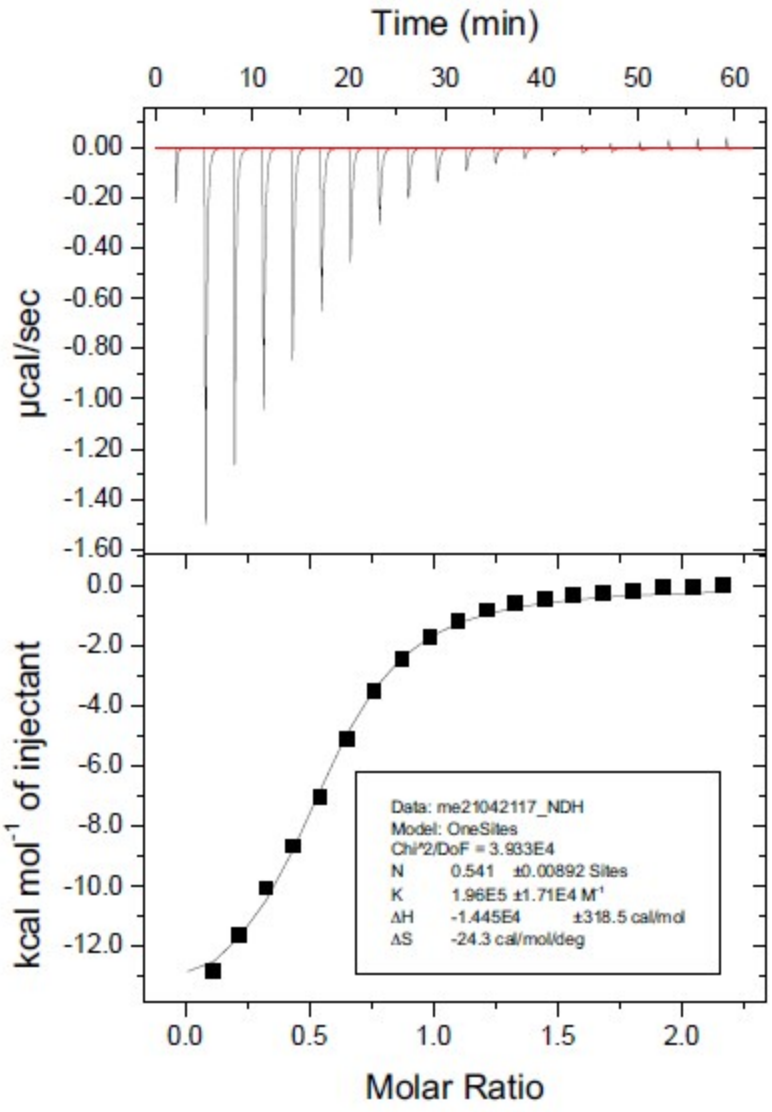


**Figure S79**. One trial of two of H3K9me$_2$ (Ac-WGGGQTARKme2STG-NH$_2$) (815 µM) titrated into **$A_2$J-1** (76 µM) at 25 $^{o}$C in 10 mM sodium borate buffer pH 8.5. (Run 1).

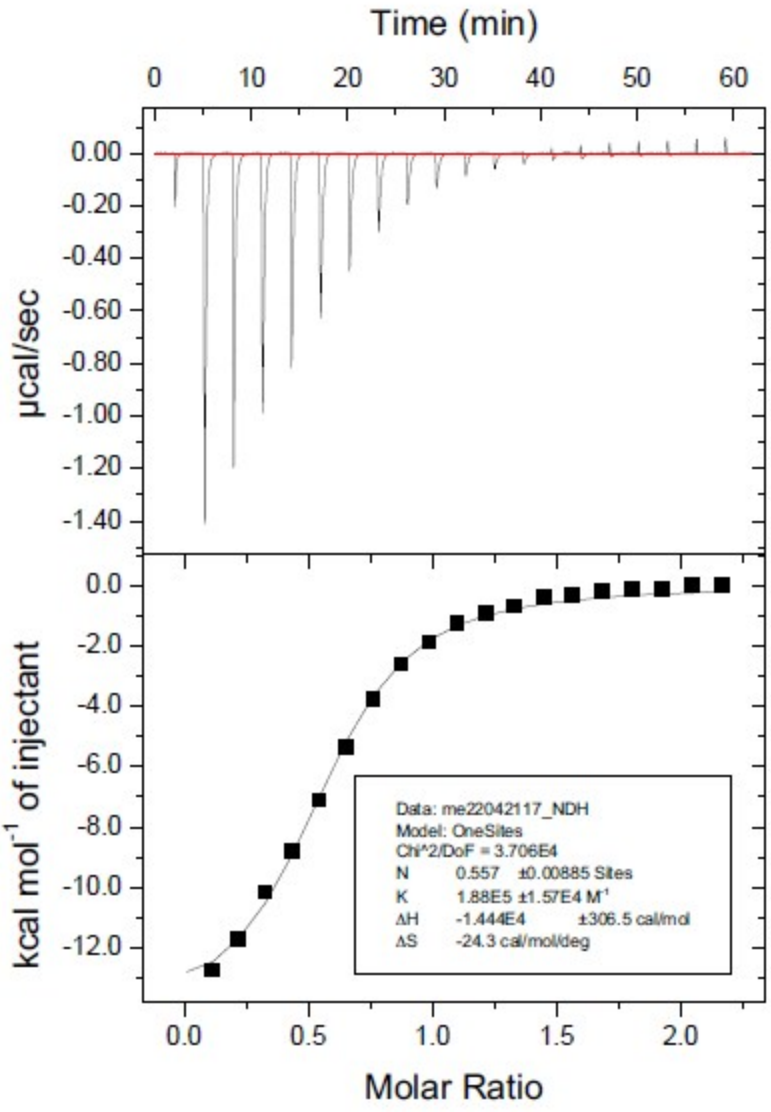


**Figure S80**. One trial of two of H3K9me$_2$ (Ac-WGGGQTARKme2STG-NH$_2$) (815 µM) titrated into **A$_2$J-1** (76 µM) at 25 $^{o}$C in 10 mM sodium borate buffer pH 8.5. (Run 2).

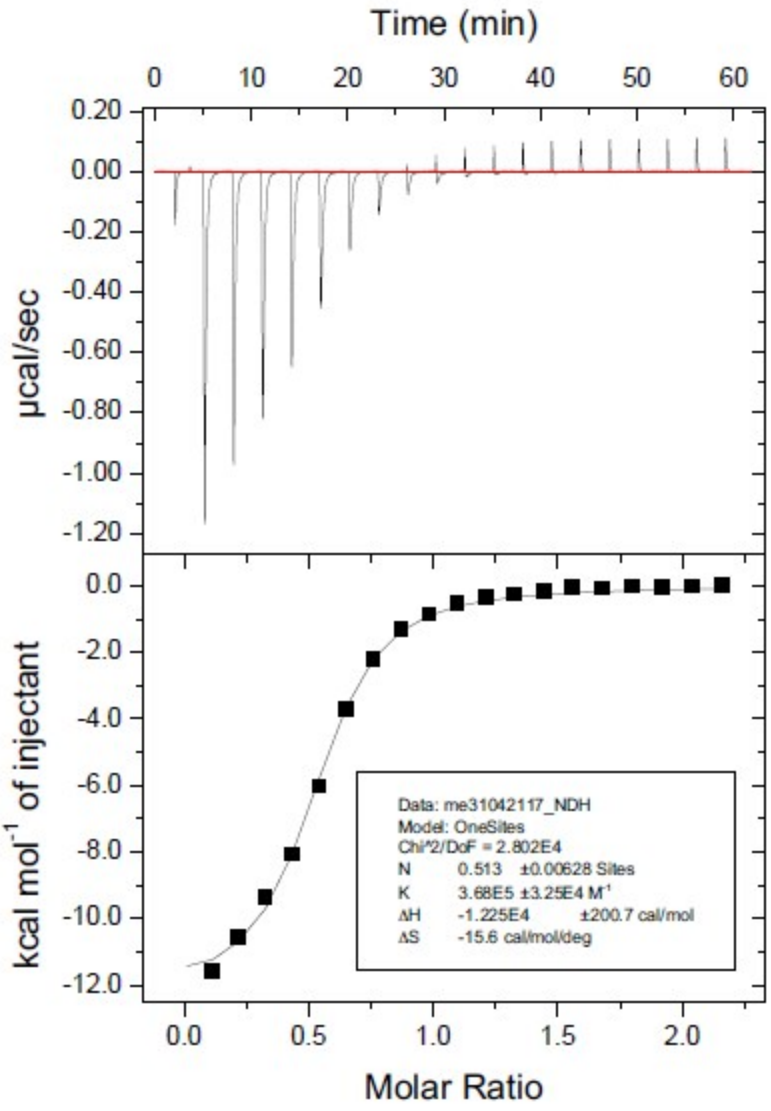


**Figure S81**. One trial of two of H3K9me$_3$ (Ac-WGGGQTARKme3STG-NH$_2$) (812 µM) titrated into **A$_2$J-1** (76 µM) at 25 $^{o}$C in 10 mM sodium borate buffer pH 8.5. (Run 1).

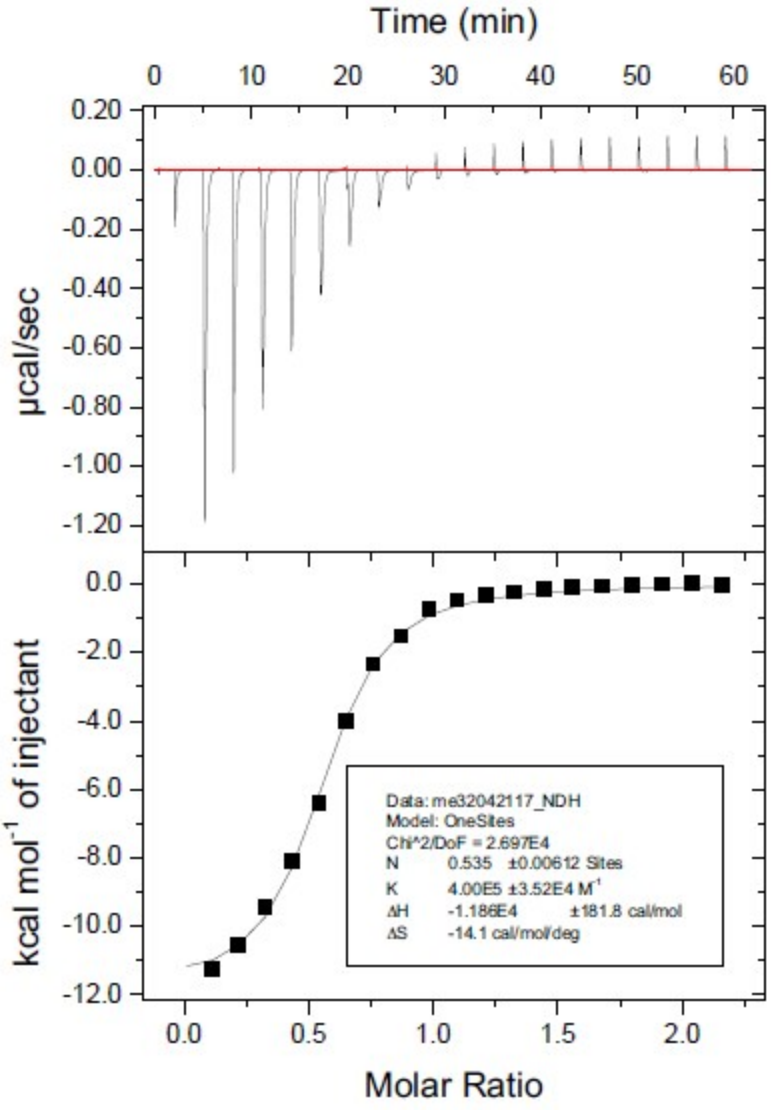


**Figure S82**. One trial of two of H3K9me$_3$ (Ac-WGGGQTARKme3STG-NH$_2$) (812 µM) titrated into **$A_2$J-1** (76 µM) at 25 °C in 10 mM sodium borate buffer pH 8.5. (Run 2).

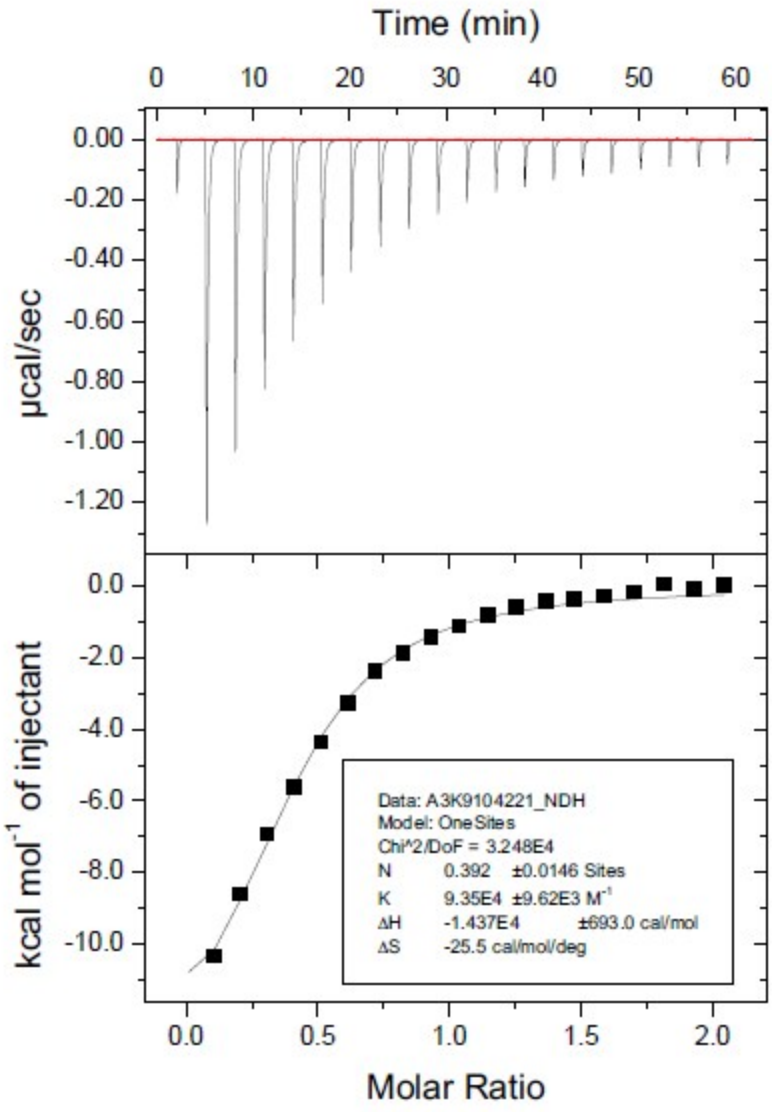


**Figure S83**. One trial of two of H3K9 (Ac-WGGGQTARKSTG-$NH_2$) (849 µM) titrated into **$A_2$J-2** (84 µM) at 25 °C in 10 mM sodium borate buffer pH 8.5. (Run 1).

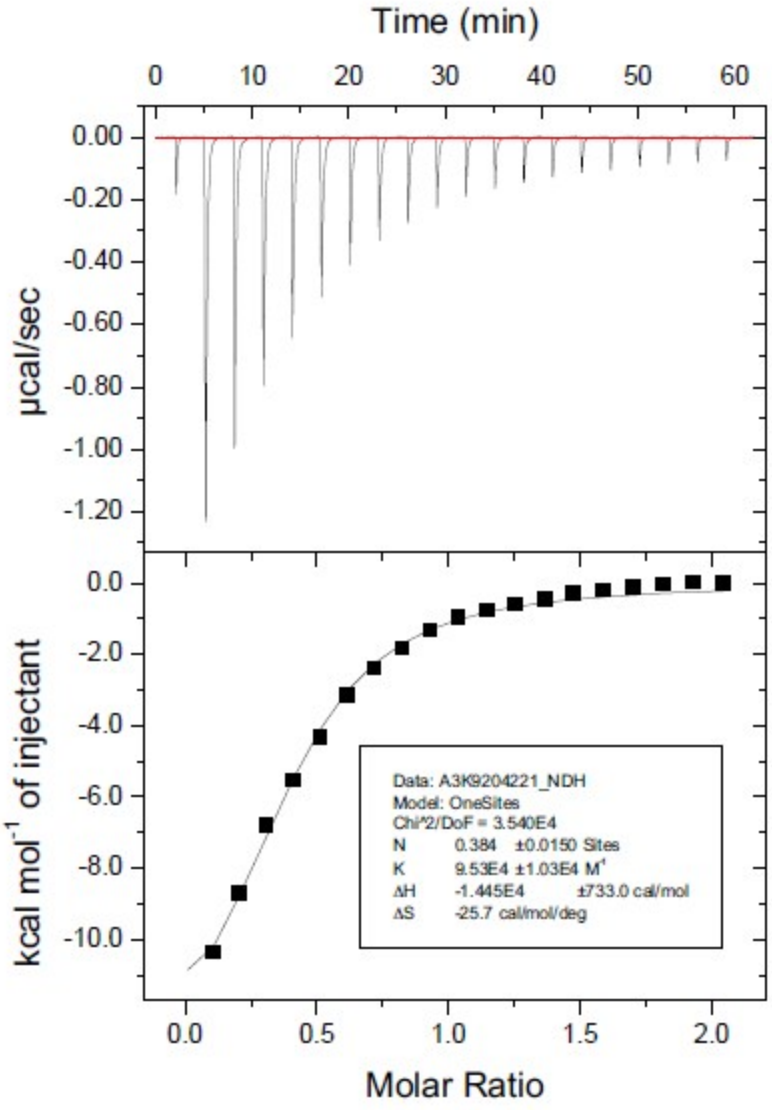


**Figure S84**. One trial of two of H3K9 (Ac-WGGGQTARKSTG-$NH_2$) (849 µM) titrated into **$A_2$J-2** (84 µM) at 25 °C in 10 mM sodium borate buffer pH 8.5. (Run 2).

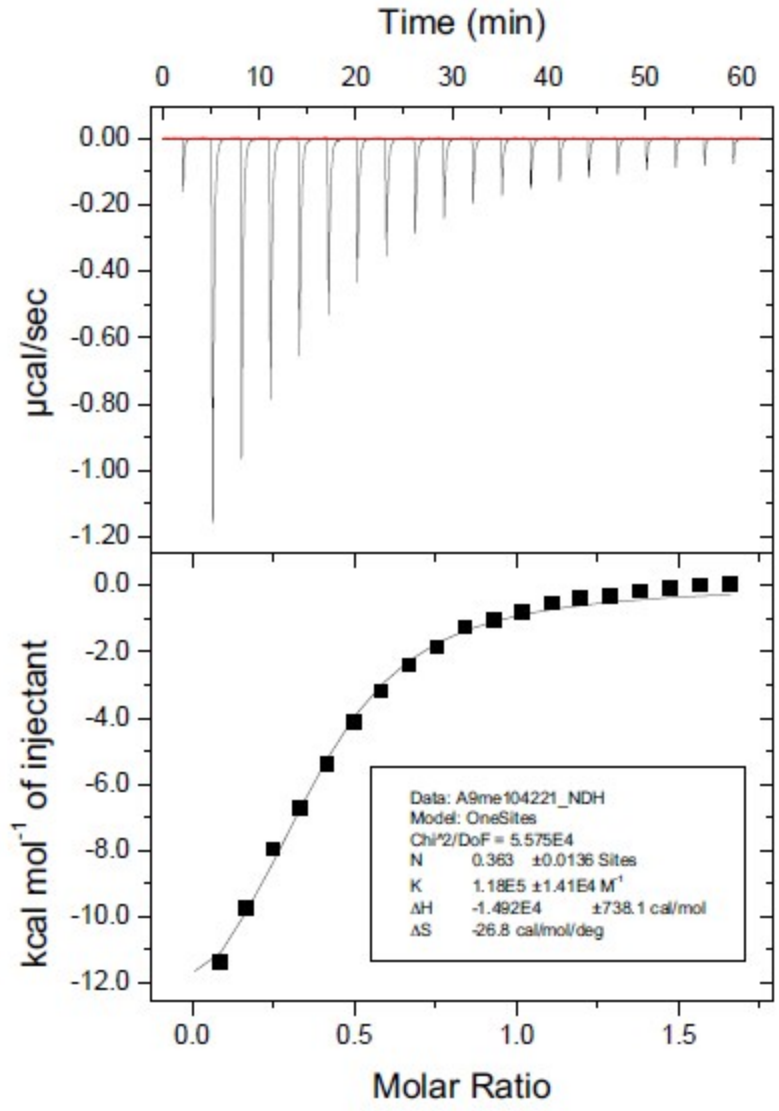


**Figure S85**. One trial of two of H3K9me (Ac-WGGGQTARKmeSTG-$NH_2$) (689 µM) titrated into **$A_2$J-2** (84 µM) at 25 °C in 10 mM sodium borate buffer pH 8.5. (Run 1).

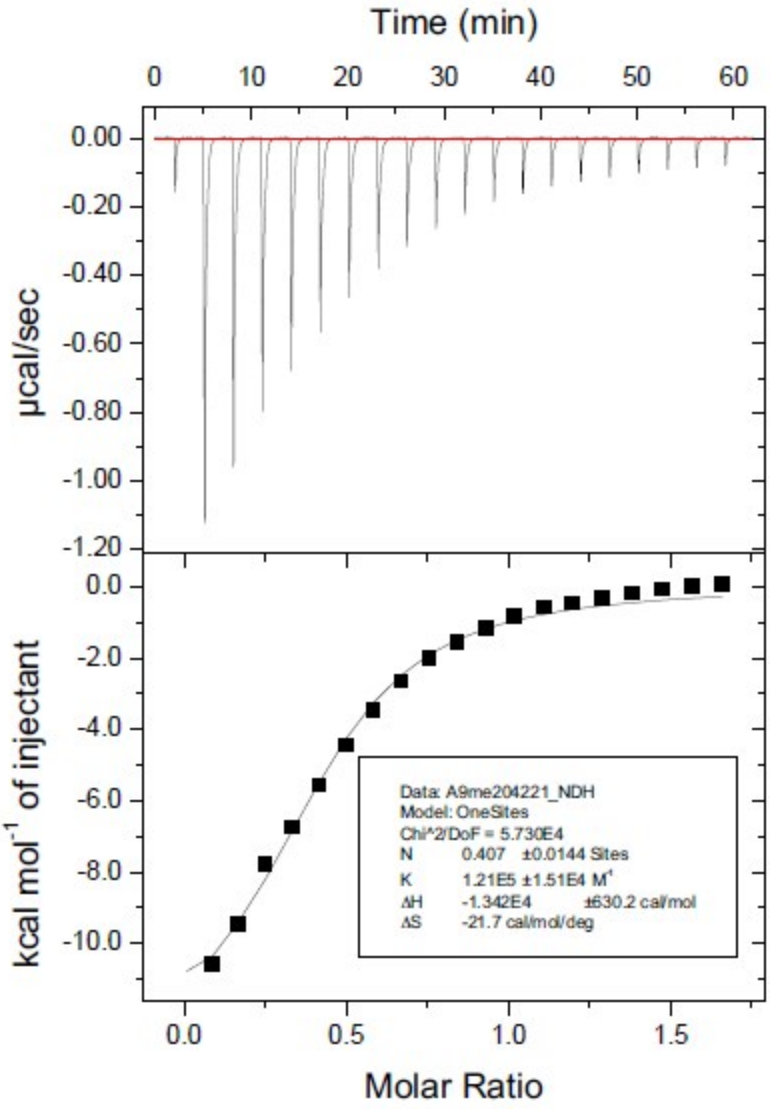


**Figure S86**. One trial of two of H3K9me (Ac-WGGGQTARKmeSTG-$NH_2$) (689 µM) titrated into **$A_2$J-2** (84 µM) at 25 °C in 10 mM sodium borate buffer pH 8.5. (Run 2).

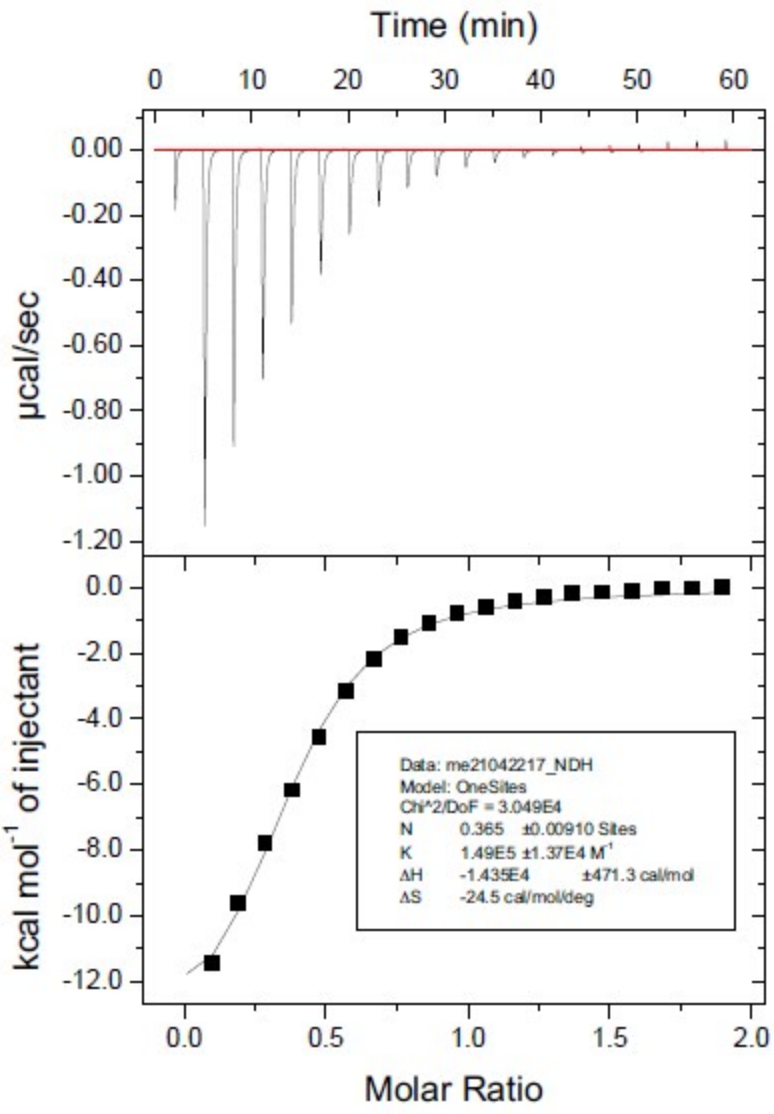


**Figure S87**. One trial of two of H3K9me$_2$ (Ac-WGGGQTARKme2STG-NH$_2$) (807 µM) titrated into **A$_2$J-2** (86 µM) at 25 °C in 10 mM sodium borate buffer pH 8.5. (Run 1).

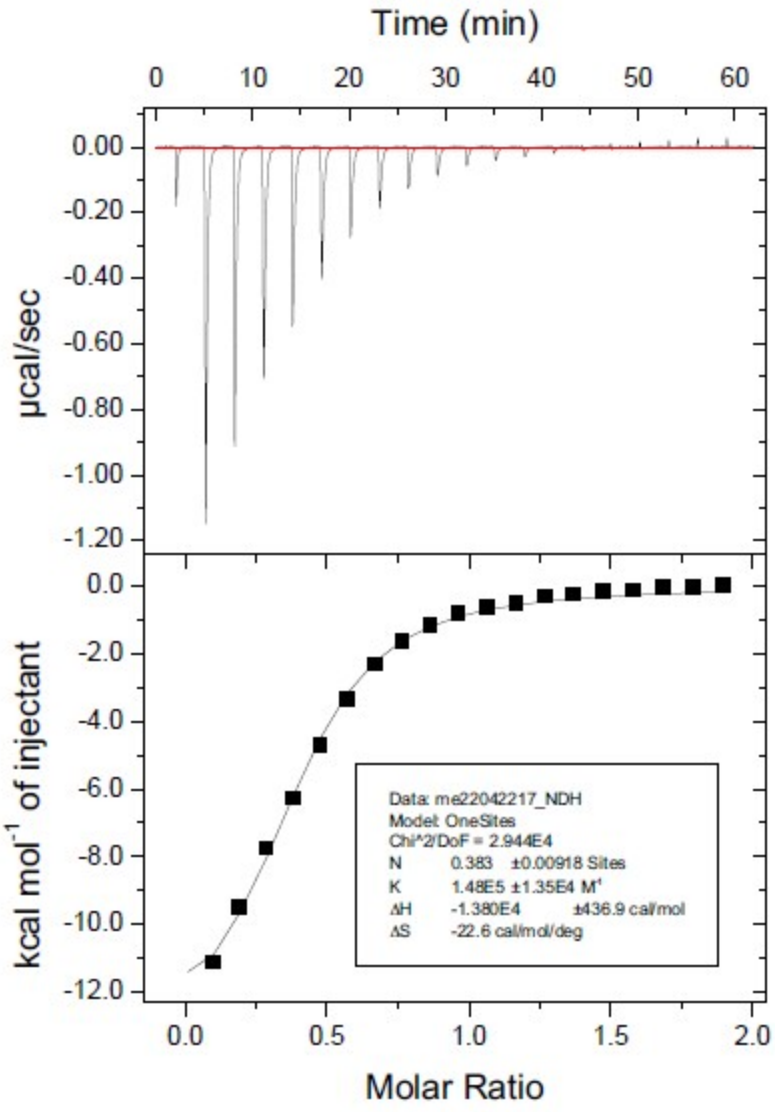


**Figure S88**. One trial of two of H3K9me$_2$ (Ac-WGGGQTARKme2STG-NH$_2$) (807 µM) titrated into **A$_2$J-2** (86 µM) at 25 $^{o}$C in 10 mM sodium borate buffer pH 8.5. (Run 2).

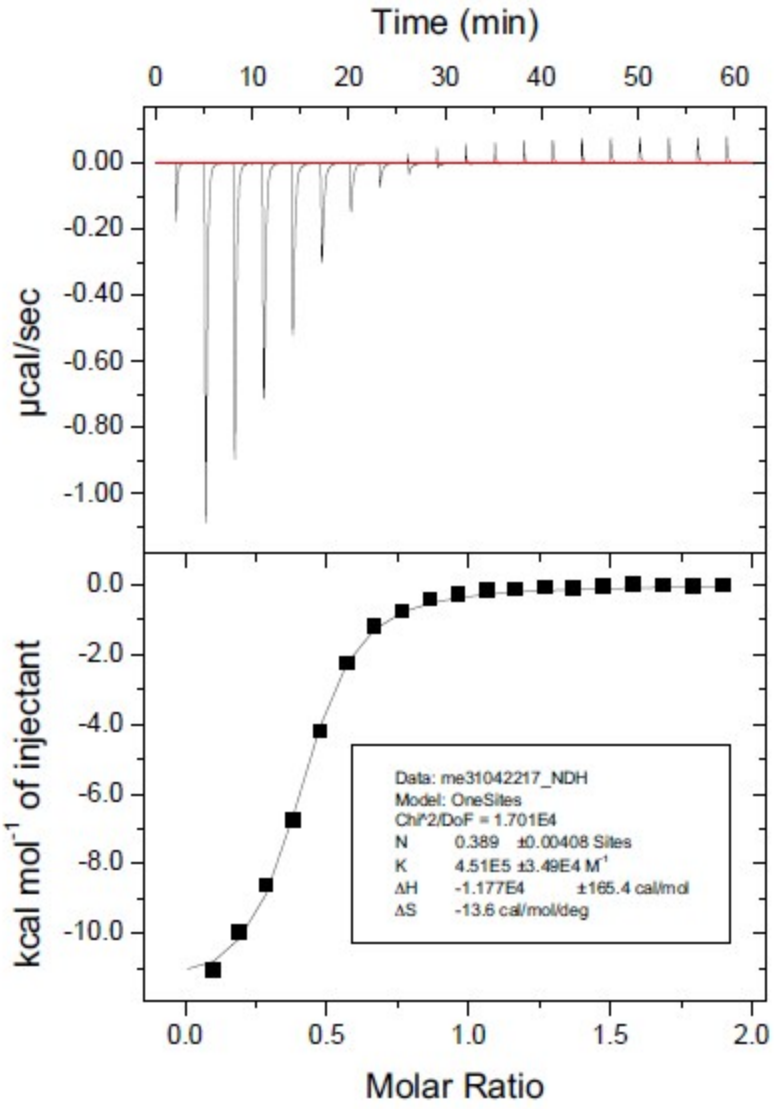


**Figure S89**. One trial of two of H3K9me$_3$ (Ac-WGGGQTARKme3STG-NH$_2$) (808 µM) titrated into **A$_2$J-2** (86 µM) at 25 °C in 10 mM sodium borate buffer pH 8.5. (Run 1).

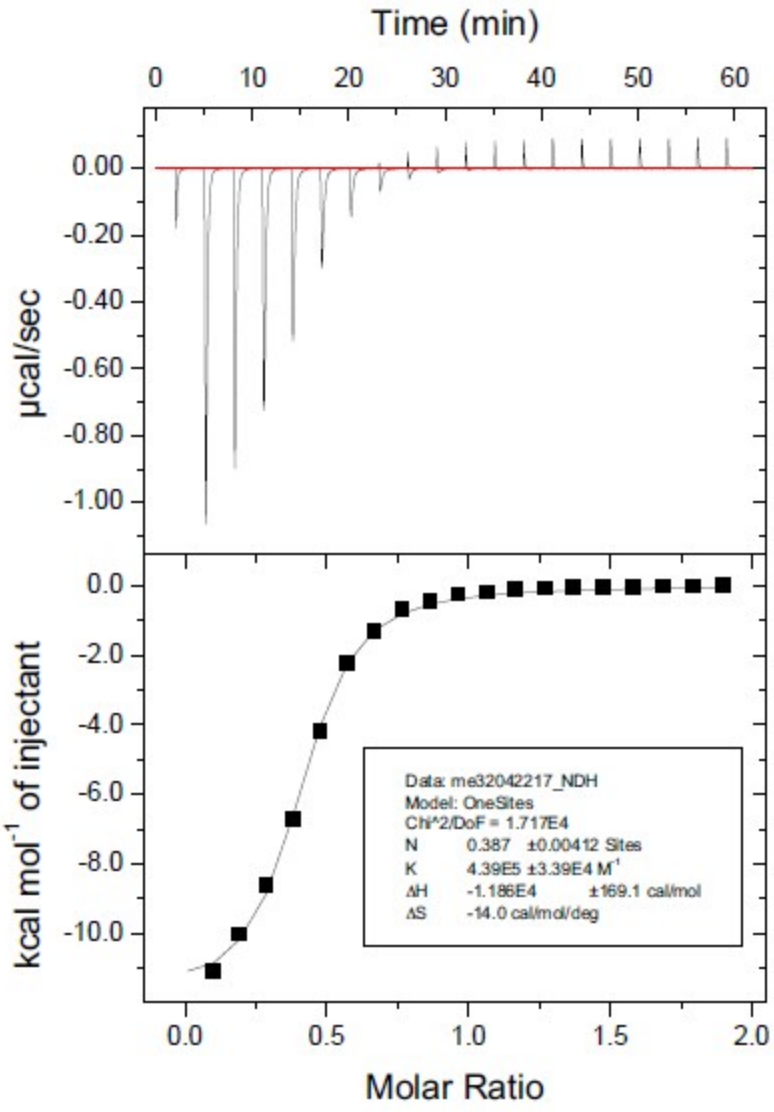


**Figure S90**. One trial of two of H3K9me$_3$ (Ac-WGGGQTARKme3STG-NH$_2$) (808 µM) titrated into **A$_2$J-2** (86 µM) at 25 °C in 10 mM sodium borate buffer pH 8.5. (Run 2).

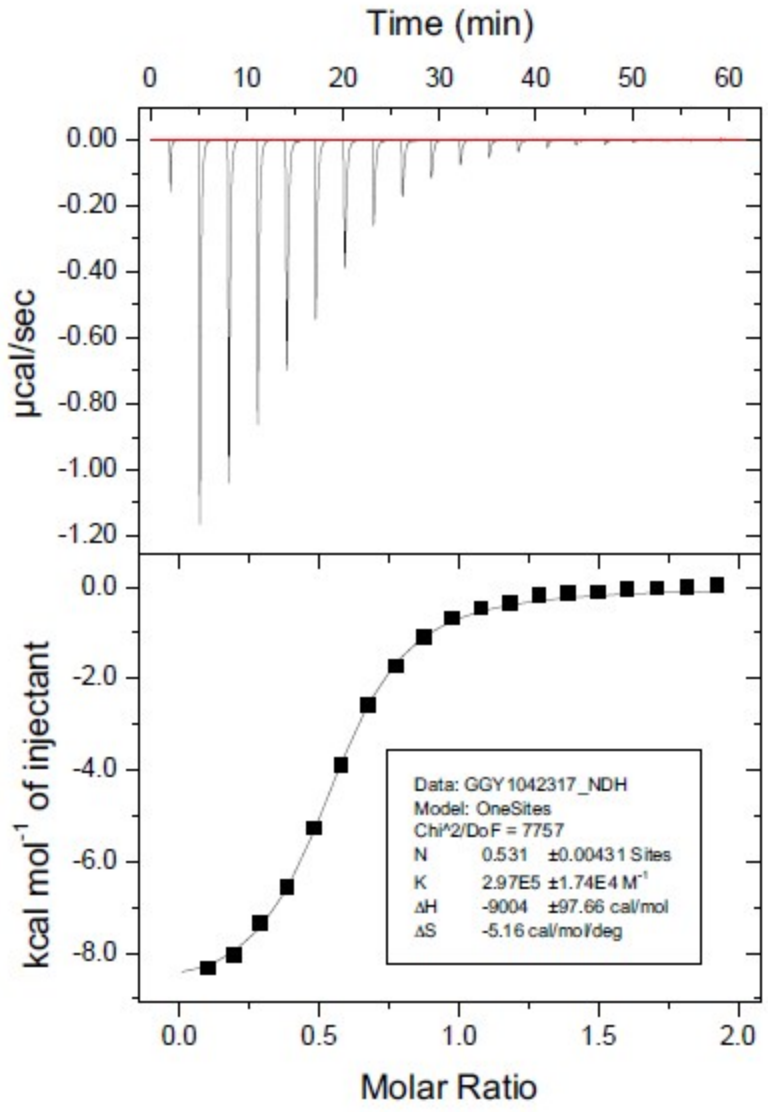


**Figure S91**. One trial of two of Kme2GGY (Ac-Kme2GGY-$NH_2$) (867 µM) titrated into **$A_2$I-2** (91 µM) at 25 °C in 10 mM sodium borate buffer pH 8.5. (Run 1).

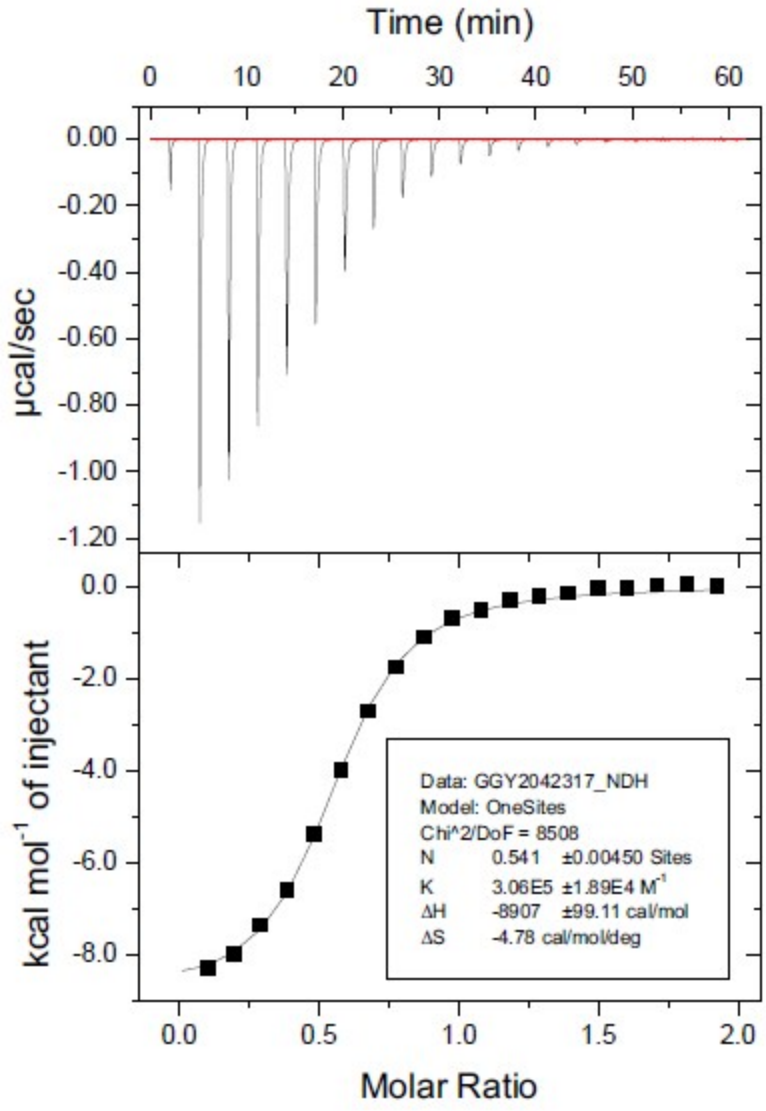


**Figure S92**. One trial of two of Kme2GGY (Ac-Kme2GGY-$NH_2$) (867 µM) titrated into **$A_2$I-2** (91 µM) at 25 °C in 10 mM sodium borate buffer pH 8.5. (Run 2).

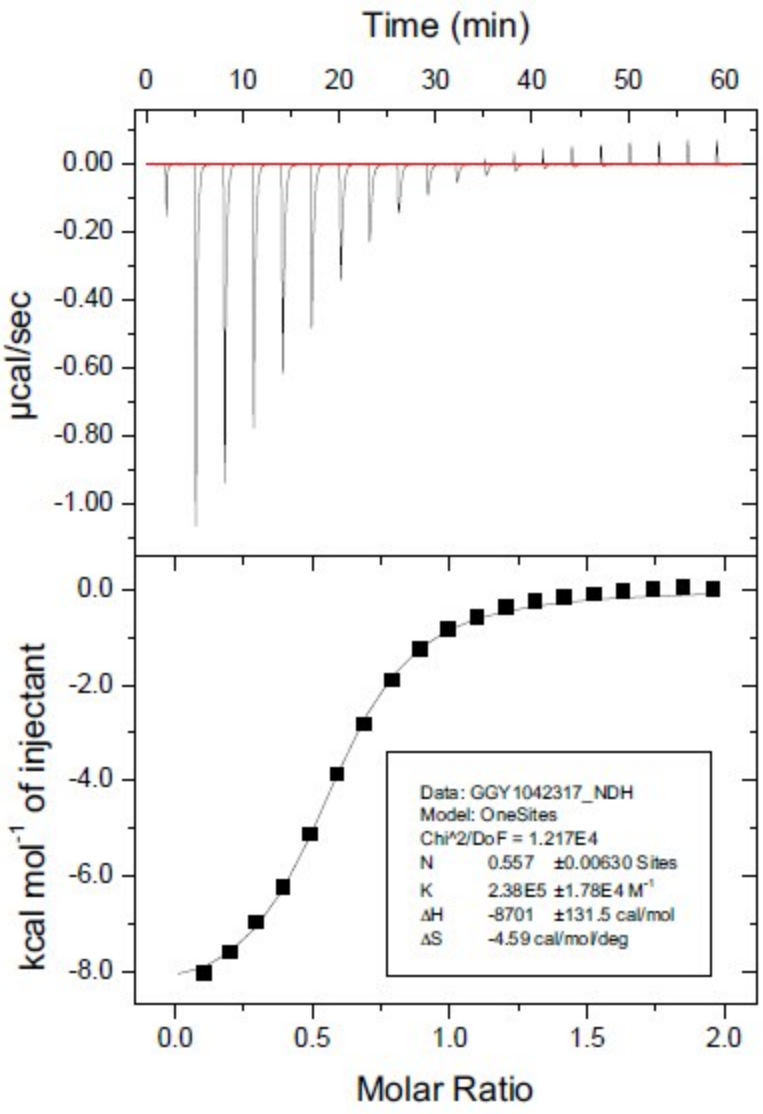


**Figure S93**. One trial of two of Kme3GGY (Ac-Kme3GGY-$NH_2$) (883 µM) titrated into **$A_2$I-2** (91 µM) at 25 °C in 10 mM sodium borate buffer pH 8.5. (Run 1).

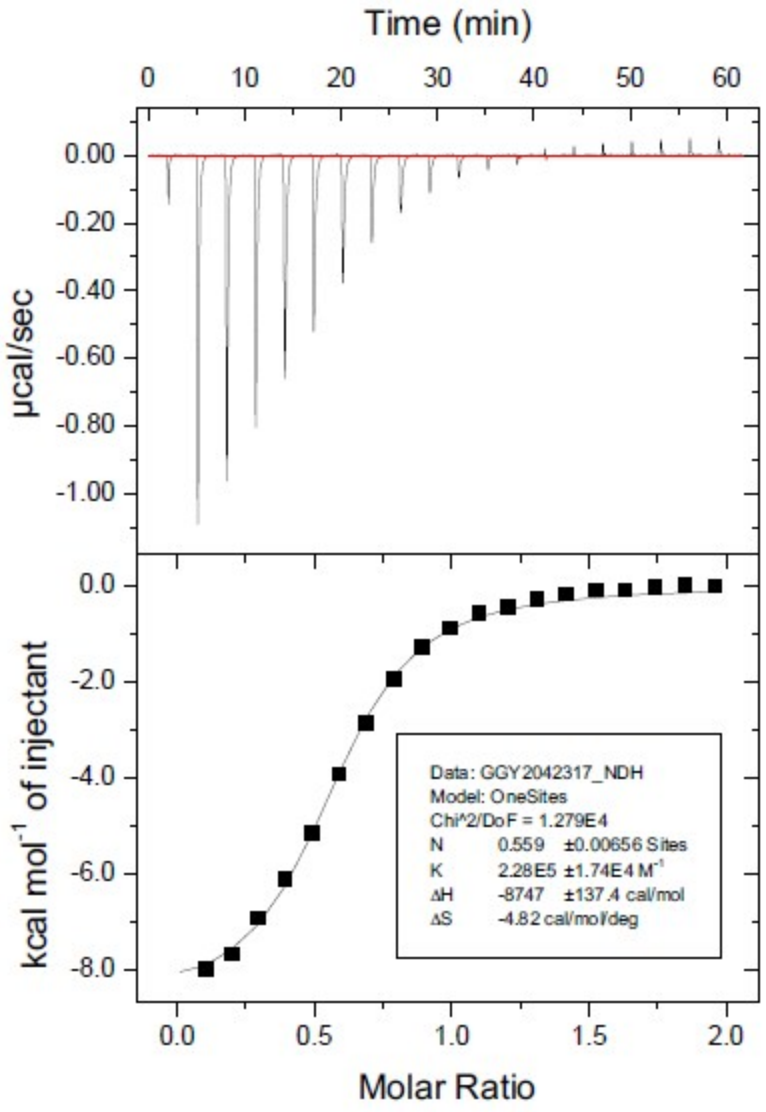


**Figure S94**. One trial of two of Kme3GGY (Ac-Kme3GGY-$NH_2$) (883 µM) titrated into **$A_2$I-2** (91 µM) at 25 °C in 10 mM sodium borate buffer pH 8.5. (Run 2).

**References**:

(1) Umemoto, T.; Garrick, L. M.; Saito, N. *Beilstein J. Org. Chem.* **2012**, *8*, 461–471.

(2) Dahl, B. J.; Branchaud, B. P. *Org. Lett.* **2006**, *8*, 5841–5844.

(3) Percec, V.; Holerca, M. N.; Nummelin, S.; Morrison, J. J.; Glodde, M.; Smidrkal, J.; Peterca, M.; Rosen, B. M.; Uchida, S.; Balagurusamy, V. S. K.; Sienkowska, M. J.; Heiney, P. A. *Chem. - A Eur. J.* **2006**, *12*, 6216–6241.